DETECTION AND CLASSIFICATION OF DIABETIC RETINOPATHY USING RETINAL IMAGES

Thesis Submitted for the Award of the Degree of

DOCTOR OF PHILOSOPHY

in

Electronics and Communication Engineering

By

Samiya Majid Baba

Registration No: 42000386

Supervised By

Prof. (Dr.) Indu Bala (23298)

School of Electronics and Electrical Engineering (Professor)

Lovely Professional University, Punjab

LOVELY PROFESSIONAL UNIVERSITY, PUNJAB

2024

DECLARATION

I, hereby declare that the presented work in the thesis entitled "DETECTION AND CLASSIFICATION OF DIABETIC RETINOPATHY USING RETINAL IMAGES" in fulfilment of degree of **Doctor of Philosophy (Ph. D.)** is outcome of research work carried out by me under the supervision of Prof. (Dr.) Indu Bala, working as Professor, in the School of Electronics and Electrical Engineering of Lovely Professional University, Punjab, India. In keeping with general practice of reporting scientific observations, due acknowledgements have been made whenever work described here has been based on findings of other investigator. This work has not been submitted in part or full to any other University or Institute for the award of any degree.

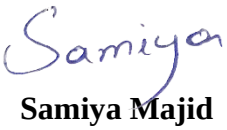

Samiya Majid
42000386
Electronics and Electrical Engineering Department
Lovely Professional University, Punjab, India

CERTIFICATE

This is to certify that the work reported in the Ph. D. thesis entitled "DETECTION AND CLASSIFICATION OF DIABETIC RETINOPATHY USING RETINAL IMAGES" submitted in fulfillment of the requirement for the award of degree of **Doctor of Philosophy (Ph.D.)** in the School of Electronics and Electrical Engineering, is a research work carried out by Samiya Majid Baba, 42000386, is bonafide record of her original work carried out under my supervision and that no part of thesis has been submitted for any other degree, diploma or equivalent course.

Prof. (Dr.) Indu Bala
Professor
23298
School of Electronics and Electrical Engineering
Lovely Professional University Punjab, India

ABSTRACT

An eye disorder known as diabetic retinopathy (DR) is often associated with diabetes. The majority of persons with long-term diabetes mellitus get this illness eventually, which may cause blindness. Regular DR screening is essential for immediately identifying the condition so that treatment can start. During regular check-ups for diabetes patients, digital retinal images are often taken. Because there are so many diabetic patients, adequately analysing these photographs might be costly and time-consuming. Therefore, automated detection techniques will be quite helpful in this field. The focus of this study is to detect and grade the diabetic retinopathy considering the training time and accuracy. The primary goal is to create an automated early-stage diagnostic method for DR lesions using machine learning. Diabetes is a condition that affects several essential human organs, including the eyes, heart, and kidneys. Approximately 80% of people may suffer variations in their blood glucose levels, which may result in a few ocular disorders. Patients who have had diabetes for more than 10 years are at risk of developing eye illnesses such as retinopathy and maculopathy. To avert eye damage at an early stage, eye-related illnesses must be identified, diagnosed, and treated effectively. If left untreated, eye disorders may lead to vision loss. When the dilated eye test indicates substantial abnormalities in the retina, such as modifications in blood vessels, newly formed blood vessels, leaky blood vessels, changes in the lens, nerve tissue loss, and enlargement of the macula, the ophthalmologist diagnoses DR. Early detection of DR helps ophthalmologists to administer appropriate treatment and so preserve patients' vision. Identifying symptoms such as microaneurysms, haemorrhages, and exudates in the retina is the first step in treating DR. Microaneurysms, the initial sign of diabetic retinopathy, may be detected early and prevented from progressing to DR and vision loss. Microaneurysms are little red patches produced by dilation of the saccular capillaries. The term retinal haemorrhage refers to abnormal bleeding of blood vessels in the retina, the light-sensitive tissue at the back of the eye. Exudates are distinguished by blood vessel released fluid and brilliant yellow lipids. .This thesis supports for the development of an automated computer-based diagnostic tool that can identify early signs of diabetic

retinopathy in retinal fundus images, assisting ophthalmologists in the screening process for the condition. The key objective of this thesis is to employ a machine learning system to identify and evaluate diabetic retinopathy based on the severity of its classes. The study's major goal is to improve accuracy with massive datasets more quickly. The retinal pictures are critical for developing an intelligent model for detecting retinal sickness. Real-time digital retinal pictures are received from SKIMS Hospital in Srinagar, Jammu and Kashmir, and publically accessible retinal image databases such as Kaggle, EyePACS, IDRiD and Messidor, are downloaded from the internet to diagnose diabetic retinopathy. Clinicians divide DR into four categories: "0","1", "2", "3" and “4” which signify "normal", "mild", "moderate", "severe", and "proliferative" respectively. The dataset from Kaggle comprises 35,126 high-resolution pictures captured under a range of imaging settings. The total number of images utilized for training and testing is 11000 and 24126, respectively. The dataset exhibits distribution of images across different DR severity levels. Specifically, there are 6149 images labelled as non-DR, while the number of images decreases considerably for mild DR (588), moderate DR (1283), severe DR (221), and proliferative DR (166). The study provides potential strategies. The pre-processed picture is made available to proposed technique. Diabetic retinopathy is categorized and its severity is identified using the DR-ResNet+ classifier as normal, mild, moderate, severe, or proliferative. In order to determine the severity of the illness, the pre-processed pictures are given to the recommended model for training with the labels normal, mild, moderate, severe, and proliferative. Using the suggested approach to diagnose the condition rather than consulting an expert may result in a faster diagnosis and report. A monthly retinal examination paired with early detection of diabetic retinopathy may lower the risk of blindness in diabetics considerably. The proposed approach performed well, with DR-ResNet+ specificity of 99%, accuracy of 98%, sensitivity of 98%, and an F1-score of 97%. According to the data, the DR-ResNet+ classifier outperforms the other classifier in terms of accuracy. The DR-ResNet+ approach provides greater accuracy with less computing time by reducing training time by 98%. The unique methodology is accomplished via improved outcomes and compared to the previous method. Thus, the study presented in this thesis may serve as a pre-screening tool to aid ophthalmologists in the screening of diabetic retinopathy for early identification and diagnosis. Jupyter

Notebook is used to carry out the planned work. The Jupyter Notebook code analyses a 2544 by 1696-pixel picture in an average of 10 seconds on a computer with an Intel (R) core i7 CPU, 16 GB of RAM, and a speed of 3.80 GHz.

Using 10 photos from an ophthalmologist, the proposed model is also verified. This results in a validation accuracy of 98 % compared to the model accuracy of 99%. Similar results are obtained using a deep learning-machine learning architecture on the Messidor dataset, which yields 98.67% accuracy. On the IDRiD dataset, a fully trained model is assessed and shown to have an accuracy of 99.6%.

Acknowledgement

I begin by expressing my deepest gratitude to Allah, the Most Merciful and Most Compassionate, for granting me the strength, guidance, and resilience throughout this academic journey.

I extend my sincere appreciation to my esteemed supervisor, Prof. (Dr.) Indu Bala whose invaluable guidance, encouragement, and expertise have shaped the trajectory of my research. Her unwavering support and insightful feedback have been instrumental in the completion of this thesis.

I am indebted to my parents, my father, Prof. (Dr.) Abdul Majid Baba, and my mother, Mrs. Nelofar, for their boundless love, unwavering encouragement, and sacrifices that made my education possible. Their belief in my abilities has been a driving force, and I am profoundly grateful for their enduring support.

To my dear brother, Dr. Mubashir Majid Baba, whose encouragement, understanding, and shared enthusiasm for knowledge have been a constant source of motivation, I extend my heartfelt thanks to him.

I dearly remember my late maternal uncle, Abdul Hamid Khan, who always felt proud and happy calling me "Doctor Sahab". His belief in me was a source of motivation throughout this journey.

Lastly, I appreciate the countless friends who have provided support, encouragement, and shared insights throughout this research endeavour.

This thesis is a testament to the collective efforts and support of these individuals, and I am truly grateful for the positive impact they have had on my academic and personal growth.

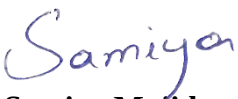

Samiya Majid
42000386
Electronics and Electrical Engineering Department
Lovely Professional University, Punjab, India

Table of Contents

List of Figures

List of Tables

List of Abbreviations

Abbreviation/s	Full Form
AI	Artificial Intelligence
CNN	Convolutional Neural Network
DL	Deep Learning
DR	Diabetic Retinopathy
GUI	Graphical User Interface
ML	Machine Learning
ROI	Region of Interest
SVM	Support Vector Machine
RGB	Red, Green, Blue
CAD	Computer-Aided Diagnosis
OCT	Optical Coherence Tomography
PDR	Proliferative Diabetic Retinopathy
NPDR	Non-Proliferative Diabetic Retinopathy
AMD	Age-Related Macular Degeneration
ROC	Receiver Operating Characteristic
AUC	Area Under the Curve
OD	Optic Disc
FOV	Field of View
DME	Diabetic Macular Edema
ResNet	Residual Network
VGG	Visual Geometry Group
InceptionNet	Inception Neural Network
MLP	Multi-Layer Perceptron
DNN	Deep Neural Network

CHAPTER 1
INTRODUCTION

1.1 Background of the Study

Diabetic Retinopathy (DR) stands as a significant and progressively prevalent complication of diabetes mellitus, posing a substantial threat to vision impairment globally. As the leading cause of blindness among working-age adults, its impact on public health is profound. Advances in medical imaging and computer vision technologies have opened avenues for enhanced diagnostics and early intervention in various medical domains. In the context of diabetic retinopathy, the utilization of retinal images for detection and classification has emerged as a promising approach.

The purpose of this study is to contribute to the ongoing efforts aimed at improving the diagnostic precision and efficiency in identifying diabetic retinopathy through the analysis of retinal images. By leveraging cutting-edge technologies such as machine learning and image processing, this research seeks to address the challenges associated with timely and accurate detection of diabetic retinopathy stages. Understanding the intricacies of image-based diagnostic systems and their potential integration into clinical practices is essential for developing effective strategies to combat the escalating threat of vision impairment caused by diabetic retinopathy.

Through this investigation, the intent is to not only enhance the accuracy of detection but also to delve into the nuances of classification methodologies, providing a comprehensive framework for characterizing different stages of diabetic retinopathy. The outcomes of this research are anticipated to contribute valuable insights to both the scientific community and healthcare practitioners, fostering advancements in the realm of diabetic retinopathy diagnostics.

In essence, this study aims to bridge the gap between medical imaging technologies and the imperative need for efficient, reliable, and accessible tools in the diagnosis and classification of diabetic retinopathy. By aligning with the broader mission of improving healthcare outcomes, the research endeavors to lay the foundation for a robust and scalable solution that can be integrated into clinical workflows, thereby

facilitating early intervention and ultimately reducing the burden of diabetic retinopathy related visual impairment.

1.1.1 The Human Eye

The human body's anatomy is made up of five senses: sight, hearing, taste, smell, and touch [1]. Each sense is critical for our daily activities, but vision is especially significant since it connects people to their surroundings. Sight is always referred to as vision. The focused light is delivered to the retina, stimulating the rods and cones. The retina then transmits these nerve impulses to the optic nerve. The optic nerve transfers these impulses to the brain, which interprets the visual pictures. The brain receives information visually via the eyes. The retina is an essential element of our eye that transmits images to the brain through the optic nerve [2]. Most eye disorders have undetectable symptoms in their early stages. If the problem is diagnosed early, it is easier to cure diseases like retinopathy and glaucoma. Otherwise, patients are put at danger; they need regular screening and diagnosis by medical specialists and trained ophthalmologists. In this case, establishing this via early identification is critical for diabetic retinal disorders. Diabetic individuals are mostly impacted by eye disorders, which may lead to serious consequences. One of the most dangerous side effects of a number of retinal disorders that cause visual impairments is diabetic retinopathy [3].

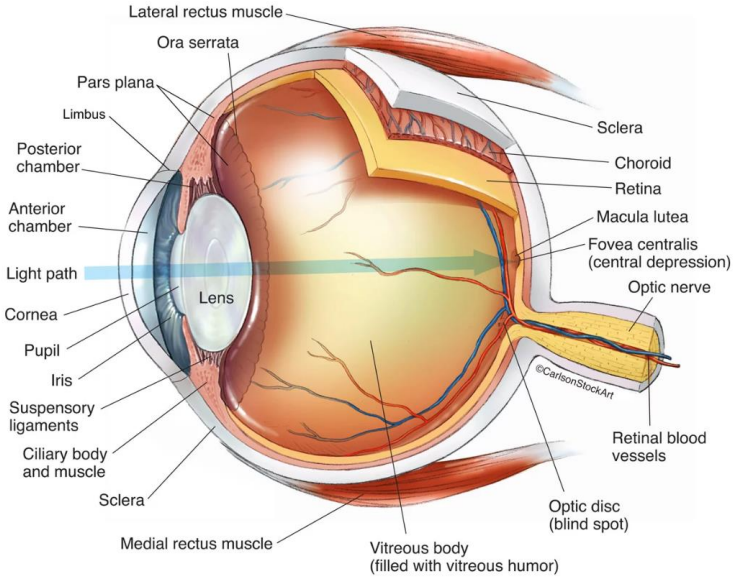

Figure 1.1: Anatomy of the Human Eye [4]

The eye is a wonderful organ in humans that is in charge of vision, which enables us to see our surroundings. Understanding the anatomy of the eye is crucial to

comprehending various eye diseases and conditions. Similar to a camera, the eye possesses a spheroid structure and functions as a receptor organ for capturing and processing light.

Figure 1.1 depicts the different parts that comprise an eye, each of which has a specific purpose. The region of the eyeball that is located behind the retina, together with the cornea, iris, and lens, are all components that collaborate to enable light from the environment to reach the retina. The retina is made up of many layers, and one of those layers contains the light-sensitive rods and cones. The retina is a single piece that connects to the optic nerve. The optic nerve transports information from the retina's rods and cones to the brain, where it is processed into a picture [5].

Diabetes is a condition that develops when the body is unable to manufacture the hormone insulin or respond appropriately to its presence. [6]. Elevated blood sugar levels occur as a consequence of carbohydrates' inability to be efficiently metabolized [7]. High amounts of blood sugar may be harmful to blood vessels as well as neurons, increasing the likelihood that patients with diabetes will develop additional disorders associated to their diabetes, including DR [8]. Diabetic retinopathy (DR) is a disease that develops with diabetes. The deterioration of the retina's tiny blood vessels is the underlying cause of this disorder. As a consequence of the diabetes syndrome's secondary effects, blood vessels in the retina may degenerate, leak, or get occluded. Vision loss develops over time when the passage of nutrients and oxygen to various parts of the retina is disrupted. As a consequence of the blockages, abnormal blood vessels may form on the retina's covering. This enlargement may increase the likelihood of bleeding and liquid spills. As a consequence of these anatomical changes, the retina may subsequently shift farther from the back of the eye, making it difficult to see well at first.

1.1.2 External Layers of the Eye

An in-depth illustration of the surface layer of the human eye, offering a comprehensive visual representation of its anatomical structures and intricate features.

1.1.2.1 Fibrous Tunic

The fibrous tunic is the name given to the most outer layer of the eye, consisting of two components - the cornea and the sclera [9].

- ***Cornea***

  This transparent and curved structure forms the eye's anterior surface. Covered by a thin membrane called the conjunctiva, the cornea is responsible for refracting light and protecting the eye [10].

- ***Sclera***

  The sclera, commonly known as the "White of the eye", is a hard, fibrous layer that protects and maintains the eye's fragile internal components [11].

1.1.2.2 Vascular Tunic (Uvea)

The vascular tunic, sometimes referred to as the uvea, is the central layer of the eye, is composed of several structures:

- ***Choroid***

  The choroid is a highly vascularized layer situated between the sclera (the white part of the eye) and the retina [12]. It is rich in blood vessels that supply nutrients and oxygen to the retina. The choroid also contains pigmented cells that help absorb excess light, preventing reflections and scattering within the eye. This function helps enhance visual clarity and reduce glare [13].

- ***Iris***

  The colorful portion of the eye known as the iris surrounds the transparent portion of the eye known as the pupil, which is the central aperture that permits light to enter the eye [14]. Muscles in the iris govern the size of the pupil, which affects how much light enters the eye. The iris dilates the pupil in low light to let more light in and constricts the pupil in bright light to reduce the amount of light entering [15].

- ***Ciliary Body***

  The ciliary body is the portion of the eye that is located right beneath the iris. It is responsible for creating the aqueous humor, which is a transparent fluid that nourishes the cornea and maintains the pressure within the eye [16].

- ***Pigmented Epithelium***

  This layer covers the inside surface of the retina and gives the photoreceptor cells the nutrients they need to function properly [17].

1.1.3 Internal Layer

1.1.3.1 Retina

The innermost layer of the eye is the retina, which contains specialized photoreceptor cells that detect light and initiate the visual process [18].

- ***Photoreceptors***

  Rods and cones are the two most fundamental types of photoreceptor cells that may be found in the retina [19]. Color perception and high-resolution center vision need cones, but low light and peripheral vision require rods [20].

- ***Fovea***

  A large concentration of cones may be found in the fovea, which is situated in the exact middle of the macula. This provides the ability for precise and detailed central vision [21].

- ***Optic Nerve***

  The optic nerve sends visual input from the retina to the brain for additional processing and interpretation [22].

1.1.4 Segment Division

1.1.4.1 Anterior Segment

The parts of the eye that are located in front of the lens are part of what is known as the anterior segment , such as the cornea, iris, and lens. This segment is responsible for focusing light onto the retina and regulating the amount of light that enters the eye [23].

1.1.4.2 Posterior Segment

The posterior segment encompasses the structures behind the lens, including the vitreous humor, retina, choroid, and sclera. It houses and protects critical components of the visual system, playing a vital role in maintaining the eye's structural integrity [24].

1.2 Structure of the Retina

The retina is an important component of the eye that is responsible for converting the light that enters the eye into neural impulses that are subsequently delivered to the brain,

which ultimately results in the ability to see. It is situated along the inner surface of the eyeball, encompassing distinct sections of varying thickness

1.2.1 Edge of the Optic Nerve Head

- *Thickness:* 0.4–0.6 mm [25]
- *Location:* The region around the optic nerve head, where the optic nerve exits the eye [26].

1.2.2 Central Fovea

- *Thickness:* 0.2–0.25 mm [27]
- *Location:* At the center of the retina [28].

1.2.3 Foveal Pit

- *Thickness:* 0.07–0.08 mm [29]
- *Location:* The central depression within the fovea, which contains a high density of cones for acute central vision [30]

1.2.4 Ora Serrata

- *Thickness:* About 0.1 mm [31]
- *Location:* The outermost boundary of the retina where it meets the ciliary body [32].

Figure 1.2 provides a visual representation of the many layers that make up the retina. The retina is made up of multiple layers, each of which is responsible for a certain function.

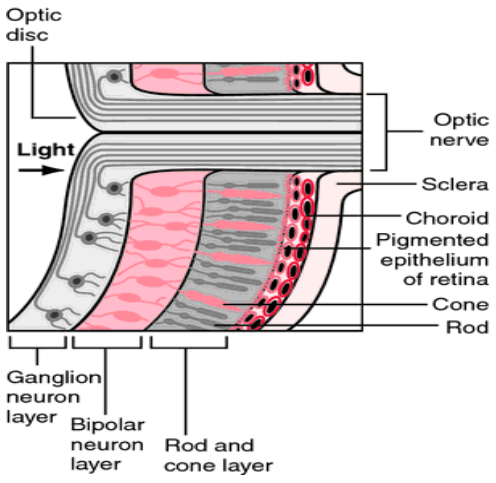

Figure 1.2: The intricate layers of the retina [33]

1.2.5 Pigment Epithelium

- *Location:* The first layer of the retina [34].
- *Function:* This layer is responsible for selectively transporting substances from the blood capillaries of the choroid to the retina [35].

1.2.6 Light-Sensitive Cells (Rods and Cones)

- *Location:* The second layer of the retina [36].
- *Function:* Rods and cones are the first neurons of the retina and serve as light receptors. There are about 7 million cones and 130 million rods in the retina. Cones are responsible for color vision and work best in well-lit environments, while rods detect motion and provide vision in low light [37].

1.2.7 Macula

- *Location:* Present at the center of the retina [38].
- *Function:* The macula is a small and light-sensitive layer of tissue responsible for sharp, clear, and detailed central vision. It plays a critical role in tasks such as reading and recognizing faces [39].

1.2.8 Fovea

- *Location:* The fovea is located at the middle of the macula [40].
- *Function:* The fovea is a tiny depression within the macula, densely packed with cones. It provides the highest visual acuity, allowing us to see fine details of objects directly in our line of sight [41].

1.2.9 Optic Disc (OD)

- *Location:* Located in the inside of the eye, behind the macula, and roughly three to four millimeters to the nasal side of the macula [42].
- *Function:* The optic disc is the brightest area on the retina and acts as the location where the optic nerve attaches to the retina. This makes the optic disc one of the most important parts of the eye. As a result of its insensitivity to light, it produces a blind area in our range of vision. The optic disc, in

contrast to the rest of the retina, does not contain any photoreceptor cells [43].

The structure of the retina is crucial for understanding its role in vision and its involvement in various eye diseases, including diabetic retinopathy. The intricate arrangement of its layers ensures the transmission of visual information from the external environment to the brain for processing and interpretation.

1.3 Working of Eye

The human eye is a very sophisticated organ that enables us to take in and analyze visual information from our surroundings. It functions by converting light signals into electrical signals that are then transmitted to the brain for interpretation [44]. Figure 1.3 demonstrates the intricate process governing the functionality of the human eye.

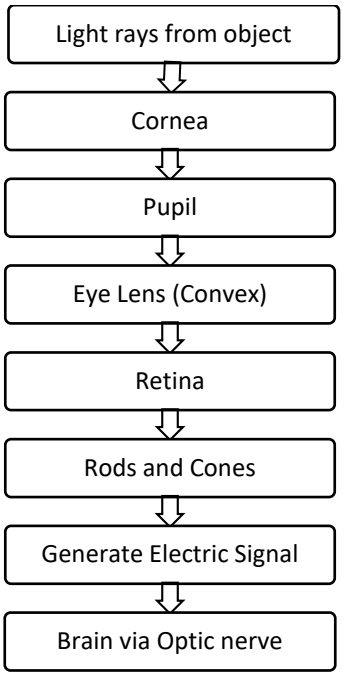

Figure 1.3: Working of eye

An overview of how the eye works is given below:

1.3.1 Light Rays from Objects

The process begins when light rays are emitted or reflected off objects in the environment. These light rays carry visual information and travel towards the eye.

1.3.2 Cornea

The cornea is the clear/transparent layer that is placed at the front of the eye and is the outermost layer of the human eye. It acts as a protective covering and also plays a crucial role in refracting or bending the incoming light rays. The cornea focuses the light rays and directs them towards the pupil.

1.3.3 Pupil and Iris

The black, circular aperture that may be found in the middle of the iris, the colorful component of the eye, is known as the pupil. Because of the quantity of light that is entering the eye, the pupil may get larger. In low light, the pupil dilates (widens) to allow more light into the eye, while in high light, the pupil constricts (shrinks) to allow less light into the eye. The iris is in charge of controlling pupil size and is responsible for the eye's distinct color.

1.3.4 Lens

Behind the pupil, there is a crystalline structure called the lens. The lens is responsible for further refraction or bending of the light rays, which helps to fine-tune the focus of the light onto the retina, which is located in the rear of the eye. The eye is able to concentrate on objects located at varying distances - process known as accommodation, which is made possible by the lens's capacity to change its shape.

1.3.5 Retina

Rods and cones are the two kinds of photoreceptor cells that may be found in the retina, which is a layer of light-sensitive cells located at the back of the eye. The process of seeing images begins when rays of light strike the retina, where photoreceptor cells transform the light's energy into electrical impulses. Cones are in charge of color vision and detailed daylight vision, while rods are morelight sensitive and in charge of night vision.

1.3.6 Optic Nerve

The electrical signals generated by the photoreceptor cells travel through the retina and are collected by nerve fibers. The optic nerve is formed when these nerve fibers join

together to create a single structure. The optic nerve acts as a pathway for the transmission of visual information from the retina to the brain.

1.3.7 Brain Interpretation

The electrical impulses are sent from the retina to the visual processing areas of the brain via the optic nerve. Electrical impulses are interpreted in the brain, and visual information is processed into pictures. Together, these processes enable us to see and understand the world around us.

1.4 Retinal Related Eye Diseases

The retina, a vital component of the eye responsible for capturing light and transmitting visual information to the brain, is susceptible to various eye diseases. Understanding these retinal-related conditions is crucial for diagnosing, managing, and treating vision problems. The following are some significant retinal-related eye diseases:

1.4.1 Diabetic Retinopathy

Diabetic retinopathy is a frequent eye disorder that damages the blood vessels in the retina (the back of the eye) [45]. Diabetes is the leading cause of vision loss in those under the age of 70. The major cause of diabetic retinopathy is uncontrolled blood glucose rise, which destroys the endothelium of blood vessels and increases their permeability. Diabetic retinopathy may progress and cause retinal detachment [46]. Early identification and treatment are essential in order to avoid patients from suffering from vision loss. Patients may not exhibit any symptoms in the early stages of the disease. Laser photocoagulation may be utilized to treat and maybe prevent the progression of diabetic retinopathy in its early stages [47]. Routine eye examinations are essential for diabetic individuals to follow the progression of diabetic retinopathy [48]. Figure 1.4 depicts the evident impact of diabetic retinopathy on eye health by contrasting a normal eye with an eye affected by the illness.

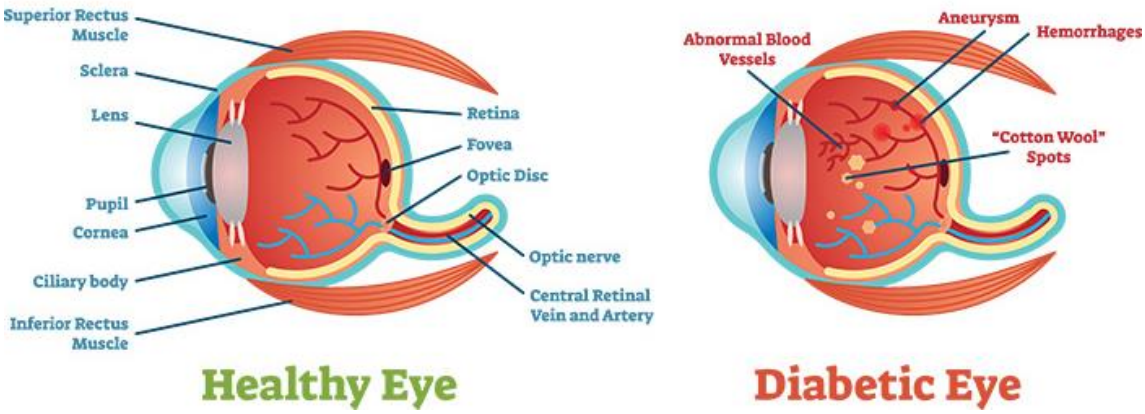

Figure 1.4: Normal Eye vs. Diabetic Retinopathy Eye [49]

1.4.2 Diabetic Macular Edema (DME)

In people with diabetes, diabetic macular edema is the most prevalent cause of visual loss and a serious consequence. The accumulation of fluid and protein deposits on or under the macula causes macular thickness or swelling, which in turn impairs vision [50]. Abnormal leakage of blood vessels surrounding the macula or diseases that damage blood vessels can cause DME [51]. Diagnosis can be achieved using techniques such as fluorescein angiography to identify blood vessel leakages and Optical Coherence Tomography (OCT) to measure retinal thickness and detect swelling [52]. Treatment options for DME may involve the use of laser therapy to stabilize vision by sealing off blood vessels. Figure 1.5 illustrates the differentiation between a normal eye and an eye with diabetic macular edema, showcasing the discernible effects of the condition on ocular characteristics

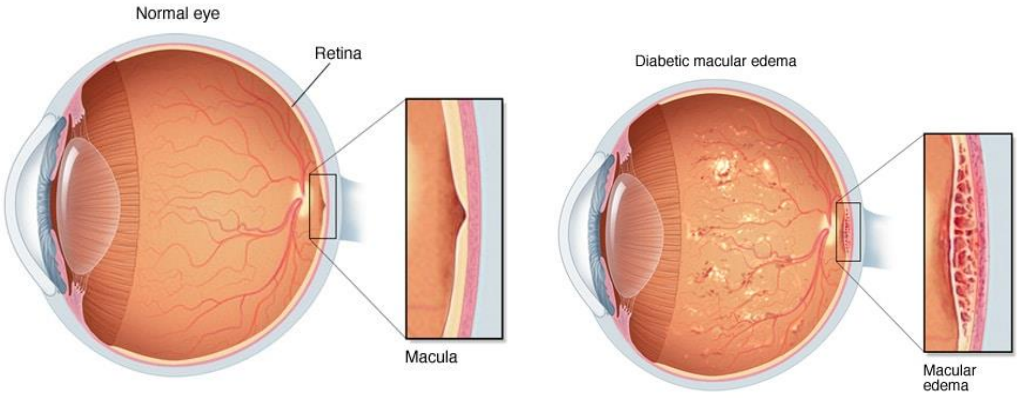

Figure 1.5: Normal Eye vs. Diabetic macular edema [53]

1.4.3 Age-Related Macular Degeneration (AMD)

Macular degeneration associated with aging is a common cause of visual impairment, especially in those aged 50 and older [54]. If treatment is not received, AMD may cause central vision to become blurry or lead to the formation of blank patches in the central vision [55]. Dry AMD and wet AMD are the two distinct forms of this condition. Dry age-related macular degeneration is an early stage of the disease that is identified by the thinning of sections of the macula or the appearance of yellow deposits that contain lipids termed drusen [56]. Wet AMD is characterized by the formation of aberrant blood vessels under the retina. These blood vessels have the potential to leak fluids and cause irreparable damage to light-sensitive cells [57]. Wet AMD is associated with a more rapid decline in vision than dry AMD. Although AMD is not curable, early intervention and management can help delay its progression and improve visual outcomes. Figure 1.6 offers a graphical representation of the comparison between a healthy eye and an eye with Age-related Macular Degeneration (AMD), elucidating the discernible ocular differences attributed to the condition.

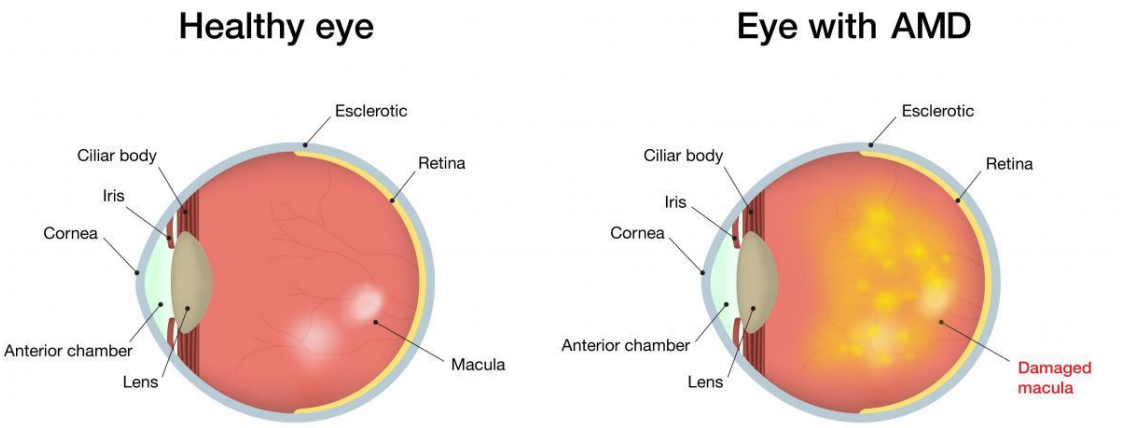

Figure 1.6: Healthy Eye vs. Eye with AMD [58]

1.4.4 Cataract

Cataracts affect the clear lens of the eye, causing it to become cloudy or opaque. This condition often occurs in individuals over the age of 40 and develops gradually, potentially affecting one or both eyes [59]. Symptoms of cataracts include blurry vision, diminished color perception, the appearance of halos around lights, trouble with bright lights, and difficulty seeing at night [60]. Cataracts are classified into three types: subcapsular cataract, occurring at the back of the lens; nuclear cataract, forming at the

center of the lens; and cortical cataract, which develops in the lens cortex [61]. Cataracts can be treated through cataract surgery to restore vision. Figure 1.7 illustrates the contrast between a healthy eye and an eye with cataract, highlighting the observable disparities in their conditions

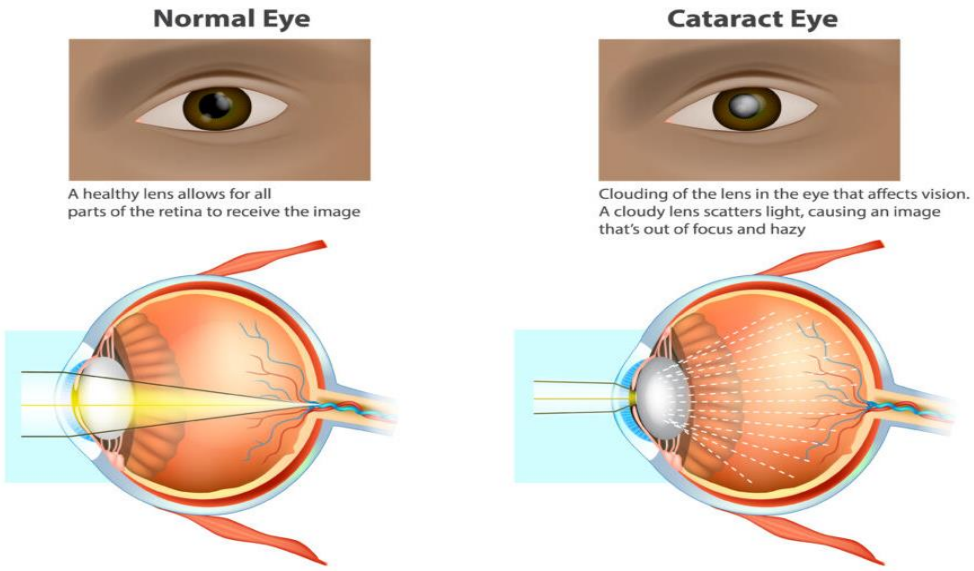

Figure 1.7: Normal Eye vs. Cataract Eye [62]

1.4.5 Conjunctivitis

An inflammation of the conjunctiva, commonly known as pinkeye or conjunctivitis, is the cause of pinkeye. The conjunctiva is a thin, transparent membrane that borders the inside of the eyelids and covers the white part of the eye [63]. Allergies, viruses, bacteria, and irritants are all possible causes. Burning and itching sensations, increased tear production, and redness in the inner or white of the eye or eyelid are all indications of conjunctivitis [64]. Treatment may involve prescribed antibiotics, although some cases of conjunctivitis caused by sexually transmitted diseases may take longer to clear up. Figure 1.8 showcases the presentation of conjunctivitis.

1.4.6 Glaucoma

Glaucoma is an umbrella term for a collection of eye diseases that may have an effect on the optic nerve and are often brought on by an accumulation of fluid in the front part of the eye [66]. This elevated fluid pressure, known as intraocular pressure, causes damage to the optic nerve, which may ultimately result in irreversible loss of eyesight [67]. Glaucoma is classified into two types: open-angle glaucoma, which appears

normal but exhibits reduced fluid drainage, and angle-closure glaucoma, where the eye does not drain due to a narrow angle between the iris and cornea, leading to a sudden increase in eye pressure [68]. Figure 1.9 is an illustrative representation of the glaucoma condition.

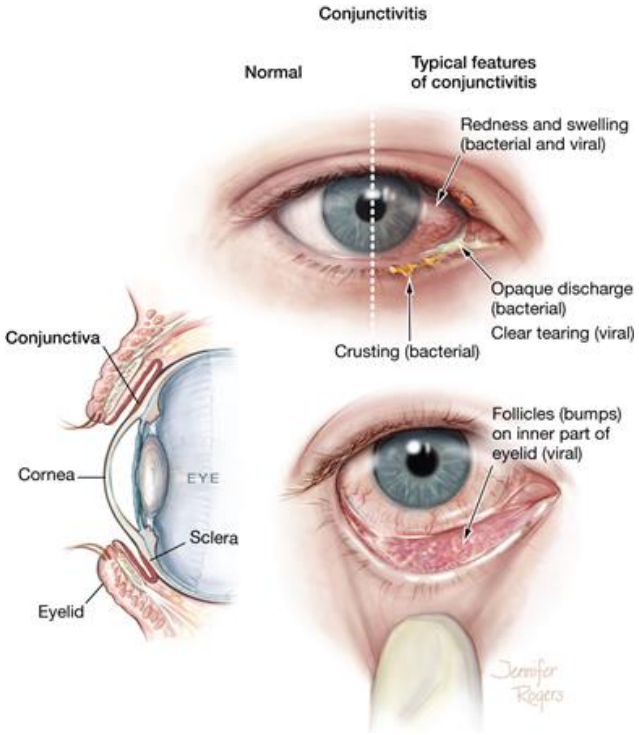

Figure 1.8: Conjunctivitis [65]

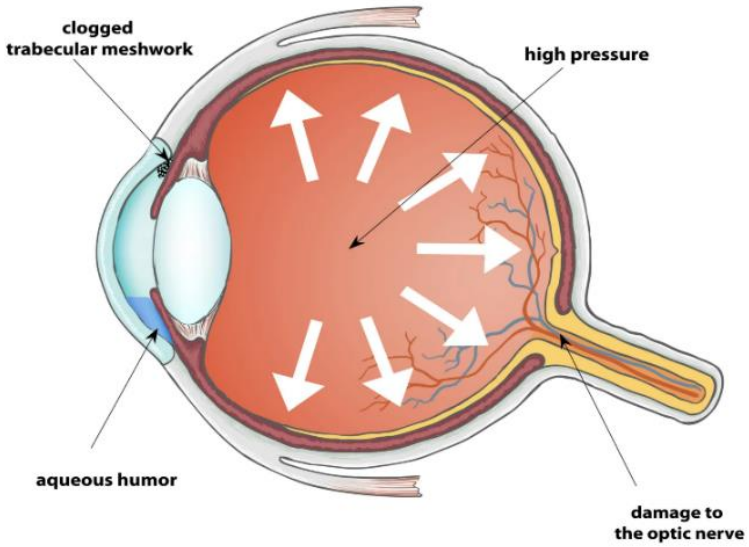

Figure 1.9: Glaucoma [69]

1.5 Diabetic Retinopathy (DR) and its Stages

Diabetic retinopathy is a progressive eye disorder that destroys the blood vessels in the retina, the light-sensitive tissue at the back of the eye. The disease can be categorized into four distinct stages, each representing different levels of severity and progressive changes within the retina. Figure 1.10 shows a graphical representation of the sequential stages characterizing Diabetic Retinopathy (DR).

1.5.1 Mild Non-proliferative Diabetic Retinopathy

In the early phases of diabetic retinopathy, patients often present with non-proliferative mild abnormalities [70]. There is weakening of the retinal blood vessel walls, leading to microaneurysms, which are small bulges or pouches that can leak fluid into the surrounding retinal tissue. This leakage can cause swelling and lead to the formation of small hemorrhages or dot-like hemorrhages. During this stage, the patient may not experience significant vision changes [71].

1.5.2 Moderate Non-proliferative Diabetic Retinopathy

As the illness advances, it moves into the stage of mild nonproliferative diabetic retinopathy. At this point, the blood vessels that feed the retina have a chance of being obstructed or deformed [72]. The reduced blood flow can lead to areas of the retina being deprived of oxygen, a condition known as retinal ischemia. In response to the lack of oxygen, the retina may release growth factors that stimulate the development of new blood vessels.

1.5.3 Severe Non-proliferative Diabetic Retinopathy

In the severe non-proliferative diabetic retinopathy stage, the retinal blood vessels become significantly blocked, resulting in a more extensive loss of blood supply to the retinal tissues. The lack of oxygen further stimulates the release of growth factors, prompting the growth of more abnormal blood vessels [73]. These new vessels can be fragile and leak blood into the vitreous, the gel-like substance that fills the eye's interior.

1.5.4 Proliferative Diabetic Retinopathy

Proliferative diabetic retinopathy, often known as PDR, is the most severe and life-threatening form of diabetic retinopathy. During this stage, the aberrant blood vessels

that were produced in the earlier phases continue to expand [74]. These new veins are prone to bleeding and may produce scar tissue, either of which can induce the creation of fibrous bands that can tug on the retina, leading to additional visual impairment. Retinal detachment is another potential complication that can result from scar tissue formation. If treatment is not received, PDR has a substantial risk of leading to serious vision loss and blindness.

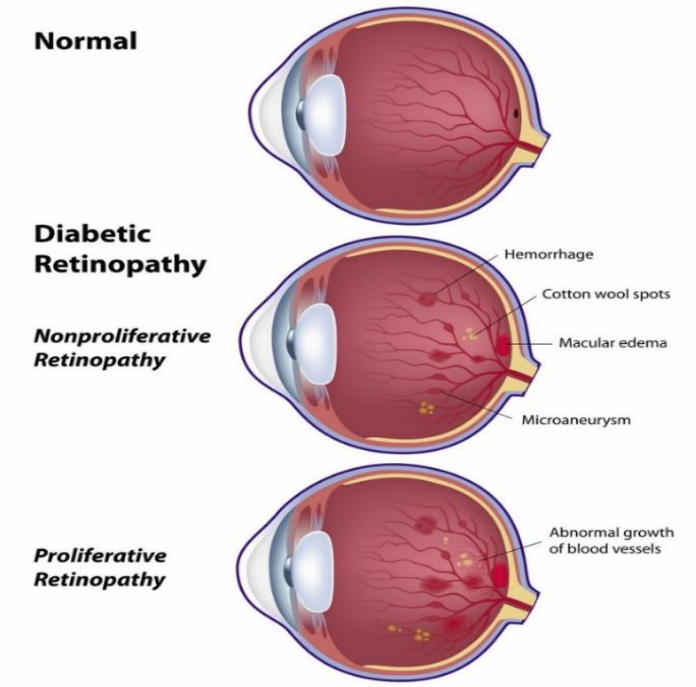

Figure 1.10: Stages of DR [75]

1.6 Pathology

The main goal of this thesis is to design an intelligent system that employs the extraction and analysis of certain retinal features to detect diabetic retinopathy (DR) early. Diabetic retinopathy, a degenerative eye disorder that affects diabetics, may lead to blindness and visual impairment if left untreated.. Detecting the disease at its early stages is crucial for implementing timely interventions and preventing irreversible damage to the retina.

In the early stages of diabetic retinopathy, patients may not experience noticeable symptoms, making regular eye screenings essential for early detection. As the disease progresses, symptoms may include blurred vision, progressive visual acuity loss, distortion, and the perception of floaters. However, by the time these symptoms

manifest, the disease may have already advanced, making early detection through retinal imaging and feature analysis a key focus of this research.

The following section outlines the clinical features of diabetic retinopathy and explains how they will be segmented and analysed. In Figure 1.11, the essential features of the retinal fundus are depicted.

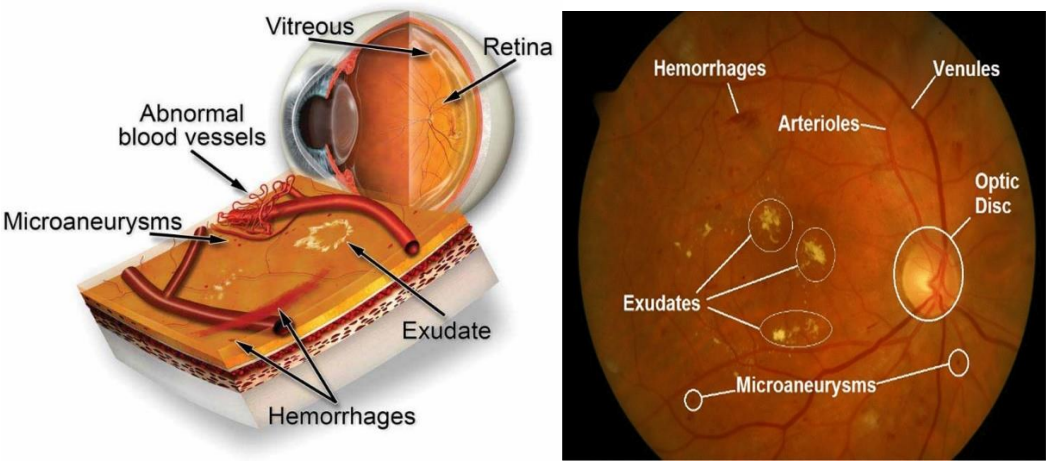

Figure 1.11: Important features of the retinal fundus. [76] [77]

1.6.1 Blood Vessels

Blood vessels in the retina play a crucial role in supplying the eye with essential nutrients, such as oxygen and blood [78]. In diabetic retinopathy, the main blood vessels may become blocked and thickened, leading to reduced blood flow and inadequate oxygen supply. As a response to this oxygen deprivation, the retina may release growth factors that stimulate the formation of new, abnormal blood vessels. These newly formed vessels are weak and prone to leakage, which can lead to the accumulation of blood and fluids, including proteins and lipids, in the surrounding retinal tissue. Such leakage can cause damage to the macula and fovea, leading to sudden vision loss.

1.6.2 Microaneurysms (MAs)

Microaneurysms are one of the earliest signs of diabetic retinopathy and are small outpouchings or dilations in the retinal capillaries [79]. The continuous exposure of retinal blood vessels to high levels of glucose leads to endothelial cell damage and weakening of the vessel walls. As a result, the weakened areas balloon out to form microaneurysms, which appear as small round red dots on the retina when examined clinically. Microaneurysms are often the first indication of vascular abnormalities in

diabetic retinopathy and can be detected through fundus examination and retinal imaging techniques [80].

1.6.3 Hemorrhages (HAs)

Hemorrhages manifest as round-shaped blot hemorrhages, resulting from blood leakage from the retinal blood vessels, predominantly in the interior layer of the retina [81]. In some cases, blood vessels may swell and leak blood or fluid, while in others, abnormal new blood vessels grow on the surface of the retina, causing hemorrhages. Microaneurysms (MAs) and hemorrhages (HAs) are commonly referred to as red lesions [82].

1.6.4 Exudates (EXs)

Exudates result from the leakage of fluid, lipids, and proteins from the retinal blood vessels [83]. These small, bright dots can be classified as hard or soft exudates. Hard exudates appear as yellow patches randomly scattered in various sizes and shapes, while soft exudates are presented as cotton wool-like spots [84]. The presence of exudates, particularly in the macular area, significantly contributes to vision loss in non-proliferative diabetic retinopathy.

1.6.5 Neovascularization

In the latter stages of diabetic retinopathy, the capillaries of the retina become more constricted, preventing the retina from obtaining adequate oxygen.. In response, the eye initiates the growth of new blood vessels, known as neovascularization, in an attempt to sustain oxygen levels in the retina [85]. Figure 1.12 displays the phenomenon of neovascularization.

Figure 1.12: Neovascularization [86]

1.7 Screening for Diabetic Retinopathy (DR)

Diabetes patients must have regular screenings for diabetic retinopathy in order to make an observation and treat any potential eye problems early on. Diabetics may acquire diabetic retinopathy, a degenerative eye ailment, and if left untreated, it can lead to severe vision impairment and even blindness. Early detection through regular screenings is essential to implement timely interventions and prevent irreversible damage to the retina.

As diabetic retinopathy progresses, it may not manifest noticeable symptoms until later stages. Therefore, timely and regular screenings are essential to detect the disease before significant vision loss occurs [87]. The screening process involves examining the back of the eyes, specifically the retina, using retinal photography. This non-invasive procedure captures detailed images of the retina, enabling ophthalmologists and retinal surgeons to determine if diabetic retinopathy is present and to what extent it has progressed.

During the screening, the patient's eyes are typically dilated with specific eye drops to provide a clearer and enlarged view of the retina. This aids in identifying characteristic abnormalities associated with diabetic retinopathy, such as microaneurysms, hemorrhages, and exudates. By thoroughly examining the retinal images, healthcare professionals can determine the appropriate course of treatment and develop individualized management plans for patients [88].

Several diagnostic techniques are commonly employed during the screening process to observe fundus images and obtain morphological information related to diabetic retinopathy. These techniques include:

1.7.1 Ophthalmoscopy (Funduscopy)

Ophthalmoscopy, also known as funduscopy, involves examining the back part of the patient's dilated eye, particularly the retina, optic disc, and macula [89]. Dilating the pupil allows experts to view larger and clearer structures within the eye. Ophthalmoscopy is a valuable screening tool for various eye diseases, including diabetic retinopathy, optic nerve damage, retinal detachment, glaucoma, macular degeneration, and diabetes-related eye conditions.

1.7.2 Fluorescein Angiography

Fluorescein angiography is a technique where a fluorescent dye (fluorescein) is injected into a vein, and the retinal circulation is visualized using a fundus camera equipped with a specialized filter [90]. The dye highlights the retinal blood vessels and helps to identify areas of leakage and neovascularization, providing valuable information about the extent and severity of diabetic retinopathy.

1.7.3 Optical Coherence Tomography (OCT)

OCT uses laser beams as a non-invasive imaging method to capture cross-sectional images of the retina. This allows retinal experts to examine each layer of the retina and measure their thickness. Such detailed measurements aid in diagnosis and provide valuable guidance for retinal-related treatments [91].

1.7.4 Scanning Laser Ophthalmoscopy (SLO)

SLO uses confocal laser scanning microscopy to obtain high-quality diagnostic images of the retina and cornea. When integrated with adaptive optics, SLO can produce even sharper images of the retina [92].

1.7.5 Stereo Fundus Photography

Stereo fundus photography captures multiple angle views simultaneously, providing a more comprehensive assessment of the retina's topography [93].

1.7.6 Hyper Spectral Imaging

Hyper spectral imaging utilizes a fundus camera to capture images with specific wavelength bands. It is particularly useful for applications like oximetry, which quantifies oxygen levels in the bloodstream [94].

1.7.7 Fundus Autofluorescence (FAF)

FAF imaging involves capturing the natural fluorescence emitted by lipofuscin, a waste product that accumulates in the retinal pigment epithelium (RPE) with age and disease [95]. FAF can reveal changes in the RPE and may help detect early signs of diabetic retinopathy and monitor disease progression.

1.7.8 Widefield Imaging

Widefield imaging utilizes specialized cameras to capture a larger area of the retina in a single image [96]. This technique allows for a more extensive view of the peripheral retina, which is essential for detecting and managing peripheral diabetic retinopathy changes.

1.8 Symptoms of Diabetic Retinopathy (DR)

Diabetic retinopathy, sometimes known as DR, is a disorder that, in its early stages, may or may not present any obvious symptoms, making regular eye examinations and screenings critical for individuals with diabetes. As the disease progresses, certain symptoms may become apparent, indicating the need for immediate attention and management. The following is a list of symptoms that may indicate the existence of diabetic retinopathy:

1.8.1 Blurred Vision

Vision impairment is a potential symptom of diabetic retinopathy in its earlier phases, while it is still in its early stages. This happens because the blood vessels in the retina have been damaged and are leaking fluid, which causes the retinal tissue to swell and take on an abnormal shape. This condition is known as retinopathy. Blurred vision may fluctuate throughout the day and can affect both near and distance vision [97].

1.8.2 Progressive Visual Acuity Loss

As diabetic retinopathy advances, visual acuity gradually diminishes. Individuals may notice a progressive decline in their ability to see clearly, impacting daily activities such as reading, driving, or recognizing faces [97].

1.8.3 Distorted Vision

Diabetic retinopathy can cause the development of abnormal blood vessels, which can exert pressure on the retina and distort vision. Straight lines may appear wavy or bent, and objects may seem distorted or out of proportion [98].

1.8.4 Floaters

Small, black patches or forms that resemble threads might seem to "float" across a person's field of vision and are referred to as floaters. They are brought on by minuscule particles of blood or other fluids that are contained inside the vitreous gel of the eye, and when they move, they create shadows on the retina [99].

1.8.5 Impaired Color Perception

As diabetic retinopathy progresses, it can affect color vision. Colors may appear washed out, faded, or less vibrant than usual [100].

1.8.6 Dark Spots or Blind Spots

Hemorrhages and fluid leakage from damaged blood vessels can create dark spots or blind spots in the visual field. These areas may block the incoming light and result in partial loss of vision [101].

1.8.7 Sudden Vision Changes

In some cases, diabetic retinopathy can lead to sudden and severe vision changes. If there is a significant amount of bleeding in the eye, sudden vision loss or a sudden increase in floaters may occur, requiring immediate medical attention [97].

1.9 Risk Factors of Diabetic Retinopathy (DR)

Diabetic retinopathy (DR) is a complex eye disease that develops as a complication of diabetes mellitus. Various factors can increase an individual's risk of developing DR, and understanding these risk factors is essential for both early diagnosis and disease prevention. While diabetes itself is the primary risk factor for DR, there are additional factors that can further elevate the likelihood of its occurrence and progression. Some of the key risk factors associated with diabetic retinopathy are as follows:

1.9.1 Duration of Diabetes

The risk of developing diabetic retinopathy increases with the duration of diabetes [102]. Individuals who have had diabetes for a longer period are at a higher risk of developing DR compared to those with a shorter history of diabetes.

1.9.2 Poor Blood Glucose Control

Maintaining stable blood glucose levels is essential for preventing complications related to diabetes, including diabetic retinopathy [103]. Poor blood glucose control, indicated by high and fluctuating blood sugar levels over time, significantly raises the risk of DR.

1.9.3 Uncontrolled Hypertension (High Blood Pressure)

High blood pressure can damage the blood vessels, including those in the retina, making it a significant a role in the development and course of the disease that [104] is a risk for.

1.9.4 Uncontrolled Hyperlipidemia (High Blood Lipid Levels)

Elevated levels of cholesterol and triglycerides in the blood can contribute to the development of DR. Proper management of lipid levels is essential in reducing this risk [105].

1.9.5 Type of Diabetes

Individuals with type 1 diabetes or type 2 diabetes are both at risk of developing diabetic retinopathy. However, the risk may be higher in those with type 1 diabetes due to its earlier onset and potential for longer disease duration [106].

1.9.6 Pregnancy

Pregnant women with pre-existing diabetes or gestational diabetes have an increased risk of developing diabetic retinopathy during pregnancy [107]. Proper monitoring and management of blood glucose levels are crucial during this period.

1.9.7 Ethnicity and Genetics

Some ethnic groups, such as Hispanics, African Americans, and Native Americans, have a higher predisposition to diabetic retinopathy [108]. Additionally, a family history of diabetes or diabetic retinopathy can increase an individual's risk.

1.9.8 Smoking

Smoking is a modifiable risk factor that significantly exacerbates the progression of diabetic retinopathy [109]. Smokers with diabetes are at a higher risk of developing severe retinopathy compared to non-smokers.

1.9.9 Nephropathy (Kidney Disease)

The presence of diabetic nephropathy is associated with an increased risk of diabetic retinopathy, a kidney-related disease [110]. Proper management of kidney disease is vital in reducing the risk of DR.

1.9.10 Macrovascular Complications

Individuals with other macrovascular complications of diabetes, such as cardiovascular disease or peripheral vascular disease, may have an elevated risk of diabetic retinopathy [111].

1.10 Complications of Diabetic Retinopathy (DR)

Diabetic retinopathy (DR), a degenerative eye disorder, may have a range of implications if neglected or untreated. As the condition progresses, the retina's blood vessels suffer damage, impairing vision and, in severe cases, resulting in permanent blindness. The following is a list of some of the most significant issues that might arise as a result of diabetic retinopathy:

1.10.1 Diabetic Macular Edema (DME)

DME is a frequent consequence of diabetic retinopathy and happens when fluid and protein leak from the damaged blood vessels into the macula, which is the core region of the retina that is important for crisp and detailed vision [112]. DME is a common complication of diabetic retinopathy. The enlargement of the macula that results from the deposition of fluid might result in vision that is distorted or unclear. People who have diabetic retinopathy are at an increased risk for developing DME, which is a primary cause of visual loss.

1.10.2 Proliferative Diabetic Retinopathy (PDR)

In the advanced stage of diabetic retinopathy, the damaged blood vasculature encourage the development of abnormally new blood vessels to form on the surface of the retina and the head of the optic nerve. These newly constructed vessels are quite fragile and prone to bleeding, causing the formation of scar tissue. PDR can lead to severe vision loss and even retinal detachment, a sight-threatening condition that requires immediate medical intervention [113].

1.10.3 Vitreous Hemorrhage

Proliferative diabetic retinopathy can cause bleeding from the newly formed fragile blood vessels, leading to the accumulation of blood in the vitreous gel and it is located between the lens and the retina and fills the gap between the two. A hemorrhage in the vitreous might result in a sudden loss of vision as well as floaters in the field of vision [114].

1.10.4 Retinal Detachment

The formation of scar tissue and the shrinking of the vitreous gel can lead to the detachment of the retina from the underlying tissue. Retinal detachment is a medical emergency and requires prompt surgical intervention to reattach the retina and restore vision [115].

1.10.5 Neovascular Glaucoma

Neovascular glaucoma may occur as a consequence of proliferative diabetic retinopathy, which can result in the formation of abnormal blood vessels on the iris and the drainage angle of the eye. This type of glaucoma is challenging to manage and can cause severe vision loss and pain [116].

1.10.6 Vision Loss

If diabetic retinopathy is left untreated or poorly managed, it can progressively lead to significant vision loss and even legal blindness. Loss of central vision and peripheral vision can profoundly impact an individual's daily activities and quality of life [117].

1.10.7 Double Vision

In some cases, diabetic retinopathy can cause double vision (diplopia) due to the misalignment of the eyes caused by impaired eye muscle function [118].

1.10.8 Vision Fluctuations

Individuals with diabetic retinopathy may experience fluctuations in their vision, with visual acuity varying throughout the day or from one day to another [119].

1.11 Medical Treatments for Diabetic Retinopathy (DR)

Diabetic retinopathy (DR) is a progressive eye disease that requires timely and appropriate medical interventions to prevent vision loss and preserve eye health. The choice of treatment depends on the stage of diabetic retinopathy, the severity of complications, and the patient's overall health. The following are some of the medical treatments commonly used for diabetic retinopathy:

1.11.1 Anti-VEGF Injections

Injections of anti-VEGF, also known as vascular endothelial growth factor, are a frequent form of therapy for proliferative diabetic retinopathy (PDR) and diabetic macular edema (DME) [120]. A protein known as VEGF is responsible for encouraging the development of aberrant blood vessels in the retina [121]. In order to inhibit VEGF activity and prevent blood and fluid leaks from damaged blood vessels, anti-VEGF medications including bevacizumab, aflibercept, and ranibizumab are injected into the vitreous gel of the eye. These drugs are injected directly into the vitreous gel. These injections may help improve eyesight and reduce the development of diabetic retinopathy in those who get them.

1.11.2 Intraocular Steroid Injections

Corticosteroids are sometimes injected into the vitreous cavity to reduce inflammation and swelling in the macula caused by diabetic macular edema. Intraocular steroid injections, such as dexamethasone implants, can help stabilize vision and provide relief from macular edema [122].

1.11.3 Laser Photocoagulation

Laser photocoagulation is a standard treatment for diabetic retinopathy, especially in its proliferative stage [123]. This procedure uses a focused laser beam to seal off and destroy abnormal blood vessels in the retina. Laser treatment can help prevent further vision loss and reduce the risk of complications like vitreous hemorrhage and retinal detachment.

1.11.4 Vitrectomy

Vitrectomy is a surgical procedure used to treat advanced cases of diabetic retinopathy with severe vitreous hemorrhage or tractional retinal detachment [124]. During vitrectomy, the vitreous gel is removed from the eye and replaced with a clear saline solution. The procedure helps improve vision by clearing the vitreous of blood and scar tissue [125].

1.11.5 Panretinal Photocoagulation (PRP)

Panretinal photocoagulation is a laser treatment that involves applying scattered laser burns to the peripheral areas of the retina. PRP is used to shrink abnormal blood vessels and reduce the risk of neovascularization in proliferative diabetic retinopathy [126].

1.11.6 Focal/Grid Laser Photocoagulation

This laser treatment is used for diabetic macular edema that affects the central part of the retina (macula). The laser is focused on specific areas of swelling or leakage to reduce macular edema and improve vision [127].

1.11.7 Combination Therapy

In some cases, a combination of different treatment modalities may be used to manage diabetic retinopathy effectively. For instance, anti-VEGF injections may be combined with laser photocoagulation to address both macular edema and abnormal blood vessels [128].

1.12 Motivation

Diabetic retinopathy (DR) is a leading cause of vision impairment globally, with millions affected each year. Early detection and accurate grading of DR are essential

for timely intervention, yet current methods are resource-intensive, relying heavily on experienced ophthalmologists for diagnosis and evaluation. This reliance on manual processes and hand-engineered features limits accessibility and scalability, particularly in resource-limited areas. Moreover, existing automated systems often require extensive training time, limiting their feasibility for real-time implementation.

This research is motivated by the critical need for a more efficient, automated framework to enhance the detection and grading of DR. Such a solution has the potential to improve patient outcomes, reduce healthcare costs, and expand access to diagnostic services. By developing a model that minimizes training time while maintaining accuracy, this study aims to bridge the gap between clinical needs and technological capabilities, paving the way for more accessible and real-time DR screening on a global scale.

1.13 Thesis Structure and Chapter Overview

This thesis is organized to provide a comprehensive examination of diabetic retinopathy detection and classification using advanced machine learning and deep learning approaches.

The study begins with **Chapter 1**, which introduces the foundational concepts of the human eye, its structure, and the pathology of diabetic retinopathy. This chapter also discusses the symptoms, risk factors, and treatment options associated with diabetic retinopathy, as well as the importance of early screening.

Chapter 2 provides a detailed literature review, covering traditional and modern methods in retinal image analysis, focusing on machine learning (ML) and deep learning (DL) techniques. The chapter also addresses specific areas such as vessel segmentation, lesion detection, and microaneurysm detection, leading to a clear identification of the research gaps and the study's objectives.

Chapter 3 discusses the dataset used for diabetic retinopathy analysis, outlining its key attributes and limitations. It also covers the grading process for classifying disease severity and presents benchmarks that establish a standard for model performance evaluation.

Chapter 4 presents the development of the proposed model, DR-ResNet+. The chapter provides an overview of the conventional ResNet model as a base and then describes

enhancements implemented to improve detection accuracy specifically for diabetic retinopathy.

Chapter 5 focuses on the results and performance evaluation of the proposed model, including a detailed comparison with existing models. This chapter further discusses the potential for real-world clinical implementation, emphasizing the benefits of the proposed model in supporting effective diabetic retinopathy screening.

Finally, **Chapter 6** concludes the thesis by summarizing the findings and contributions of this research and offering directions for future work that can build upon these advancements to further improve diabetic retinopathy detection in clinical practice.

CHAPTER 2

LITERATURE REVIEW

This second chapter, embarks on a comprehensive exploration of the ever-evolving landscape surrounding the detection and classification of diabetic retinopathy (DR) through the analysis of retinal images. The timely diagnosis and accurate grading of DR are pivotal in preventing vision impairment and blindness among individuals afflicted by diabetes mellitus. This chapter is dedicated to unraveling the multifaceted tapestry of research and innovation that has shaped the field, tracing the trajectory of advancements, and identifying the current state of knowledge in this critical domain of medical imaging and healthcare.

As we delve into the wealth of literature on DR detection and classification, a survey of the various methodologies, techniques, and algorithms that have been developed over the years has been explored. Our exploration will not only span the technological aspects but will also scrutinize the clinical implications of these advancements. The goal is to not only understand where we stand in the present but also to uncover opportunities for further enhancement and innovation, ultimately contributing to the improvement of healthcare outcomes for diabetic patients.

2.1 Existing Approaches for DR Detection and Classification

2.1.1 Traditional Methods

Diabetic Retinopathy (DR) is a complex and progressive eye disease that poses significant challenges for early detection and accurate diagnosis. Over the years, various methods have been employed to detect and assess DR, with manual grading and human expert assessment being the conventional approaches. In this section, we delve into the details of these methods, their limitations, and the driving factors behind the need for more sophisticated and automated techniques.

2.1.1.1 Manual Grading

Manual grading involves the visual inspection and assessment of retinal images by trained ophthalmologists or medical professionals [129]. This labor-intensive process

requires experts to meticulously examine retinal images for characteristic features of DR, such as microaneurysms, hemorrhages, exudates, and vascular abnormalities [130]. While manual grading benefits from the expertise of skilled professionals, it is inherently subjective and prone to interobserver variability. Different experts may interpret the same image differently, leading to inconsistent results [131]. Moreover, this approach becomes increasingly impractical when dealing with a large volume of images, as it requires considerable time and resources.

2.1.1.2 Human Expert Assessment

Human expert assessment takes advantage of the deep knowledge and clinical experience of ophthalmologists. These experts analyze retinal images to diagnose and grade DR accurately [132]. The process involves identifying subtle signs and patterns indicative of the disease's progression. However, like manual grading, human expert assessment suffers from subjectivity and variability [133]. The reliance on individual expertise introduces the risk of misinterpretation and inconsistencies in diagnosis, which can impact patient care [134].

2.2 Limitations of Traditional Methods

The utilization of traditional methods for the detection and assessment of Diabetic Retinopathy (DR) has been associated with a range of inherent limitations. These shortcomings, including subjectivity, time-consuming procedures, and interobserver variability, underscore the pressing need for more advanced and automated techniques. In this section, we delve into the specific constraints posed by these traditional methods and their implications for effective DR diagnosis and management.

2.2.1 Subjectivity in Interpretation

One of the prominent limitations of traditional methods, such as manual grading and human expert assessment, is their reliance on subjective interpretation [135]. Expert evaluators, while skilled, are still susceptible to individual biases and variations in judgment. This subjectivity introduces a degree of uncertainty into the diagnostic process, leading to discrepancies in the identification and grading of DR features. Such

inconsistencies hinder the reliability and reproducibility of results, potentially compromising patient care decisions.

2.2.2 Time-Consuming Procedures

Traditional methods are notorious for their time-consuming nature. Manual grading and human expert assessment demand extensive periods for the evaluation of each retinal image [136]. This elongated process becomes impractical when dealing with large datasets or when rapid intervention is crucial. The delay in diagnosis and treatment initiation can lead to missed opportunities for early intervention, exacerbating the progression of DR and its associated complications.

2.2.3 Interobserver Variability

Interobserver variability, the phenomenon where different evaluators arrive at different conclusions when assessing the same retinal images, is a significant challenge in traditional DR detection approaches [137]. Multiple experts analyzing the same image may arrive at divergent diagnoses or severity gradings due to inherent differences in perception and interpretation. This variability introduces a level of unpredictability and inconsistency in results, undermining the reliability of traditional methods.

2.2.4 Impact on Clinical Workflow

The limitations of traditional methods have implications for the overall clinical workflow. Subjectivity, time constraints, and interobserver variability can collectively hinder the efficiency of healthcare practices [138]. Valuable clinician time is allocated to manual assessments, diverting resources from other critical tasks. Moreover, the need for continuous training and expertise maintenance adds to the operational burden, limiting the scalability of traditional approaches.

2.2.5 The Imperative for Automation

In light of these limitations, there is a growing consensus within the medical community about the imperative to transition toward automated and objective techniques [139]. By harnessing the power of advanced technologies, such as machine learning algorithms and computer-aided diagnosis systems, healthcare practitioners can overcome the challenges posed by subjectivity, time consumption, and interobserver

variability [140]. These innovative approaches hold the promise of enhancing the accuracy, efficiency, and accessibility of DR detection and classification, ultimately leading to improved patient outcomes and the effective management of Diabetic Retinopathy.

2.3 Machine Learning and Deep Learning Techniques in Medical Image Analysis

Advancements in medical image analysis have been significantly propelled by the emergence of Machine Learning (ML) and Deep Learning (DL) techniques. ML and DL offer a paradigm shift in how complex patterns and information can be extracted from medical images, including those of retinal structures, facilitating more accurate and efficient disease detection and diagnosis [141]. This section provides an overview of the key concepts of ML and DL and discuss their profound impact on the field of medical image analysis, particularly in the context of Diabetic Retinopathy (DR).

2.3.1 Machine Learning (ML) and its Application in Medical Imaging

Machine Learning refers to a computational approach where algorithms are designed to learn from data and subsequently make predictions or decisions without being explicitly programmed. In medical imaging, ML techniques encompass a diverse range of methodologies that enable computers to autonomously identify patterns, anomalies, and relevant features within images [142]. Common ML techniques include Support Vector Machines (SVM), Random Forests, Decision Trees, and k-Nearest Neighbors, among others [143]. These techniques have been employed for tasks such as image segmentation, feature extraction, and classification of medical conditions.

In the context of DR detection, ML has been instrumental in the development of automated systems that can accurately distinguish between healthy retinal images and those with various stages of DR [144]. By training on large datasets containing labeled images, ML algorithms can learn to recognize subtle textures, shapes, and structures associated with different retinal abnormalities [145]. The application of ML techniques has demonstrated promising results in improving the efficiency and accuracy of DR screening, aiding healthcare practitioners in making informed clinical decisions [146].

2.3.2 Deep Learning (DL) and its Role in Medical Image Analysis

Deep Learning represents a subset of ML techniques that have garnered significant attention and acclaim for their ability to handle complex and high-dimensional data [147]. DL models, specifically Convolutional Neural Networks (CNNs), have exhibited remarkable prowess in image recognition and understanding. These networks consist of multiple layers that automatically learn hierarchical representations of features from raw input data, making them particularly well-suited for medical image analysis [148].

In the domain of DR detection, DL techniques have demonstrated exceptional performance. DL models trained on large annotated datasets have shown the capability to accurately segment retinal structures, detect lesions such as microaneurysms and exudates, and classify the severity of DR [149]. The depth and complexity of CNN architectures allow them to capture intricate details and variations in retinal images, leading to enhanced diagnostic accuracy [150].

2.3.3 Advantages and Challenges

The integration of ML and DL techniques into medical image analysis offers several advantages, including reduced subjectivity, increased efficiency, and improved diagnostic accuracy [151]. These technologies have the potential to revolutionize DR screening by providing objective and consistent assessments, thereby alleviating the limitations associated with traditional manual methods.

However, it is important to acknowledge that the successful implementation of ML and DL techniques requires robust data collection, preprocessing, and algorithm design [152]. Additionally, the black-box nature of some DL models may raise concerns regarding interpretability and transparency, necessitating efforts to enhance model explainability in medical contexts [153].

2.4 ML and DL Approaches in Diabetic Retinopathy Detection, Classification and Grading

In recent years, the integration of Machine Learning (ML) and Deep Learning (DL) techniques has revolutionized the field of Diabetic Retinopathy (DR) diagnosis [154]. This section presents an extensive review of studies that have harnessed these

computational methodologies to enhance the accuracy and efficiency of DR detection, classification, and grading.

2.4.1 ML-Based Approaches

Numerous investigations have explored the efficacy of traditional ML algorithms in DR analysis. Support Vector Machines (SVM), Decision Trees, Random Forests, and k-Nearest Neighbors have been widely applied to extract features and classify retinal images [155]. These techniques have exhibited notable potential in distinguishing between various DR severity levels based on features like microaneurysms, hemorrhages, and exudates.

R Sarki et al. [156] employed SVM for multi-class classification of DR images, achieving an impressive accuracy of 85%. Additionally, Yu et al. [157] combined k-Nearest Neighbors with texture analysis to improve DR grading accuracy, demonstrating the versatility of ML techniques in addressing the complexity of retinal image analysis.

2.4.2 DL-Based Approaches

The emergence of Deep Learning, particularly Convolutional Neural Networks (CNNs), has ushered in a new era of precision in DR diagnosis. DL models possess an innate capability to learn intricate patterns from vast datasets, enabling more nuanced identification of retinal abnormalities.

Bosale et al. [158] traces the progression of diabetic retinopathy (DR) detection methods from conventional to deep learning, emphasizing convolutional neural networks (CNNs). It also points out the untapped potential of integrating pretrained language models with segmented image inputs for improved diagnostic accuracy in web applications.

2.4.3 Hybrid Approaches and Ensemble Learning

In pursuit of optimal accuracy, some studies have adopted hybrid approaches that synergistically combine traditional ML algorithms with DL techniques. This fusion of methodologies capitalizes on the strengths of both paradigms, leading to improved diagnostic outcomes.

Furthermore, ensemble learning techniques, including stacking and bagging, have gained traction for their ability to enhance classification performance. By aggregating predictions from multiple models, ensemble methods mitigate overfitting risks and enhance model robustness [159].

2.5 Retinal Image Analysis Techniques

2.5.1 Image Processing

In both manual and automated diagnostics, the integrity and accuracy of identification depend heavily on the quality of retinal images. Multiple factors contribute to the potential degradation of retinal image quality, encompassing challenges such as uneven illumination, deficient contrast, obscured media clarity, the wide-angle perspective of fundus cameras, inadequate pupil dimensions, variations in sensor array geometry, and the inherent effects of eye movement [160]. Therefore, the enhancement of image quality emerges as a pivotal consideration in the analysis process. Diverse methodologies have been extensively explored to ameliorate the uniformity of illumination and contrast levels across various research domains. The subsequent section delineates prevalent techniques employed to optimize the preparation of ocular retinal images, thereby striving to ensure consistency and clarity for accurate diagnostics.

2.5.2 Noise Reduction Approach

Prior to the application of illumination correction and contrast enhancement procedures, a tailored noise reduction filter was strategically employed to effectively mitigate disruptive background noise inherent in each image. During the execution of this filtration, a dual consideration of the neighborhood's mean value and its variance was thoughtfully incorporated [161]. Among order-statistic filters, the median filter has garnered notable recognition, primarily due to its proficiency in addressing specific noise types, encompassing Gaussian, random, and salt-and-pepper noise [162]. This strategic implementation of noise reduction measures serves as a foundational step in optimizing the quality and fidelity of retinal images for subsequent analysis.

2.5.3 Illumination Compensation Technique

In the pursuit of rectifying suboptimal illumination conditions, a commonly employed approach involves shadow correction [163, 164]. Within this methodological framework, a significant advancement is achieved by effectively eliminating the background components that contribute to illumination irregularities. The foundational principle underlying this technique involves extracting an image that predominantly captures the underlying backdrop from the original image. This process is facilitated by strategically implementing a median filter with dimensions surpassing those of the most prominent retinal features, thereby resulting in the derivation of the comprehensive background image. By successfully integrating this illumination correction strategy, the inherent challenges associated with inconsistent lighting are adeptly addressed, subsequently enhancing the overall quality and interpretability of retinal images.

2.5.4 Enhancement of Contrast

Efforts aimed at enhancing the contrast of retinal images commonly encompass two predominant strategies, namely histogram processing and the polynomial transformation operator. Among these, the Contrast Limited Adaptive Histogram Equalization (CLAHE) technique stands out as a noteworthy approach [165]. Distinctively, CLAHE operates on targeted segments of the image rather than applying a uniform enhancement to the entire image. This nuanced methodology results in a more precise and discerning enhancement of picture contrast compared to conventional histogram equalization methods.

In contrast to conventional approaches, the CLAHE method excels in executing image contrast enhancement with heightened efficiency and effectiveness [165]. Notably, Walter et al. have introduced a distinctive avenue for global polynomial contrast enhancement [166], wherein a specially designed polynomial gray level conversion operator is enacted upon the green channel image. This technique holds promise for elevating the perceptibility of vital and salient areas within the retinal image [167]. Renowned for its applications in biomedical image processing, the CLAHE enhancement methodology has proven instrumental in rendering significant anatomical

details more vividly and effectively apparent, thereby contributing to enhanced diagnostic accuracy and interpretation [167].

2.6 Extraction of Retinal Blood Vessels

Ophthalmologists can identify patients with DR by checking for lesions in the retina that are associated to the condition. The technique proposed works effectively in certain areas where diabetes is prevalent and DR diagnosis and treatment are often needed owing to a lack of resources and competence. While ophthalmologists labor hard to avoid blindness and the number of diabetics grows, DR infrastructure and skill are deteriorating. Over the past 10 years, there has been a boom in interest in automated retinal blood vessel segmentation. Fraz et al. [168] created both supervised and unsupervised segmentation algorithms. Unsupervised algorithms learn as they segment photos, while supervised segmentation approaches depend on the ground truth of a training set of images. Approaches used in unsupervised research include vessel tracking, matched filtering, contour models, Laplacian operators, morphological transformations, and perceptual transformation approaches. The proposed study defines datasets gathered from public and hospital sources as "normal", "mild", "moderate", and "severe", and then trains the network using supervised learning techniques. Staal et al. [169] created the ridge-based vessel identification approach, which separates the image into segments based on the closeness of each pixel to a ridge element. A kNN classifier is used to evaluate and apply a set of 27 characteristics for each pixel. When the feature set is small, this strategy speeds up the process; when the feature set is large, it slows down. The method's reliance on training data and susceptibility to fake edges are also disadvantages. Marin et al. [170] describe an approach without network learning features based on a single expert person. Its AUC is also good. To generate neural network classifiers, he proposed utilizing an independent training dataset and a seven-feature set built using neighborhood parameters and the moment invariants-based technique. Soares et al. [171] recommend employing a GMM classifier after retrieving the six-feature set using Gabor wavelets. The training data differs in this scenario as well, and it takes longer to train GMM models that integrate 20 distinct Gaussian distributions. Fraz et al. [172] extract a nine-feature set using 200 decision trees, boosting and bagging algorithms, and Gabor filters in their vessel classification

approach. The high computational cost of this method is a disadvantage. The morphology-based technique, according to Roychowdhury et al. [173], classifies more pixels than the Gaussian mixture model (GMM) and can distinguish blood vessels and background areas. Roychowdhury et al. [173] provided a strategy in which the morphology-based method recognizes blood vessels and background areas while the CNN categorizes a larger number of pixels, which served as motivation for the proposed work for the vascular segmentation approach utilizing CNN in Tensorflow. It is advised to increase the number of test and training images, the classifier's accuracy, and the number of characteristics used for classification. Liskowski et al. [174] used unsupervised techniques to build a deep neural network and extract vessel pixels from fundus images. Ramlugun et al. [175] employed retinal blood vessel segmentation from digital fundus images to detect proliferative DR (PDR). The blood vessels are segmented using a double-sided thresholding approach, then enhanced using 2D-Match (Gabor) filters and contrast limited adaptive histogram equalization (CLAHE). This vascular extraction process has a high accuracy of 93.1%. Vasanthi and Wahida Banu [176] extracted the blood vessel using preprocessing, feature extraction, and classification. To accomplish this extraction, (i) a feature vector is generated by extracting nine features, and this feature vector is then classified using ELM. (ii) To extract seven characteristics, grey level and moment invariants are employed, and ELM is used for classification. Vessel segmentation provides the foundation for recognizing exudates, optic discs, and microaneurysms. As part of a computer-based diagnostic approach, Franklin and Rajan [177] proposed employing a feed forward network and a back propagation algorithm to adjust the effective weights in the previously mentioned neural network. To recognize retinal blood vessels, a multilayer perceptron neural network is utilized. Gabor and moment invariants-based features provide input. He also saw exudates in the retinal picture. Yogesh et al. [178] developed a bi-orthogonal wavelet filter for blood vessel extraction. The statistical properties are computed, and the results reveal that the accuracy is 0.9516 and the sensitivity is 0.9567. Numerous research have used the vessel-tracking technique using line tracking and particle filters, respectively [179, 180]. Badsha et al. [181] offered Kirsch's technique for edge improvement, object classification, and morphology-based strategies for obtaining retinal images. Akram et al. [182] employed the 2D Gabor wavelet approach and

stacked thresholding. Using the 2D Gabor wavelet, the image's noise is decreased and its structures are enhanced. In the multilayered thresholding technique, several thresholds are used to monitor the vessel's edges and their connection. The performance measures' accuracy, as measured using publicly available datasets such as DRIVE and STARE, was 94.69% and 95.02%, respectively.

2.7 Detection of Microaneurysm

Early non-proliferative diabetic retinopathy, the first stage of DR, is distinguished by dark lesions in the retina such as microaneurysms and haemorrhages. Early diagnosis of these illnesses may aid in rehabilitation and the avoidance of visual loss. Several research efforts have been conducted to automate the examination of retinal abnormalities and the diagnosis of MA and HA. The discovery of microaneurysms, which are typically smaller than the major optic veins, is crucial in determining the severity of DR. It appears as a little circular area that forms when two thin blood vessels intersect. The circular specks are very small in both size and shape. The most common ways for seeing the clear picture of MAs are shade correction, filtering, or noise reduction. The green channel is most often utilised for segmentation. When the blood vessel walls weaken and bulge, this is the first sign of DR. On the retinal surface, tiny, spherical red spots with diameters smaller than 125 m may be detected. These dots may be observed alone or in groups. Sopharak et al. [183] developed a technique for identifying MAs in retinal images using morphological operators. Preprocessing is done using mathematical morphology, and the blood vessels are extracted using a shade correction approach. For MA identification, local thresholding approaches and the extended minima transform are applied. The statistical report has a sensitivity of 81.66% and a specificity of 99.99%. A decision support system based on the location and number of MAs and HA was implemented to aid in the diagnosis of DR. Saleh and Easwaran [184] employed morphological transformation approaches for segmentation. The top-hat and bottom-hat are utilized in contrast enhancement procedures. To detect dark lesions, multilayer thresholding and the H-maxima transform are used. MAs were discovered to have sensitivity and specificity of 84.31% and 93.63%, respectively, in this investigation. It detects HAs similarly, with sensitivity and specificity of 87.53% and 95.08%, respectively. Zhang et al. [185] developed the Multiscale Correlation

Filtering (MSCF) and dynamic thresholding approach for the effective detection and localization of MAs. It utilises two approaches, employing fine level detection to classify true MAs and coarse level detection to collect MAs. MAs were recognised at the coarse level by calculating the correlation coefficient, using a sliding neighbourhood filter, and employing a multiscale Gaussian kernel. MAs are classified finely based on features such as shape, colour, grayscale intensity, Gaussian filter output, and correlation coefficient values. Tavakoli et al. [186] extracted MAs using a fluorescein angiogram (FA) on a radon transform and numerous overlapping windows. The sensitivity and specificity are 94% and 75%, respectively. Tavakoli et al. [186] employed a cutting-edge approach for identifying lesions to diagnose the DR disease. The optic nerve's head was first recognised and covered. The preprocessed image was divided into sub-images, and each sub-image was subjected to the radon transform. By segmenting the blood vessels and the optic nerve head, MAs may be detected using the proper thresholding and radon transform. Lazar and Hajdu [187] proposed a strategy for identifying microaneurysms using directed cross section profiles by using the local maxima pixels of the preprocessed image. In each profile, peak detection is employed, and peak parameters such as size, height, and shape are determined. To exclude phoney possibilities, naive Bayes classification is used. Reduced false positive rates result in higher sensitivity. Dupas et al. [188] devised a diameter-closing approach for finding microaneurysms using k-nearest neighbours (kNN). Antal and Hajdu [189] investigated how to improve MA recognition using contextual data and an adaptive weighting approach. An ensemble-based technique assigns weights to the lesions of the ensemble members based on their contrast and geographical location. Pereira et al. [190] provide a multi-agent system paradigm for MA identification. It progresses from the pre-processing step to the environment construction stage. Niemeijer et al. [191] developed a technique to identify microaneurysms using a vascular segmentation approach. A pixel classification method is used to create the vessel map and identify its structure. Adal et al. [192] developed a scale-invariant interest-point or blob detection theory to detect possible microaneurysms.

2.8 Detection of Haemorrhages

Blot haemorrhages are circular haemorrhages that occur in the inner layer of the retina as a result of blood seeping from the retinal blood vessels. In certain cases, blood vessels may widen and leak blood or fluid, while in others, abnormal new blood vessels may sprout on the surface of the retina. Blood vessels that are swollen or abnormally or newly produced blood vessels that leak blood may cause haemorrhages. Haemorrhages and microaneurysms are referred to as red lesions in medicine. Grisan et al. [193] use a simple local thresholding strategy to find hemorrhagic lesions in retinal pictures. Pixel values are evaluated using the cluster's spatial density.

2.9 Detection of Exudates

Exudates are small, bright spots that form when the retinal blood vessels haemorrhage proteins, lipids, and water. Exudates are classified into two types: soft and hard. The initial stage of exudates is hard exudates, which appear as intermittent yellow colour patches of varying sizes, shapes, and placements. The soft exudates, which often resemble cotton wool, are the most severe stage of exudates. These types of exudates are responsible for the bulk of vision loss in NPDR. Both hard and soft exudates are referred to as bright lesions.

Harangi and Hajdu [194] use an automated technique for identifying exudates in digital fundus images. It is performed by using a grayscale morphology-based approach to detect any exudates evident in the fundus image. Following the contour detection, non-exudate lesions were excluded using a region-wise classifier. This task is completed using the Naive Bayes classifier and region-based characteristics. Karegowda et al. [195] proposed decision trees and Genetic Algorithm-Correlation-based Feature Selection (GA-CFS) techniques to detect and extract exudates from retinal fundus images. A back propagation neural network classifier is utilised to classify the exudates. Mookiah et al. [196, 197] employ colour, shape, and morphological traits to identify exudates. The optic disc was excised and deleted using the Intuitionistic Fuzzy Histon (A-IFSH) method. Li and Chutatape [198] present integrated region growth and edge detection techniques to identify exudates. A clever edge detector is employed to detect exudates on each of the 64 sub-images that comprise the retinal fundus image, and a

Personal Component Analysis classifier is used to detect OD. Sinthanayothin et al. [199] employed recursive area expanding segmentation to detect exudates, with sensitivity and specificity of 88.5% and 99.7%, respectively. Osareh et al. [200] employ fuzzy C-Means clustering to detect exudates in retinal fundus images. Exudates are separated based on global and local thresholding criteria. A neural network classifier is used to identify the fundus image's attributes such as colour, size, edge strength, and texture. To rank the traits and identify the subset, a genetically based technique is used. Its sensitivity and specificity are 93.5% and 94.6%, respectively. The training technique requires more computational effort, which decreases the training velocity. Sanchez et al. [201] use combination models to dynamically threshold the images and isolate the exudates from the background of the retinal image. A post-processing approach was employed to differentiate between hard exudates, cotton wool patches, and other artifacts. The result was obtained using a database of eighty retinal images. Agurto et al. [202] demonstrate high computational complexity. His method employs the most sophisticated DR frequency and amplitude features. Ali et al. [203] developed a statistical atlas-based approach for identifying the presence of exudates. Based on mathematical morphology, Welfer et al. [204] developed a superior approach for recognizing exudates in colored fundus images. It achieves 70.48% sensitivity and 98.84% specificity using DIARETDB1 as the performance measure. Fathi and Naghsh-Nilchi [205] demonstrated the multi-scale vessel augmentation approach using a sophisticated continuous wavelet transform. To extract thick and thin vessels, low-resolution and high-resolution sub-bands are employed, respectively. The diameter of the vessels is calculated by acquiring the circular structure vessel diameter. Giancardo et al. [206] developed a unique approach for diagnosing diabetic macular edema (DME) that combines automated lesion segmentation, wavelet decomposition, and color features. A classifier based on these criteria was constructed to identify DME with exudates. The performance metric is generated using 164 photographs from the publicly available dataset. The detection of exudates in retinal images was accomplished using a novel approach termed adaptive thresholding developed by Jaafar et al. [207]. Using mathematical morphology, the adaptive thresholding outcomes based on the coarse segmentation findings are clarified. Harangi et al. [208] developed an automated method for detecting exudates. Exudates in the retinal fundus image were discovered

utilising an active contour-based method and grayscale morphology. Filter banks are employed to separate exudate-producing locations, and a Bayesian classifier is utilised to distinguish between exudate- and non-exudate-producing regions, according to Akram et al. [209]. Reza et al. [210] provide a unique method for detecting exudates and the optic disc. The region is segmented using a marker-controlled watershed segmentation method, and the resultant image is improved via average filtering and contrast correction methods.

2.10 Segmentation of OD

The identification and extraction of the optic disc is the most important job in automated retinal screening. The optic disc is initially discovered to identify it from the other spectacular lesions. As a result, OD extraction is critical for the development of an automated retinal grading system. On the basis of active contour modeling and back propagation and the Fuzzy C-Means (FCM) algorithm, Muramatsu et al. [211] developed a feed-forward neural network for OD detection. In order to determine the boundary of the optical disc, a perceptive edge detector is employed. Aquino et al. [212] and Yu et al. [213] developed a template-based approach for the purpose of segmenting OD from retinal fundus images. An algorithm of the voting kind is used to find the OD. The borders of the OD, red, and green channels are established using morphological and edge detection algorithms. For OD boundary estimation, the circular Hough transform is implemented. Ellipsoidal disc images are less successful. In order to detect OD, Kavitha and Ramakrishnan [214] developed the Ant Colony Optimisation (ACO) technique for edge recognition of retinal images. Morphological methods may be used to identify OD. Li and Chutatape [215] improved their identification technique by utilising an active shape model based on PCA to identify the form of the OD. Youssif et al. [216] employ a two-dimensional Gaussian matching filter to generate a direction map of the segmented retinal arteries. The vessel direction and the difference in matching filter output are both monitored. The smallest difference is utilised to calculate OD's coordinates. The watershed transform (Walter & Klein [217]; Hajer et al. [219]) and the Hough transform (Zhu & Rangayyan [218]) were used to determine the OD borders and centre. The vessels in the OD area are removed, and contours are

found using the watershed transform. The watersnake transform, a mix of active contours and the watershed transform, was utilised by Hajer et al. [219].

2.11 Vessel Segmentation of Retinal Images

Vessel segmentation plays a pivotal role in the accurate analysis of retinal images, aiding in the identification and characterization of blood vessels within the intricate network of the retina. Several distinct characteristics contribute to the uniqueness of retinal vessels, encompassing their distinct dark red color, inherent contrast against the retinal background, and the discernible gradient exhibited along the contours of these vessels. The representation of these vessels through piecewise linear functions provides an effective framework, with their cross-sectional intensities resembling the bell-shaped Gaussian distribution.

Vessel segmentation methodologies have been classified into three primary categories, each guided by distinctive principles: matched filtering, mathematical morphology, and vessel tracking. The foundational utilization of the Gaussian filter for blood vessel segmentation was initially introduced by Chaudhuri et al. [220]. In addition to exploiting the piecewise linear nature of vessels, the application of a two-dimensional Gaussian filter was aptly employed. This filter's dimensions were tailored to encapsulate a distance that aligns with the anticipated transition to vessel linearity. Convolving the retinal image with this filter, oriented to accommodate vessels at various orientations, resulted in an enhanced depiction known as the Matched Filter Response (MFR). Subsequent steps involved binary vessel mapping through a global threshold, although it's important to acknowledge that the matched filtering method responds not only to vessel edges but also to other edge types.

Li et al. [221] proposed a segmentation method that enhances accuracy by combining a multiscale matching filter with a dual-threshold algorithm. Aguirre-Ramos et al. [222] introduced an enhancement through the integration of the Gabor filter and Gaussian distribution derivatives, refining both vessel structure and profile. A matched filtering technique centered on the Gumbel probability distribution function was advocated by Singh and Srivastava [223], aimed at augmenting retinal vascular segmentation.

Despite the strengths of these approaches, methods relying on windows require pixel-level processing, leading to substantial computational demands and prolonged segmentation durations. Mendonca's variance in distance Gaussian filter [224] facilitated the extraction of vessel centerlines, while the utilization of morphological operators and iterative region-growing advanced the segmentation process.

In a distinct vein, Cree [225] adopted a two-dimensional Gaussian model for vessel tracking, yielding precise measurements of vessel width and orientation through a nonlinear least squares approach. Frangi et al. [226] introduced the Hessian matrix for extracting directional features from images, while Fathi and Naghsh-Nilchi [227] presented a continuous wavelet transform-based multiscale vessel segmentation method. Notably, Ghoshal et al. [228] proposed a comprehensive strategy integrating both vascular area and axial ratio considerations to enhance the detection of smaller blood vessels.

These diverse methods collectively underscore the dynamic landscape of vessel segmentation techniques, showcasing the multifaceted approaches employed to unravel the complex intricacies of retinal vasculature in pursuit of accurate Diabetic Retinopathy detection and classification.

2.12 Image Feature Analysis

Image feature extraction is a fundamental process that involves the transformation of pixel information into a structured feature space. This crucial step enables efficient image retrieval, navigation, and indexing within databases by encapsulating essential attributes derived from the visual content. The extraction of texture attributes from images encompasses a diverse array of methodologies, including statistical, structural, and spectral techniques.

Statistical methods play a pivotal role in characterizing texture descriptors by analyzing the statistical properties of the distribution of grey levels across spatial domains. Given the intricate and diverse nature of retinal structures, statistical texture analysis emerges as a suitable approach. A notable technique in this realm is the Grey Level Co-occurrence Matrix (GLCM), also referred to as the spatial grey level dependence matrix (SGLDM). Rooted in second-order statistics, the GLCM focuses on the analysis of

pixel pairs positioned within defined spatial relationships. This matrix effectively quantifies the frequency with which specific permutations of pixel intensity values occur within a given area, direction, and separation distance, surpassing the limitations of first-order measures that merely rely on gray level intensity histograms.

Another significant texture descriptor is the Local Binary Pattern (LBP), which adeptly captures local image primitives such as edges, flat regions, and spots. LBP translates these primitives into a comprehensive feature histogram, showcasing resilience against image rotation and brightness variations. The foundation of LBP lies in the analysis of grey level relationships within localized neighborhoods, ultimately resulting in the generation of binary codes.

Researchers such as Sandra Morales et al. [229] have probed the potential of LBP as a texture descriptor for retinal images, conducting comparisons with other techniques like matched filtering and local phase quantization. Additionally, Dhiravidachelvi et al. [230] harnessed statistical characteristics like the Grey Level Co-occurrence Matrix (GLCM) to extract features that were subsequently employed by classifiers to accurately identify microaneurysms.

Structural methodologies delve into the decomposition of textures into fundamental constituents, often referred to as primitives or texels. These primitives are defined by shapes and their spatial configurations, forming the basis for defining and identifying repeated textural elements. The core objective of structural approaches lies in discerning these textural primitives and establishing rules governing their arrangement. These methods prove particularly effective for regular textures characterized by repetitive patterns.

Images may be expressed in other spaces (such as the frequency space or the scale space) using transform techniques, whose coordinate system has an expression that is tightly tied to texture properties. One method for extracting texture information from digital photos is outlined by Filter Banks Law, which employs relatively basic filters. This technique is divided into two steps. First, twenty-five masks with dimensions of three by three or five by five are created by combinatorially converging a number of one-dimensional arrays. Following that, a texture field is convolved with the latter,

highlighting the object's microstructure. This produces an image from which the energy of the microstructure, as well as its other properties, may be measured. One of Law's measures' flaws is that they are not rotationally invariant. Veiga et al. [231] exploited textural properties of laws to identify MA.

Transform methods, including Fourier transform-based techniques, further contribute to texture analysis by decomposing images into harmonic constituents. These methods leverage the observation that spatial edges manifest low frequencies in specific directions and higher frequencies in orthogonal orientations. The Fourier transform facilitates the representation of images as collections of sinusoids, each characterized by its frequency. Although valuable, the Fourier transform encounters challenges in explaining local texture fluctuations. To address this limitation, techniques like Gabor decomposition and wavelets have been introduced.

Notably, Agurto [232] introduced a multiscale amplitude modulation frequency modulation (AM-FM) approach for characterizing retinal structures. This method involves analyzing microaneurysms, hemorrhages, exudates, and more across various frequency scales using a filter bank. Gabor filtering is another compelling technique, employing Gaussian kernel functions modified by plane waves. While effective, Gabor filters may produce duplicated features due to their non-orthogonal nature. Vijayan et al. [233] harnessed Gabor Filters for DR classification, extracting 60 characteristics from retinal images.

Vocabulary learning comprises recognising patterns in data by grouping local descriptors in the feature space. K-means or Gaussian mixture models may be utilised for this. The clusters' centres serve as representations for words in a visual dictionary. As a consequence, visual patterns may be thought of as words; the dictionary has examples of numerous patterns. A string of words with the same meaning that were grouped together inside the property extent may be used to detect a recurring pattern or texton. Dictionary learning includes key-point exposure, local descriptor elicitation, dictionary clustering (using techniques such as K-means), and image pooling (using methods such as occurrence count histogram). Clustering image descriptors yields the codebook (the specified dictionary). The vector of locally aggregated descriptors (VLAD), the extended Fisher vector, and the Fisher vector may all be used for feature

encoding. Multifeature fusion dictionary learning is a novel technique for MA identification that was proposed by Wei Zhou et al. [234]. The foundation of the recommended approach for automatic MA recognition is a framework that combines dictionary learning with multifeature learning advantages. Those who proposed Discriminative Dictionary Learning (DDL) are Malihe Javidi et al. [235]. This process has two main goals: the first is to correctly place veins; the second is to detect MA. The Convolutional Neural Network (CNN) paradigm is a popular supervised learning approach due to its superior feature representation capabilities. CNNs are made up of a number of locally linked layers, including convolutional layers. Convolutional layers in a processing algorithm use kernels with a limited range to process the whole input picture. Because of their hierarchical structure, deep learning models may automatically learn high-level attributes from the original image. CNN performance, on the other hand, is affected by how much of the training sample is annotated. Many different CNN models were utilised for feature extraction.

2.13 Detection Techniques for Microaneurysms

Microaneurysms (MAs) serve as the initial indicators of Diabetic Retinopathy (DR), underscoring the importance of their timely detection to identify the disease at its nascent phase [236]. Vascular dilation within minuscule blood vessels stands as a primary cause of MAs in Non-Proliferative Diabetic Retinopathy (NPDR) [237]. The approaches used to identify MAs may be generally divided into two groups: those based on more modern Deep Learning (DL) techniques and those based on conventional Machine Learning (ML) techniques [238]. In the pursuit of robust MAs detection, various approaches leveraging ML techniques have been devised. These methods harness the power of well-established classification algorithms to discern the presence of MAs within retinal images. By capitalizing on features extracted from the images, ML-based classifiers are trained to distinguish between healthy retinal structures and those afflicted by microaneurysms.

Conversely, the emergence of DL has ushered in a transformative era for MAs detection. Deep Learning techniques, particularly Convolutional Neural Networks (CNNs), have garnered attention for their ability to automatically learn intricate features from raw data [239]. These networks, characterized by their multilayered architecture

and convolutional layers, exhibit exceptional capabilities in recognizing and localizing MAs within retinal images.

The choice between ML and DL-based techniques for MAs detection hinges on various factors, including the availability of annotated data, computational resources, and the desired level of accuracy. These approaches have the potential to improve the precision and effectiveness of MAs detection, which will aid in the early identification of diabetic retinopathy [240].

2.13.1 Microaneurysms Detection via Machine Learning Approaches

A new method for the identification of Microaneurysms (MAs) is presented by Derwin et al. [241] via the introduction of a unique characteristic known as the Local Neighborhood Differential Coherence Pattern (LNDCP). This method reduces the possibility of False Positives (FPs) from blood vessels and background noise by extracting certain MA characteristics using the singular value decomposition-based LNDCP. The coherence of pixel intensity variations among spatially connected areas in retinal fundus pictures is exploited by the LNDCP approach. Image Pre-processing, Segmentation, Candidate Extraction, Feature Extraction, and Classification are the steps that make up the proposed approach. To separate the optic disc during the Segmentation stage, the Circular Hough Transform (CHT) is used. Following this, morphological methods are used to separate putative MAs, so improving their visibility. The LNDCP, which includes a coherence pattern, is used to extract features, and an ANN classifier is used to differentiate between microaneurysms and non-microaneurysms.

In order to accomplish early DR identification, Long et al. [242] presented a system for MAs detection that makes use of local contrast directions (DLC). A number of machine learning techniques were looked at, including K-Nearest Neighbors (KNN), Support Vector Machine (SVM), and Naive Bayesian. The initial phase of the process involves the enhancement and categorization of blood vessels using an advanced enhancement function based on Hessian matrix eigenvalues. Shape features and linked component analysis are subsequently employed to isolate potential microaneurysm locations outside the blood vessel network. Through the segmentation of the image into patches,

relevant properties of each microaneurysm candidate patch are extracted. These properties serve as the basis for labeling the patches as microaneurysms or non-microaneurysms, facilitating effective differentiation through the employed machine learning algorithms.

Dharani et al. [243] and Joshi et al. [244] propose mathematical morphology-based techniques for detecting microaneurysms in retinal fundus images. Computer-Aided Detection (CAD) methods, as suggested by Dharani et al. [243], involve two distinct phases: coarse segmentation to identify potential MAs, and fine segmentation to eliminate false positives. Candidate MAs are segmented using the bottom hat transform, thresholding, and the hit or miss transformation. Enhanced morphological contrast and multiple structuring elements within the hit or miss transform are then employed to enhance the detection accuracy of MAs. Joshi et al. [244] present a three-part approach: morphological processing for image enhancement, extraction, and removal of red structures, and identification and analysis of bright artifacts. They introduce the novel concept of the "MA factor", an area-based feature designed to characterize the structure of microaneurysms.

Colomer et al. [245] propose a method that eliminates the need for prior segmentation or potential map generation. Their approach involves generating local binary patterns and granulometric profiles at each pixel, providing information about the texture and morphology of retinal images. Various permutations of this data are then input into classification algorithms, such as random forests (RF), support vector machines (SVM), and Gaussian processes for classification (GPCs), to achieve accurate discrimination between lesions and healthy tissue. The proposed technique is validated using publicly available fundus databases, including eophtha and DIARETDB1.

A patch-based approach is presented by Wen Cao et al. [246] for MA classification with feature reduction. Raw patches of 25 by 25 pixels are created, and features are extracted from them. Principal Component Analysis (PCA) and the random forest feature importance method are employed to reduce the dimensionality of the features. The reduced features are then fed into Random Forest (RF), Neural Network (NN), and Support Vector Machine (SVM) classifiers.

Melo et al. [247] introduce an innovative method for MA identification, involving the use of sliding band filters (SBF) to enhance microaneurysms before appropriate feature selection. Local gradient convergence filters prove robust against varying lighting conditions, background noise, and poor contrast. The proposed method combines filter responses with intensity, contrast, and shape-based information, achieving improved differentiation between genuine and spurious microaneurysms. Classification is performed using the RUSBoost classifier, and the technique is validated using Receiver Operating Characteristic (ROC) analysis and the e-ophtha dataset.

An inventive method for detecting MA is presented by Jingyu Du et al. [248]. It functions without relying on the division of blood vessels and optic discs. To find MA candidates, they use block filtering and Local Minimum Region (LMR) extraction in their methodology. Block filtering, based on intensity differences and directed gradient histogram analysis, helps remove non-MAs, while LMR extraction efficiently captures most true MAs. Then, utilizing edge detection, saliency analysis of the surrounding area, local cross-section transformation, intensity and boundary analysis, and edge detection, various properties of each candidate are generated. To finish the MA identification, a classification method based on undersampling and boosting (RUSBoost) is used.

Veiga et al. [249] present a two-step classification method for categorizing MAs based on texture masks. The concept is to utilize texture, specifically Laws texture masks, to characterize pixels belonging to MAs. The first stage involves candidate detection using Laws texture energy features and an SVM classifier. To mitigate false positives, the second stage extracts additional characteristics from each candidate identified in the first stage. The second SVM performs conventional object classification, combining texture-based features with context-based attributes such as intensity and shape.

Deepa et al. [250] propose a method for classifying DR at the image level by leveraging the characteristics of MAs. They utilize the discrete orthonormal Stockwell transform (DOST) for spatial frequency representation, akin to the discrete wavelet transform, along with statistical measures from the GLCM. These features are then fed into various classifiers, with the Artificial Neural Network (ANN) classifier demonstrating superior performance.

Selcuk et al. [251] suggest a microaneurysm segmentation and classification method using an evolutionary algorithm. They employ Frangi filters for vascular anatomy recovery from color fundus images, followed by the successful application of an ant colony algorithm for microaneurysm segmentation. Performance evaluation is conducted using Dice and Jaccard similarity index values, with datasets such as Messidor and Diaretdb1.

Pundikal et al. [252] present a two-level approach involving blood vessel segmentation prediction prior to MA categorization. Hessian filter-based blood vessel segmentation is initially performed, followed by the use of the Grey Wolf Optimizer (GWO) to predict segmented microaneurysm areas' accuracy. Shape and GLCM features are then utilized to extract attribute vectors from MA regions, and the Modified MKNN classifier is employed to categorize both MA and non-MA regions. Their work is validated using datasets like e-ophtha and DIARETDB1.

Kumar et al. [253] propose improved methods for detecting microaneurysms and hemorrhages, contributing to the early analysis of DR. Their approach involves preprocessing and blood vessel identification through mathematical morphological techniques. Optical disc segmentation is accomplished using the watershed transform, and a radial basis function Neural Network (NN) is utilized for disorder classification.

2.13.2 Microaneurysms Detection using Deep Learning Techniques

Eftekhari et al. [254] present a comprehensive approach employing a two-stage Convolutional Neural Network (CNN) for rapid and automated microaneurysm detection in images. The process involves initial pre-processing, followed by a probability map generation using the first CNN, referred to as the base CNN. Subsequently, the final CNN assigns a MA or non-MA classification to each pixel in test images, utilizing the probability map from the previous stage to select example inputs. The final result is a smoothed probability map over all images indicating the likelihood of each pixel being a MA or non-MA. The basic CNN model consists of 10 layers, while the final CNN model includes 13 layers. Their approach is evaluated on widely-used datasets, including the Retinopathy Online Challenge dataset and the E-Ophtha-MA dataset.

For MA identification, Shan et al. [255] introduce a stacked Sparse Autoencoder (SSAE), a type of deep learning technique. Their method involves generating smaller image patches from original fundus photos. The SSAE is trained to learn high-level features based solely on pixel intensities, aiming to capture distinctive MA characteristics. These high-level features are then fed into a softmax classifier, which categorizes each image patch as either containing a MA or being non-MA.

Xinpeng Zhang et al. [256] propose a feature-transfer network based on a single Sparse Autoencoder (SAE) for abundant feature extraction in MA detection. They apply a feature-distance-based approach during preprocessing to suppress local background noise. The feature-transfer mechanism involves transferring ideal weights and biases from each training process to the next, iteratively refining the network until an optimal configuration is achieved. This approach aims to enhance the feature extraction process for effective MA identification.

Piotr Chudzik [257] developed a fully convolutional neural network (FCNN) architecture integrated with Batch Normalization (BN) layers and a Dice coefficient loss function for segmenting and detecting microaneurysms (MAs). The approach encompasses three main steps: pre-processing, patch extraction, and pixel-wise categorization. Patches are classified as MA patches (containing at least 1 MA pixel) or non-MA patches (lacking MA pixels). The architecture follows a similar structure to a convolutional autoencoder for training purposes.

Deepa R [258] introduced a CNN architecture with 10 layers for MA detection. The preprocessing phase involves scaling images from the database, followed by automated feature extraction using a basic CNN. Through training, the CNN learns to differentiate between diseased and healthy images.

Kou et al. [259] proposed a hybrid architecture, DRU-Net, for MA segmentation by combining a deep residual model and a recurrent residual convolutional neural network (RRCNN). The architecture extends the U-Net by substituting conventional convolutional layers with RRCNN blocks. DRU-Net comprises seven RRCNN blocks and two basic blocks, with experiments conducted using Keras and Tensor Flow in

Python 2.7 on a single GPU computer. Patches of size 48x48 were utilized for training, and the E-Ophtha and IDRiD datasets were employed.

For MA detection, Qomariah et al. [260] developed MResUNet, a modified U-net design. Convolutional layers and batch normalization are used in conjunction with a modified identity mapping to improve features and mitigate feature deterioration as the network becomes deeper. During training, a mean weighted loss function is used to take into consideration the difference in pixels between MAs and the background. The datasets for architectural analysis were DiaretDB1 and IDRID.

Zhang et al. [261] introduced a novel deep learning architecture for MA detection utilizing a multilayer attention mechanism. The architecture involves image quality enhancement through equalization procedures, followed by the fusion of multiple feature layers based on an attention process. This approach exploits spatial associations between MAs and blood vessels for secondary screening of preliminary results, ultimately achieving accurate MA detection. The architecture includes a basic feature extraction network, layer-wise feature fusion, and channel-wise feature fusion.

To identify microaneurysms (MAs), a deep convolutional encoder-decoder network is constructed in [262]. Rather than using traditional skip concatenation, the network concentrates on taking use of the peculiarities found in skip connections. The network enhances MA-related information that would have been lost during the encoder process by using skip layer differences. A longer-tail sigmoid activation function is used to improve the probability map's ability to discriminate. Training and testing of the model are carried out on a server that has four NVIDIA Tesla P40 24G GPUs, an Intel Xeon Gold 6152 CPU, and 256GB of RAM. The ROC dataset and the e-ophtha-MA dataset, two publicly accessible datasets, are used for the experiments.

Another innovative approach for MAs and hemorrhages (HEs) identification associated with diabetic retinopathy (DR) is introduced in [263]. This method is built around a deep symmetric convolutional neural network composed of three main stages: preprocessing, feature filtering and extraction, and classification. The preprocessing stage involves selecting the center of MAs and HEs in the fundus image for 27x27 sampling. The deep symmetric convolutional structure is employed to provide greater

depth and breadth to the network, addressing potential overfitting and compensating for imbalances between positive and negative samples. The categorization system operates on patches. In the exploration of existing literature, a comprehensive analysis of relevant studies and methodologies has been conducted. Table 2.1 provides a structured overview of key parameters extracted from pertinent research papers in the field of diabetic retinopathy detection and classification. The table encompasses critical details such as the title of the paper, the dataset employed, the class of diabetic retinopathy considered, unique insights offered by each study, reported accuracy, and the corresponding references. This compilation serves as a valuable resource for synthesizing the current landscape of research efforts, highlighting trends, and discerning gaps that propel the focus of this thesis.

Table 2.1: Key Parameters of Selected Diabetic Retinopathy Studies

S.No.	Title of the paper	Dataset used	Class	Insight	Accuracy	Ref.
1.	"Diabetic Retinopathy Grading Base on Contrastive Learning and Semi-supervised Learning"	Datasets employed include EyePACS, Messidior, IDRiD, and FGADR datasets.	Binary and multiclass classification.	A new strategy based on contrastive learning and semi-supervised learning was proposed. To train the lesion segmentation model, a tiny quantity of open-source pixel-level annotation information was used.	Results are superior to earlier approaches.	[264]
2.	"Fusing dual-tree quaternion wavelet transform and local mesh based features for grading of diabetic retinopathy using extreme learning machine classifier"		Multiclass	A comprehensive micro-macro feature extraction approach for DR grading - A feature extraction algorithm based on the fusion of dual-tree	The best classification accuracy obtained is 93.2%. The suggested approach has a high level of accuracy and sensitivity.	[265]

				quaternion wavelet transform with local mesh patterns.		
3.	"Encoding Retina Image to Words using Ensemble of Vision Transformers for Diabetic Retinopathy Grading"	Testing a public DR dataset from the 2015 Kaggle competition. Data that is very unbalanced, with five severity levels: No DR, Mild, Moderate, Severe, and Proliferative DR.	Multiclass classification - Five levels of severity: No DR, Mild, Moderate, Severe, and Proliferative DR.	Based on an ensemble of vision transformers, the proposed technique outperforms previous methods in DR grading.	Precision: 47% Recall: 45%	[266]
4.	"DR|GRADUATE: Uncertainty-aware deep learning-based diabetic retinopathy grading in eye fundus images"	Kaggle DR detection training set. Multiple datasets were evaluated.	Binary classification	DR|GRADUATE is a proposed deep learning-based DR grading CAD system. Explanation and prediction uncertainty are medically interpretable.	Achieved quadratic-weighted Cohen's kappa (κ) between 0.71 and 0.84 in five different datasets. High κ values occur for images with low prediction uncertainty, indicating high accuracy.	[267]
5.	"Few-shot Learning Based on Multi-stage Transfer and Class-Balanced Loss for Diabetic Retinopathy Grading"	Multiple datasets with different scales were used. The specific datasets used	Multiclass	Multi-stage transfer learning is introduced for DR grading, and a class-balanced loss function is suggested for DR	Accuracy is increased by class-balanced loss and multi-stage transfer. The best possible result on the DR grading was obtained.	[268]

		are not mentioned.		datasets that are unbalanced.		
6.	"Diabetic Retinopathy Grading Based on a Hybrid Deep Learning Model"	Two benchmark datasets were used in the study.	Multiclass classification. Diagnosing different DR grades (normal, mild, moderate, severe, and proliferative DR (PDR))	Achieved great accuracy in identifying various DR grades using the hybrid deep learning model that was proposed for diabetic retinopathy grading.	Average accuracy (ACC) equals 91.6%. The proposed system achieved promising results.	[269]
7.	"Severity Grading and Early Retinopathy Lesion Detection through Hybrid Inception-ResNet Architecture"		Multiclass	Hybrid Inception-ResNet architecture for feature extraction is proposed as a framework for severity grading and early detection.	Suitable outcomes compared to previous approaches.	[270]
8.	"Diabetic Retinopathy Grading Using 3D Multi-path Convolutional Neural Network Based on Fusing Features from OCTA Scans, Demographic, and Clinical Biomarkers"	Dataset of 100 patients used for grading DR.	Binary classification	A computer-aided diagnostic approach for identifying and evaluating diabetic retinopathy is proposed. - A 3D convolutional neural network was created to segment blood vessels and categorize retinal vasculature properties.	Average accuracy of 96.8%. Sensitivity of 98.1% and specificity of 88.8%	[271]
9.	"A Deep Learning Based Approach for Automated Diabetic Retinopathy Detection and Grading"	IDRiD database	Multiclass	Transfer learning and ensemble learning methodologies	Accuracy for DR identification: 99.5%.	[272]

				were used in the proposed strategy for automatic DR identification and grading.	Accuracy for grading of DR: 99.6%	
10.	"Robust Collaborative Learning of Patch-level and Image-level Annotations for Diabetic Retinopathy Grading from Fundus Image"	Datasets of different distributions (label and camera).	Binary classification	Collaborative utilization of patch-level and image-level annotations. Exploitation of more discriminative features for DR grading	Better performance than state-of-the-art algorithms and ophthalmologists.	[273]
11.	"BiRA-Net: Bilinear Attention Net for Diabetic Retinopathy Grading"		Multiclass classification	Proposed BiRA-Net architecture for DR grading. Introduced grading loss function for improved training convergence	Superior performance demonstrated in experimental results.	[274]
12.	"Automated feature-based grading and progression analysis of diabetic retinopathy"	Training dataset: 2251 images with detailed annotations. Public database: 89 retinal images with expert annotations	Binary classification	Well-annotated datasets from diverse global populations Independence from specific grading schemes for adaptability	Overall agreement between DAPHNE and human grading was above 85%. Software did not miss any sight-threatening cases	[275]
13.	"Diabetic retinopathy classification based on multipath CNN and machine learning classifiers"	IDRiD, Kaggle (for DR detection), and MESSIDOR. Publicly available databases used for evaluation.	Binary classification	Automated DR grading using deep learning and ML. M-CNN with J48 classifier achieves best results.	The average accuracy obtained for the proposed work is 99.62% for DR grading.	[276]

14.	"Automated identification and grading system of diabetic retinopathy using deep neural networks"	Dataset included PDR and NPDR images - Data augmentation techniques used to enhance training set	The first task of the system is a binary classification to identify the presence of DR. The second task of the system is a multi-classification to predict the level of DR severity.	Automated DR identification and grading system called DeepDR Exploration of different combination methods for best integration performance	Identification model accuracy: 97.7%. Grading model accuracy: 96.5%	[277]
15.	"Lesion-Aware Transformers for Diabetic Retinopathy Grading"	Messidor-1 dataset Messidor-2 dataset EyePACS dataset	Binary classification	Proposed a lesion-aware transformer (LAT) for DR grading and lesion discovery. Introduced mechanisms for identifying diverse lesion regions.	The proposed LAT performs favorably against state-of-the-art DR grading and lesion discovery methods. Extensive experimental results on three challenging benchmarks demonstrate the effectiveness of the proposed LAT.	[278]
16.	"Coarse-to-fine classification for diabetic retinopathy grading using convolutional neural network"	IDRiD and Kaggle fundus image datasets.	Binary classification: No DR and DR Multiclass classification: mild, moderate, severe NPDR, PDR	Proposed CF-DRNet for automatic DR grading. Improved classification performance of five-class DR grading.	CF-DRNet outperforms some state-of-art methods - Enables efficient and reliable DR grading diagnosis	[279]
17.	"Deep Multi-Task Learning for Diabetic	DDR dataset (Li et al. 2019b).	Multiclass	Proposed a deep multi-task learning method	DeepMT-DR method achieves improved	[280]

	Retinopathy Grading in Fundus Images"	EyePACS dataset (Graham 2015)		for diabetic retinopathy grading in low-resolution fundus images. Developed a task-aware loss to focus on pathological regions.	accuracy for DR grading. DeepMT-DR method performs considerably better than other methods.	
18.	"Diabetic Retinopathy Diagnosis Based on RA-EfficientNet"	APTOS 2019 dataset. ImageNet dataset (for transfer learning)	Binary classification: Diagnose DR or not DR. Multiclass classification: 5 grades of DR diagnosis (No DR, mild DR, moderate DR, severe DR, proliferative DR)	Preprocessing of DR images to address size difference, information redundancy, and data imbalance in the APTOS 2019 dataset. - Proposal of a new network called RA-EfficientNet, which incorporates a residual attention block to extract more features and address small differences between lesions.	Accuracy of 98.36% in 2-grade classification. Accuracy of 93.55% in 5-grade classification	[281]
19.	"A Benchmark for Studying Diabetic Retinopathy: Segmentation, Grading, and Transferability"	FGADR dataset with 2,842 images - 1,842 images with pixel-level DR-related lesion annotations and 1,000 images with image-level labels graded by	The paper does not mention whether the tasks are binary or multiclass.	Construction of a large fine-grained annotated DR dataset. Introduction of benchmark tasks for evaluation and transfer learning method	N/A	[282]

		ophthalmologists				
20.	"Diabetic retinopathy classification using deeply supervised ResNet"	Kaggle dataset used.	Binary classification	Proposed deeply supervised ResNet approach for DR classification. Introduced multi-scale learning and cost sensitive learning	The proposed method outperforms the state-of-the-art method. The accuracy value is not provided in the paper.	[283]
21.	"A Deep Learning Ensemble Approach for Diabetic Retinopathy Detection"	Kaggle dataset used for training and evaluation.	The problem of diabetic retinopathy detection is classified as multiclass. - The proposed model classifies DR into five different stages.	Detecting all stages of Diabetic Retinopathy (DR). Using end-to-end deep ensemble networks for detection	Accuracy is biased towards the negative class. Other parameters like recall, precision, specificity, F1-score, and ROC-curve are used for unbiased results.	[284]
22.	"SE-MIDNet Based on Deep Learning for Diabetic Retinopathy Classification"		Binary classification	Proposed an improved Inception module for efficient feature extraction Used dense connection method for multi-scale feature reuse and enhanced feature representation	Accuracy of DR automatic classification: 88.24%	[285]
23.	"Diabetic Retinopathy Grading System Based on Transfer Learning"	IDRiD dataset used for training. Multi-label dataset used for training	Multi-label classification	Development of a DL CAD system for diagnosing DR Utilization of a customized efficientNet model for diagnosis	Accuracy of the proposed DL CAD system is 86%.	[286]

24.	"An automated grading system for diabetic retinopathy using curvelet transform and hierarchical classification"	Messidor database	The SVM classifier used in the proposed system is a binary classifier. The binary nature of the SVM classifier is expanded using hierarchical classification to create a multi-level classification.	Automated grading system for Diabetic Retinopathy. Classification into four severity levels: normal, mild, moderate, severe	86.23% accuracy achieved by the proposed system.	[287]
25.	"Automatic Diabetic Retinopathy Grading via Self-Knowledge Distillation"	Messidor dataset. IDRID dataset	Binary classification	Proposed a deep-learning technique for grading diabetic retinopathy. Used self-knowledge distillation and CAM-Attention for improved performance	Accuracy of 92.9% for the Messidor dataset. Accuracy of 67.96% for the IDRID dataset.	[288]
26.	"A complete modelling of Local Binary Pattern for detection of diabetic retinopathy"	STARE database used for the dataset.	Binary classification	Proposed detection of DR using texture feature characteristic. Utilized CLBP as feature extraction method	CLBP-SC (CLBP sign and mean value) has an accuracy of 97.16%. CLBP-SM (CLBP sign and magnitude) also has an accuracy of 97.16%.	[289]
27.	"Diabetic Retinopathy Detection using Deep Learning"	- Dataset used: APTOS	Multiclass	Analysis of different DR stages using Deep	Accuracy of DR detection: 0.9611. Quadratic	[290]

		(available on Kaggle)		Learning - Trained model (DenseNet) for automatic DR detection	weighted kappa score: 0.8981	

2.14 Research Problem

The problem addressed in this thesis is the need for an intelligent and accurate system for the early detection and classification of diabetic retinopathy (DR) using retinal images. Diabetic retinopathy is a serious eye disease that affects individuals with diabetes and is a leading cause of vision loss and blindness. Early detection and timely treatment are crucial to prevent the progression of the disease and preserve visual function.

Currently, the diagnosis and grading of diabetic retinopathy often rely on manual examination by ophthalmologists, which can be time-consuming, subjective, and prone to inter-observer variability. Additionally, with the increasing prevalence of diabetes globally, the demand for diabetic retinopathy screenings is rising, posing challenges to healthcare resources and the availability of ophthalmologists.

The research aims to develop an automated system that can accurately detect signs of diabetic retinopathy in retinal images and classify the disease into different stages based on its severity. The model proposed is efficient, scalable, and capable of processing large volumes of retinal images to cater to the growing demand for diabetic retinopathy screenings. The proposed system's accuracy and reliability are critical for minimizing false positives and false negatives, ensuring the appropriate diagnosis and treatment of diabetic retinopathy.

The research problem can be further broken down into the following key components:

1. ***Automated Detection***

   Developing an algorithm that can automatically detect signs of diabetic retinopathy in retinal images is essential to streamline the screening process and ensure early detection. The algorithm should be capable of identifying key features such as microaneurysms, hemorrhages, exudates, and other abnormalities associated with diabetic retinopathy.

2. ***Classification and Grading***

   Once the signs of diabetic retinopathy are detected, the system should be able to accurately classify and grade the severity of the disease. Classifying diabetic retinopathy into different stages, such as mild non-proliferative diabetic retinopathy, moderate non-proliferative diabetic retinopathy, severe non-proliferative diabetic retinopathy, and proliferative diabetic retinopathy, is crucial for guiding appropriate treatment decisions.

3. ***Accuracy and Reliability***

   The developed system should achieve high accuracy and reliability in detecting and classifying diabetic retinopathy. Minimizing false positives and false negatives is essential to avoid unnecessary treatments or overlooking potential cases of diabetic retinopathy.

4. ***Efficiency and Scalability***

   The proposed system should be efficient in processing large volumes of retinal images to cater to the increasing demand for diabetic retinopathy screenings. Scalability is critical to ensure its feasibility in real-world clinical settings and public health programs.

5. ***Validation and Comparison***

   Validating the developed algorithm against existing diagnostic methods and conventional grading systems is essential to establish its effectiveness and superiority. A comparison with manual examination by ophthalmologists will help determine the algorithm's robustness and potential for clinical adoption.

6. ***Generalization and Adaptability***

   The research problem also includes ensuring that the developed system is generalizable and adaptable to different populations and retinal image datasets. Accounting for variations in image quality, patient demographics, and diabetes types will enhance the algorithm's applicability across diverse settings.

Addressing these aspects of the research problem will contribute to the advancement of technology in ophthalmology and healthcare. An accurate, efficient, and automated system for diabetic retinopathy detection and classification can lead to early interventions, better patient outcomes, and reduced burden on healthcare resources. Moreover, it can facilitate broader access to timely diabetic retinopathy screenings,

especially in underserved areas and resource-limited settings, ultimately leading to improved vision health and quality of life for individuals with diabetes.

2.15 Research Gap Identified

Based on the difficulties and challenges noted in over 50 relevant works related to the identification of vessel segmentation, microaneurysms, hemorrhages, and exudates in diabetic retinopathy, the following research gaps and areas of improvement can be identified:

1. **Enhancing Detection of Tiny Lesions**

   There is a need to develop advanced algorithms and image processing techniques that can effectively identify tiny microaneurysms and thin arteries in low contrast retinal images. Improving the sensitivity of the detection process for these small lesions can lead to earlier diagnosis and intervention.

2. **Comprehensive DR Screening Method**

   Existing automatic diabetic retinopathy screening methods often focus solely on vessel identification and may neglect the detection of important features like hemorrhages. There is a scope for the development of integrated screening methods that consider multiple lesion types, thereby providing a more comprehensive and accurate assessment of diabetic retinopathy.

3. **Efficiency and Speed of Algorithms**

   While neural networks and statistical classifiers have shown promise in diabetic retinopathy screening, they can be computationally intensive and time-consuming. There is a need for more efficient algorithms that can achieve high accuracy without compromising on speed, allowing for quicker and more scalable screening processes.

4. **Integration of Lesion Segmentation and Grading**

   Many existing methods for segmenting lesions and grading diabetic retinopathy focus on individual lesions separately. Integrating the segmentation of dark and

bright lesions and developing grading methods that consider all lesions together can improve the sensitivity and precision of the overall diagnostic process.

5. **Access to Diabetic Retinopathy Screening in Rural Regions**

   With the increasing number of diabetic retinopathy patients, specialists may face challenges in delivering timely and effective screenings, particularly in rural and underserved areas. The research should explore ways to improve access to diabetic retinopathy screening through telemedicine, mobile health applications, or other innovative approaches.

2.16 Research Goals and Novelty

The primary research goals of this thesis are to develop effective algorithms for the detection and classification of diabetic retinopathy using retinal images. The specific aims of the study are as follows:

1. ***To develop an algorithm for the detection of Diabetic Retinopathy using the retinal images.***

The first objective of this research involved the successful development of an advanced algorithm for the detection of Diabetic Retinopathy (DR) using retinal images. The algorithm was meticulously designed to analyse retinal images and automatically identify crucial features associated with DR. Leveraging state-of-the-art data augmentation techniques, machine learning, and computer vision algorithms, our approach enabled accurate and early detection of DR.

The application of machine learning algorithms, particularly DR-ResNet, allowed for efficient and accurate classification and identification of different lesions in the retina, facilitating a detailed assessment of DR severity. To ensure optimal performance, the algorithm was trained on a substantial dataset of annotated retinal images, encompassing both normal cases and those affected by DR. During the training process, the algorithm's parameters were fine-tuned and optimized to ensure effective differentiation between healthy retinas and those with various stages of DR. The successful development of this algorithm represents a significant achievement, as it lays the foundation for the creation of a robust and automated DR screening system. This

system can be seamlessly integrated into existing healthcare frameworks, enabling early detection and intervention in DR cases. The algorithm's implementation holds the potential to reduce the risk of vision loss and improve the overall management of Diabetic Retinopathy, thus enhancing the quality of life for individuals affected by this sight-threatening condition.

2. ***To develop an algorithm for the classification and grading of the retinal images for the detection of Diabetic Retinopathy.***

The second objective of this research was to develop a sophisticated algorithm capable of classifying and grading retinal images for the accurate detection of Diabetic Retinopathy (DR). The algorithm was designed to categorize retinal images into different stages of DR severity, providing valuable insights to aid in effective disease management and treatment. To achieve this objective, the algorithm incorporated advanced machine learning methodologies. The algorithm was trained on a diverse dataset of retinal images, comprising varying degrees of DR progression. Through the development of DR-ResNet+ model, the algorithm learned to recognize characteristic features associated with different stages of DR, such as microaneurysms, hemorrhages, exudates, and other abnormalities and reducing the training time. The classification and grading algorithm employed a multi-class approach to categorize retinal images into various DR severity levels, ranging from mild non-proliferative diabetic retinopathy (NPDR) to severe proliferative diabetic retinopathy (PDR). This granular classification enabled the algorithm to provide detailed information on the disease's advancement, allowing for more personalized and targeted treatment strategies. The algorithm's robustness was thoroughly tested using an independent validation dataset to assess its accuracy and reliability in classifying retinal images. Parameters and hyperparameters of the algorithm were fine-tuned to optimize its performance and ensure consistent and precise grading results.

3. ***To optimize the sensitivity, specificity, and accuracy of the proposed Algorithm.***

The third objective of this research was to optimize the performance metrics of the proposed algorithm, specifically focusing on sensitivity, specificity, and accuracy. Sensitivity refers to the algorithm's ability to correctly identify true positive cases of

Diabetic Retinopathy (DR) from the dataset. Specificity, on the other hand, measures the algorithm's capability to correctly identify true negative cases, i.e., healthy retinas, in the dataset. Lastly, accuracy measures the overall correctness of the algorithm's classifications. To achieve this objective, an iterative process was undertaken to fine-tune and optimize the algorithm's parameters and hyperparameters. The algorithm was trained on various subsets of the dataset, and different configurations were tested to assess their impact on sensitivity, specificity, and accuracy.

To increase sensitivity, the algorithm was designed to become more adept at detecting even subtle signs of DR, ensuring that a greater number of true positive cases were identified correctly. Special attention was given to refining the features extracted from retinal images to minimize the risk of false-negative results.

Similarly, efforts were directed towards enhancing specificity by reducing false positive cases. The algorithm was fine-tuned to minimize the chances of misclassifying healthy retinas as having DR, thus increasing the true negative detections.

In addition to sensitivity and specificity, overall accuracy was a crucial focus. The algorithm's performance was measured against the ground truth annotations, and adjustments were made to achieve the highest level of overall accuracy.

The optimization process involved cross-validation and validation on an independent dataset to validate the generalization ability of the algorithm. Continuous evaluation and adjustments were made to achieve the best possible balance between sensitivity, specificity, and accuracy.

By optimizing the sensitivity, specificity, and accuracy of the proposed algorithm, we have significantly enhanced its diagnostic capabilities and reliability. The algorithm's ability to precisely identify DR cases while minimizing false positives and false negatives is pivotal in providing accurate assessments to healthcare professionals. This optimization has reinforced the algorithm's potential as a robust and effective tool for early detection and diagnosis of Diabetic Retinopathy, ultimately contributing to better patient outcomes and vision preservation.

4. ***To validate the proposed algorithms for diabetic retinopathy by comparing the same with the conventional algorithms.***

The fourth objective of this research was to validate the effectiveness and superiority of the proposed algorithms for Diabetic Retinopathy (DR) detection and classification in comparison to conventional algorithms. The validation process aimed to assess the algorithm's performance in real-world scenarios and establish its potential as an improved alternative to existing methods.

To achieve this objective, a comprehensive evaluation was conducted, involving a set of experiments and comparative analyses. The proposed algorithm, developed in previous objectives, was put to the test against a selection of well-established conventional algorithms commonly used for DR detection and grading.

A diverse and representative dataset of retinal images was used to ensure a fair and unbiased comparison. This dataset encompassed a wide range of DR severity levels and included normal retinas as well. Both algorithms, the proposed one and conventional ones, were applied to this dataset under identical conditions.

The performance metrics used for comparison included sensitivity, specificity, accuracy, precision, and recall. Statistical analyses were carried out to ascertain significant differences in the performance of the algorithms.

Additionally, the processing time and computational efficiency of each algorithm were evaluated to gauge their practicality for real-time applications in clinical settings.

The validation process followed a rigorous and systematic methodology to eliminate biases and ensure reliable results. Cross-validation and independent validation were also incorporated to verify the generalization ability of the proposed algorithm.

The results of the validation process were analyzed and presented in a clear and comprehensive manner, allowing for an informed and evidence-based comparison between the proposed algorithm and conventional ones.

By validating the proposed algorithm against conventional methods, we have demonstrated its superiority and potential for enhanced DR detection and classification. The findings of this validation process provide concrete evidence of the algorithm's

effectiveness and pave the way for its adoption as a state-of-the-art tool for DR diagnosis and grading. The validation process has strengthened the credibility of the proposed algorithm, assuring its accuracy and reliability for the benefit of healthcare professionals and patients alike.

2.17 Methodology

This study presents a structured approach for developing, training, and validating an automated model for diabetic retinopathy (DR) detection and grading. The methodology consists of several stages, each designed to ensure robust performance, accuracy, and efficiency in real-world clinical settings.

1. **Dataset Preparation**

The initial stage involves acquiring and pre-processing images from a reputable dataset, which contains labeled fundus images across different DR severity levels. Key steps in this process include:

- **Data Acquisition**: Collection of retinal images from the Kaggle Diabetic Retinopathy dataset.
- **Image Pre-processing**: To enhance model performance, images undergo resizing, normalization, and data augmentation techniques (e.g., rotation, flipping). This process increases dataset diversity and reduces overfitting.
- **Data Splitting**: The dataset is divided into training, validation, and test sets to enable unbiased model evaluation.

2. **Model Architecture**

This study builds upon the conventional ResNet architecture, proposing a custom DR-ResNet+ model tailored to the specific requirements of DR detection and grading. The architecture incorporates skip connections to address the vanishing gradient problem, enabling effective training of deep layers.

- **Baseline Model (ResNet)**: A standard ResNet model serves as a baseline for comparative analysis.

- **Proposed DR-ResNet+ Model**: The DR-ResNet+ model introduces modified layers and additional connections to enhance feature extraction and representation, particularly for subtle DR indicators in retinal images.

3. **Training Procedure**

The model training involves several key hyperparameters and techniques optimized for this problem domain.

- **Loss Function**: Categorical Cross-Entropy is employed to minimize classification error across multiple DR severity levels.
- **Optimizer**: It is utilized for its efficiency in handling sparse gradients in complex neural networks.
- **Hyperparameter Tuning**: Various configurations of learning rates, batch sizes, and dropout rates are evaluated to optimize model performance.

4. **Performance Evaluation**

The trained model's effectiveness is assessed using multiple evaluation metrics to ensure reliability across diverse clinical scenarios.

- **Evaluation Metrics**: Accuracy, sensitivity, specificity, and F1 score are calculated to measure classification performance. The area under the receiver operating characteristic (ROC) curve (AUC) is also analyzed for each severity level.
- **Comparison with Baseline**: The performance of DR-ResNet+ is compared against the baseline ResNet model and other conventional approaches to validate its enhanced capability in DR grading.

5. **Real-World Implementation**

To demonstrate clinical applicability, the model is tested in a simulated real-world environment. This includes assessing inference time and testing the model on additional, unseen images to validate its generalizability and potential for real-time screening applications.

CHAPTER 3

DATASET FOR DIABETIC RETINOPATHY

This chapter delves into the dataset employed for diabetic retinopathy analysis, exploring its origins, characteristics, and significance to the study. The dataset's relevance is established by detailing its specific attributes and limitations, including considerations around data variability and potential biases that may impact results. Additionally, the process of grading diabetic retinopathy severity is outlined, along with standardized benchmarks, to provide a framework for assessing disease stages and enhancing the dataset's value for clinical and research applications.

3.1 Dataset used

The present research uses a dataset of 35,126 retinal fundus images from Kaggle [291]. Two sets of these photographs are created using random selection for training and validation separately. The photos devoid of diabetic retinopathy are kept apart to ensure the dataset's suitability for training and testing. Based on the severity of the condition, diabetic retinopathy (DR) is divided into five types: proliferative DR (grade 4), severe DR (grade 3), severe DR (grade 3), and no DR (grade 0). In the proposed work, the percentage of pictures is kept in the training and validation sets to maintain balance in the distribution of DR classes shown in Figure 3.1 as pie chart showing the percentage of samples per class and Figure 3.2 as visualization of 5 images per class. The number of photographs is divided into five classes namely, no DR, mild DR, moderate DR, severe DR, and proliferative DR. A total of 11,000 images are used in the training dataset. Most of the images are with no DR and moderate DR classes. Most of the images in this dataset are high-resolution, with a color depth of 24-bit RGB, which supports a broad range of color representation. This level of depth and resolution ensures that the images capture fine visual details, making them suitable for accurate retinal analysis. Since the performance of the model on the less prevalent classes of diabetic retinopathy is impacted by the class imbalance in the training dataset, data augmentation strategies are used to increase the number of photographs. Therefore, class weight is introduced during training.

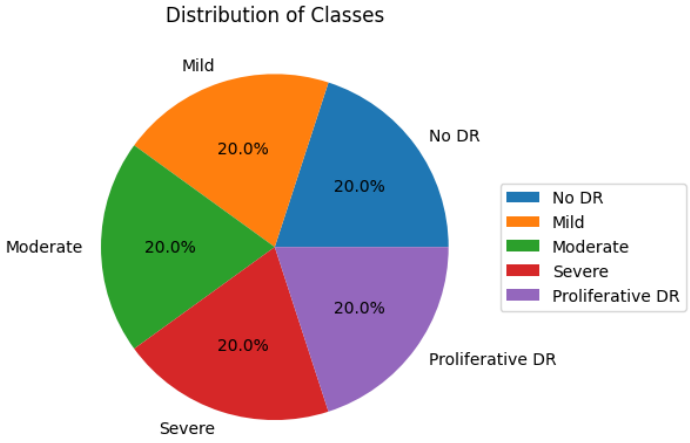

Figure 3.1: Pie chart showing the percentage of samples per class

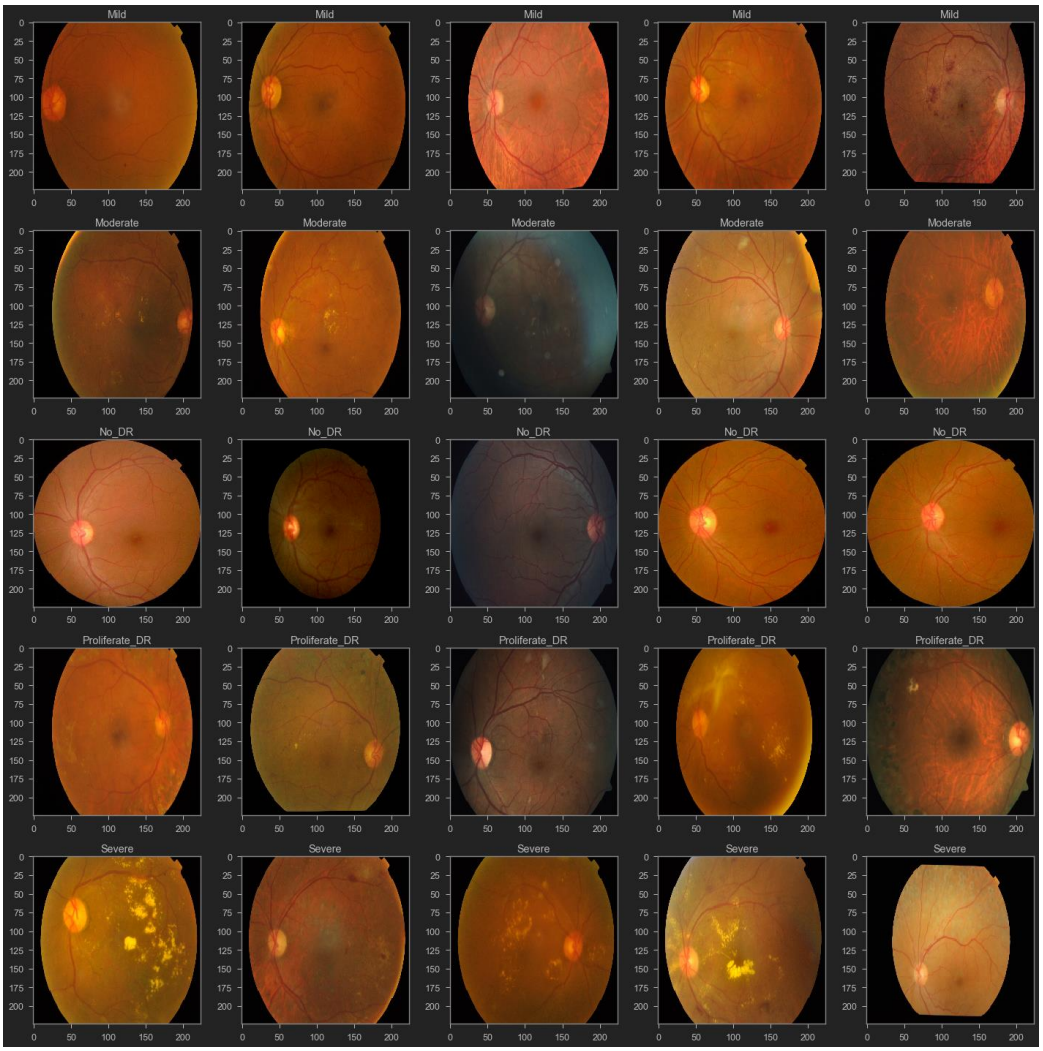

Figure 3.2: Visualization of 5 images per class

3.2 Dataset Limitations

The dataset utilized in this investigation exhibits certain limitations that need to be acknowledged. Such as

i. ***Lack of Severity Categorization***

The lack of a clear categorization of diabetic retinopathy (DR) pictures into distinct groups based on the severity levels of the disease is a significant shortcoming of the dataset utilized in this investigation. The Kaggle dataset does not contain specific folders for labels identifying the degree of DR severity for each image. Instead, details regarding the categories to which each photograph belonged were included in an attached Excel file. This constraint makes it difficult to undertake a thorough investigation of the impact of various severity levels on the study's goals.

ii. ***Imbalanced Distribution***

The dataset exhibits an imbalanced distribution of images across different DR severity levels. Specifically, there are 6149 images labeled as non-DR, while the number of images decreases considerably for mild DR (588), moderate DR (1283), severe DR (221), and proliferative DR (166). This imbalance may have implications for the performance and accuracy of machine learning models.

iii. ***Limited Image Clarity and Quality***

A portion of the dataset contains images that are characterized by lower image quality, such as blurriness, noise, or artifacts. These limitations in image clarity and quality can pose challenges in accurately analyzing and extracting meaningful information from the images and thus potentially impact the performance.

3.3 Severity Grading Process and Standard Benchmarks

The accurate grading of severity in diabetic retinopathy (DR) is crucial for effective diagnosis and management of the disease. The severity grading process involves the evaluation of various retinal features and lesions observed in fundus images.

Ophthalmologists and trained graders visually assess these features, including microaneurysms, hemorrhages, exudates, cotton wool spots, intraretinal microvascular abnormalities (IRMA), venous beading, and neovascularization. The presence, extent, and characteristics of these features are considered in assigning severity grades to determine the stage of DR. Two widely recognized standard grading systems for DR severity assessment are the American Academy of Ophthalmology (AAO) and the International Clinical Diabetic Retinopathy Disease Severity Scale [292]. These grading systems categorize DR into different levels, ranging from mild non-proliferative DR (NPDR) to severe NPDR and proliferative DR (PDR). These grading scales provide a consistent framework for clinicians to assess and communicate the severity of DR. To ensure reliability and comparability across studies, several benchmark datasets have been established. One prominent benchmark is the Early Treatment Diabetic Retinopathy Study (ETDRS) dataset, which comprises retinal images graded by expert ophthalmologists following standardized protocols [293]. To ensure reliability and comparability across studies, several benchmark datasets have been established such as the International Diabetic Retinopathy (IDRiD) dataset [294] and the EyePACS-Kaggle dataset. These datasets consist of retinal images annotated by trained graders based on established severity scales.

In the thesis, the American Academy of Ophthalmology (AAO) and the International Clinical Diabetic Retinopathy Disease Severity Scale (Refer Table 3.1) is used for DR severity assessment on the Kaggle dataset to ensure the validity, reliability, and comparability of our results. The severity grading used in this work are enlisted in Table 3.2.

Table 3.1: The International Clinical Diabetic Retinopathy Disease Severity Scale [292]

Severity Level	**Name of the Severity**	**Findings Observable on Dilated Ophthalmoscopy**
Grade Level 0	No apparent retinopathy- No DR	No signs of diabetic retinopathy are observed, and the retina appears normal without any abnormalities.
Grade Level 1	Mild Non proliferative diabetic retinopathy (NPDR)	During the examination, small tiny balloon-like bulges, known as microaneurysms, are observed on the retinal blood vessels.

Grade Level 2	Moderate Non proliferative diabetic retinopathy (NPDR)	During the examination, there are retinal changes that indicate a stage between mild NPDR and severe NPDR. These changes are more significant than microaneurysms but have not reached the severity seen in severe NPDR.
Grade Level 3	Severe Non proliferative diabetic retinopathy (NPDR)	During the examination, any of the following characteristics are observed 1. More than 20 intraretinal hemorrhages in each of the 4 quadrants: There are multiple dot-like bleedings within the retinal layers, and they are distributed in more than 20 locations in each of the four quadrants of the retina. 2. Definite venous beading in 2 quadrants: Abnormal dilations or constrictions (beading) are present in the retinal veins, and this is observed in two of the four quadrants of the retina. 3. Prominent intraretinal microvascular abnormalities (IRMAs) in 1 quadrant: There are noticeable abnormal new blood vessels that have formed within the retina, and this is observed in one of the four quadrants.
Grade Level 4	Proliferative diabetic retinopathy (PDR)	During the examination, one or more of the following signs are observed: 1. Neovascularization: Abnormal new blood vessels, also known as neovascularization, have formed on the retina's or optic disc's surface. These new blood vessels are fragile and prone to leakage, causing complications such as vitreous hemorrhage or retinal detachment. 2. Vitreous/preretinal hemorrhage: There is bleeding that occurs either into the vitreous humor (gel-like substance inside the eye) or in the space between the retina and the vitreous humor (preretinal space). This bleeding can

		significantly impair vision and cause floaters or dark spots in the visual field.

Table 3.2: Severity grading distribution for Kaggle, MESSIDOR and IDRiD dataset

Grade	Grading Description	Number of Images in Kaggle Dataset	Number of Images in the MESSIDOR dataset	Number of Images in IDRiD dataset
Grade 0	($N_{MA} = 0$) and ($N_{HM} = 0$)	6149	546	168
Grade 1	($0 < N_{MA} \leq 5$) and ($N_{HM} = 0$)	588	153	25
Grade 2	($5 < N_{MA} < 15$) or ($0 < N_{HM} \leq 5$)	1283	247	168
Grade 3	($N_{MA} \geq 15$) or ($N_{HM} \geq 5$)	221	254	93
Grade 4	$N_{MA} \geq 20$ in each of 4 quadrants, venous beading in 2 quadrants, and prominent intraretinal microvascular abnormalities in 1 quadrant	166	-	-

*N_{MA} represents the number of microaneurysms

**N_{HM} represents the number of hemorrhages

Table 3.3: Different Dataset Available

Dataset Name	Published in Year	Captured by	No. of Persons from which images are taken	Total no. of images	Image format	Type	Used for	Ref
FGADR	2020	NA	NA	2842	JPEG	Fundus	DR and DME grading	[295]
Dataset from fundus images for the study of DR	2021	Visucam 500 camera of the Zeiss brand	NA	757	JPEG	Fundus	DR grading	[296]
Retinal Lesions	2020	Selected from EPACS dataset	NA	1593	JPEG	Fundus	Implemented for DR	[297]

							grading and lesion segmentation	
Bahawal Victoria Hospital	2020	Vision Star, 24.1 Megapixel Nikon D5200 camera	500	2500	JPEG	Fundus	DR grading	[298]
AGAR300	2020	45-degree field-of-view	150	300	JPEG	Fundus	DR grading and MA detection	[399]
Zhongshan Hospital and First People's Hospital	2019	Multiple colour fundus camera	5278	19,233	JPEG	Fundus	DR grading and lesion segmentation	[300]
OIA-DDR	2019	NA	9598	13,673	JPEG	NA	DR grading and lesion segmentation	[301]
ODIR-2019	2019	Fundus camera (Canon), Fundus camera (ZEISS), and Fundus camera (Kowa)	5000	8000	JPEG	Fundus	DR, HT, AMD and Glaucoma	[302]
OCTAGON	2019	DRI OCT Triton (Topcon	213	213	JPEG & TIFF	OCTA	DR detection	[303]
CSME	2019	NIDEK non-mydriatic AFC-330 auto-fundus camera	NA	1445	JPEG	Fundus	DR grading	[304]

APTOS	2019	DFC	NA	5590	PNG	Fundus	DR grading	[305]
UoA-DR	2018	Zeiss VISUCAM 500 Fundus Camera FOV 45 degree	NA	200	JPEG	Fundus	DR grading	[306]
OCTID	2018	Cirrus HD-OCT machine (Carl Zeiss Mediatec)	NA	500+	JPEG	OCT	DR, HT, AMD	[307]
IDRID	2018	NA	NA	516	JPEG	Fundus	DR grading and lesion segmentation	[308]
Singapore National DR Screening Program	2017	NA	14,880	494,661	JPEG	Fundus	DR, Glaucoma and AMD	[309]
Ophthalmic Data Repository DR	2017	TRC-NW65 non-mydriatic DFC (Topcon)	70	1120	PNG	Fundus	DR detection	[310]
JICHI DR	2017	AFC-230 fundus camera (Nidek)	2740	9939	JPEG	Fundus	DR grading	[311]
DR HAGIS	2016	TRC-NW6s (Topcon), TRC-NW8 (Topcon), or CR-DGi fundus camera (Canon)	38	39	JPEG	Fundus	DR, HT, AMD and Glaucoma	[312]
Rabbani	2015	Heidelberg SPECTRALIS OCT HRA system	24	24 images & 24	TIFF	OCT	Diabetic Eye diseases	[313]

				videos				
EyePACS	2015	Centervue DRS (Centervue, Italy), Optovue iCam (Optovue, USA), Canon CR1/DGi/CR2 (Canon), and Topcon NW (Topcon)	NA	88,702	JPEG	Fundus	DR grading	[314]
Srinivasan	2014	SD-OCT (Heidelberg Engineering, Germany)	45	3231	TIFF	OCT	DR detection and grading, DME, AMD	[315]
Lotus eyecare hospital	2014	Canon non-mydriatic Zeiss fundus camera 90_ FOV	NA	122	JPEG	Fundus	DR detection	[316]
MESSIDOR 1	2014	Topcon TRC NW6 non-mydriatic retinography, 45_ FOV	NA	1200	TIFF	Fundus	DR and DME grading	[317]
FFA Photographs	2014		70	70	JPEG	FIFA	DR grading and Lesion detection	[318]
DRIMDB	2014	CF-60UVi fundus camera (Canon)	NA	216	JPEG	Fundus	DR detection and grading	[319]
DR2	2014	TRC-NW8	NA	520	TIFF	Fundus	DR detection	[320]

		retinography (Topcon) with a D90 camera (Nikon, Japan)						
DR1	2014	TRC-50_ mydriatic camera Topcon	NA	1077	TIFF	Fundus	DR detection	[320]
RITE	2013	Canon CR5 non-mydriatic 3CCD camera with a 45_ FOV	40	40	TIFF	Fundus	Retinal vessel segmentation and ophthalmic diseases	[321]
22 HRF	2013	CF-60UVi camera (Canon)	45	45	JPEG	Fundus	DR detection	[322]
Longitudinal DR screening data	2013	Topcon TRC-NW65 with a 45 degrees field of view	70	1120	JPEG	Fundus	DR grading	[323]
eOphtha	2013		NA	463	JPEG	Fundus	Lesion detection	[324]
DRiDB	2013	Zeiss VISUCAM 200 DFC at a 45_ FOV	NA	50	BMP	Fundus	DR grading	[325]
Fundus Images with Exudates	2012		NA	35	JPEG	Fundus	Lesion detection	[326]
FFA Photographs & CF	2012		60	120	JPEG	FIFA	DR grading and lesion detection	[327]
19 CF	2012		60	60	JPEG	Fundus	DR detection	[328]

HEI-MED	2010	Visucam PRO fundus camera (Zeiss, Germany)	910	169	JPEG	Fundus	DR detection and grading	[329]
National Taiwan University Hospital	2007–2017	Heidelberg retina tomography with Rostock corneal module	30	30	TIFF	Fundus	DR, pseudo exfoliation	[330]
DIARETDB 1	2007	50_ FOV DFC	NA	89	PNG	Fundus	DR detection and grading	[331]
DIARETDB 0	2006	50_ FOV DFC	NA	130	PNG	Fundus	DR detection and grading	[332]
DRIVE	2004	Canon CR5 non-mydriatic 3CCD camera with a 45_ FOV	400	40	JPEG	Fundus	Retinal vessel segmentation and ophthalmic diseases	[333]

This chapter outlined the dataset utilized in this study, examining its structure, inherent limitations, and the grading benchmarks that guide severity classification for diabetic retinopathy. Understanding these factors is crucial in the design and training of a reliable model for DR detection. Insights gathered from the dataset enlighten the architectural and methodological decisions of the proposed model, elaborated upon in the next chapter.

CHAPTER 4

PROPOSED MODEL

This chapter introduces the proposed DR-ResNet+ model, designed to enhance diabetic retinopathy detection. Beginning with an overview of the ResNet model's structure, the chapter then describes the architectural enhancements specific to DR-ResNet+. These adaptations are tailored to address challenges such as vanishing gradients and to improve feature extraction, ultimately leading to more accurate retinal image analysis. Through advanced deep learning techniques, DR-ResNet+ is presented as a robust tool for diabetic retinopathy detection.

4.1 Conventional ResNet Model

In the conventional CNNs, as it becomes deeper, vanishing gradients occur, which has a negative impact on network performance. This gradient is back propagated to the previous layer and disappears, resulting in a very small gradient. Residual neural networks provide a "skip connection" function that allows for 152-layer training without vanishing gradient concerns [334]. It works by superimposing "identity mappings" on top of the CNN and creates skip connection/identity shortcut connections that skip one or more parameter/weight layers and feed the input directly bypassing one or more layers to a layer ahead. Moreover, the stacking of the layers should not degrade the performance of its shallow counterpart. As shown in Fig. 3, the output of the skip path *is* $H(x) = x + F(x)$, where *x* denotes the input to the layers and $F(x)$ is the activation implemented on two layers that are skipped. Therefore, $F(x)$ in this case will be $H(x) - x$ i.e., $F(x) = H(x) - x$ in actuality. $(H(x) - x)$ is a residual learned by the layers that are skipped and known as a skipped connection or residual network.

Weight layer learns F(x) = H(x)-x

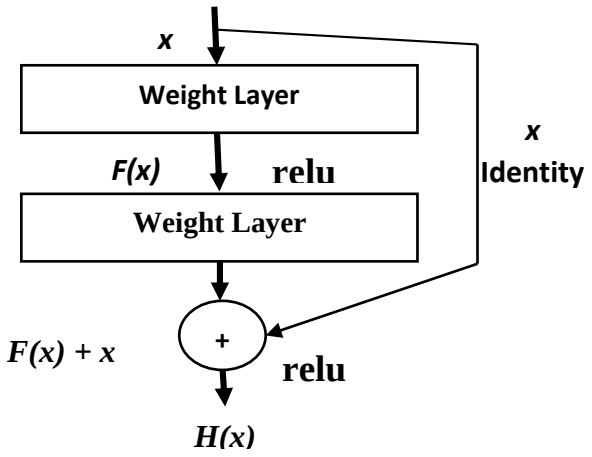

Figure 4.1: ResNet Model [335]

During the training phase, the error gradient propagates backward from the output to the input side of the network, in the case of the skipped connection, the gradient can directly flow to those connections as well and vanishes the error gradient. Figure 4.2 shows 34 layers residual network [336]. All the bypass connections which are shown by the curved arrows represent all the skip connections that skip the number of layers in between to pass the information to the next layers as shown in Fig. 4.2. Key variables involved in forward and backpropagation within the residual network are presented below.

a^l: The activation at layer *l*. This variable represents the output of neurons at a particular layer after applying the activation function.

f: The activation function, which applies a non-linear transformation to the weighted sum of inputs to add non-linearity to the model.

$W^{l-1,l}$: The weight matrix connecting layer $l-1$ to layer *l*. It represents the learned parameters that modify the input activations as they pass from one layer to the next.

b: The bias term. This term is added to the weighted sum of inputs to adjust the activation function's threshold, allowing the model to shift the activation function as needed.

Z^l: The weighted sum of inputs at layer *l* before applying the activation function. This is computed as $W^{l-1,l} \cdot a^{l-1} + b$, representing the net input to layer *l*.

δ^l: The error gradient at layer *l*. This gradient shows how the error changes with respect to the activation a^l, indicating how much each parameter should adjust to reduce the output error.

$\nabla W^{l-1,l}$: The gradient of the weights $\nabla W^{l-1,l}$in the normal path. It shows how the error changes with respect to these weights, guiding the adjustments during backpropagation.

$\nabla W^{l-2,l}$: The gradient of the weights in the skip path that connects layer *l−2* directly to layer *l*. This gradient indicates the effect of the skip connections on the error, ensuring the error propagates efficiently to earlier layers.

Forward Flow: $a^l = f\left(W^{l-1,l} \,.\, a^{l-1} + b + W^{l-2,l} \,.\, a^{l-2}\right) = f\left(Z^l + W^{l-2,l} \,.\, a^{l-2}\right)$ *(i)*

$$a^l = f(Z^l + a^{l-2}) \quad \text{if same dimension} \qquad \textit{(ii)}$$

Back Propagation: $\nabla W^{l-1,l} = -a^{l-1}.\delta^l$ Normal path *(iii)*

$\nabla W^{l-2,l} = -a^{l-2}.\delta^l$ Skip path *(iv)*

As shown in Fig. 4.3, during backpropagation, the error gradient propagates backward from layer l to layer $l-1$. This gradient can flow from layer l to layer $l-2$ following the skip connection.

It has been observed that in backpropagation, the error gradient propagates back from both the normal path and the skipped paths to avoid the vanishing gradient problem in the residual network.

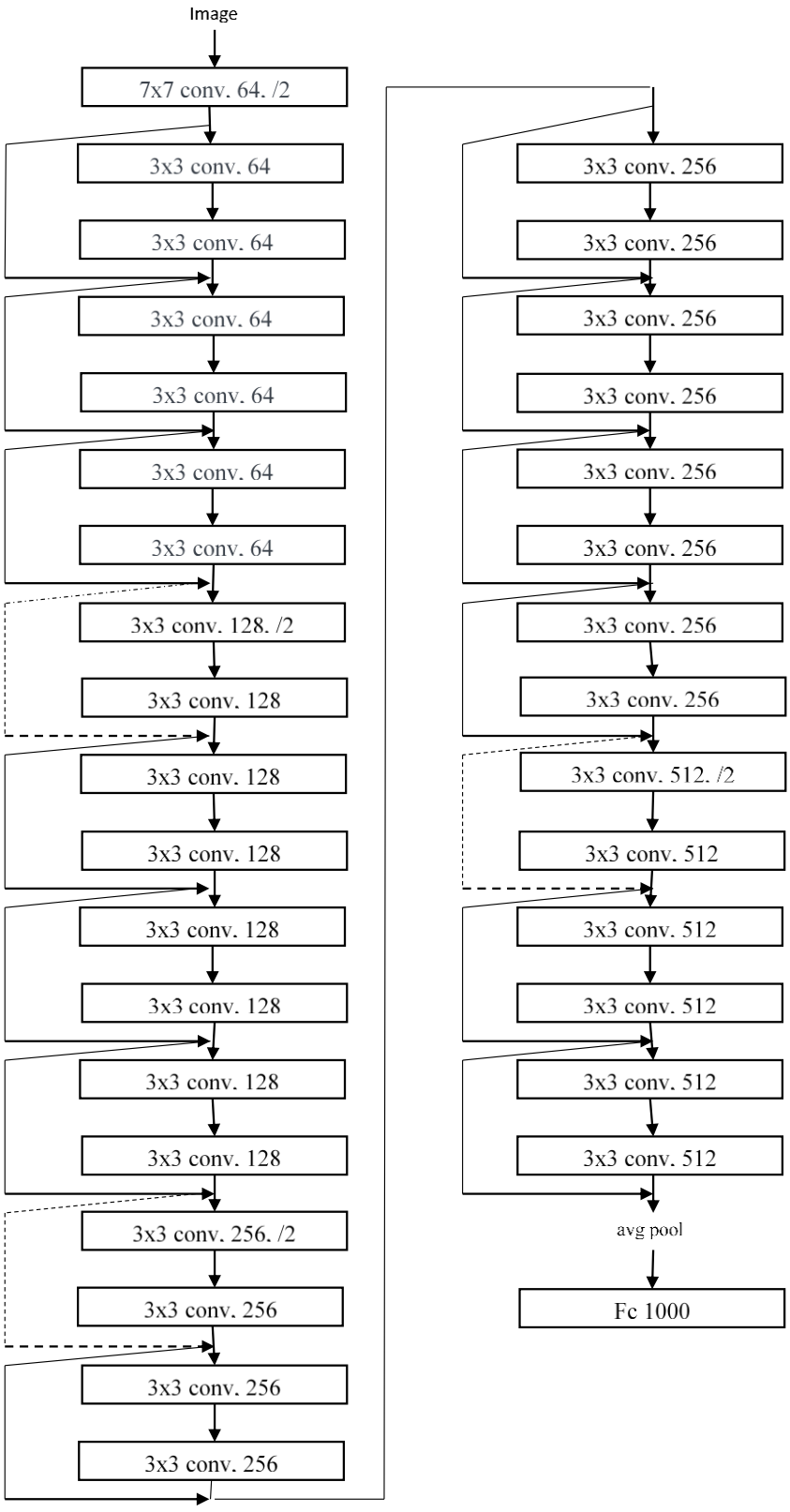

Figure 4.2: 34-layer residual network [337]

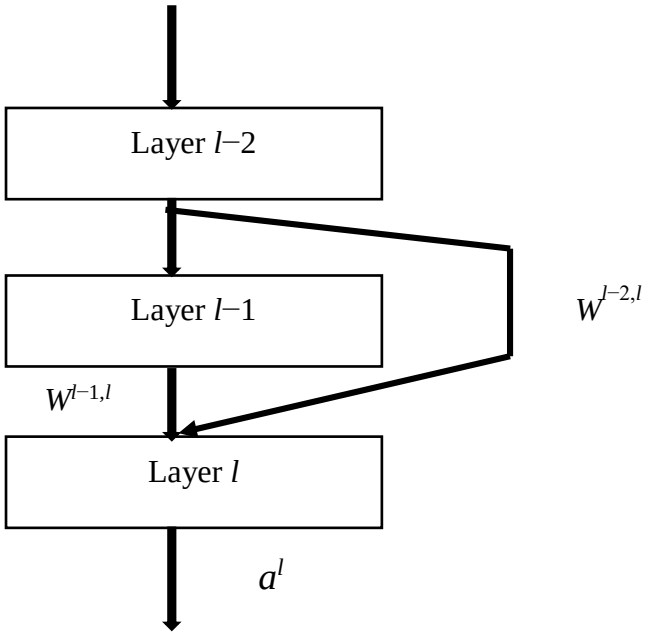

(a)

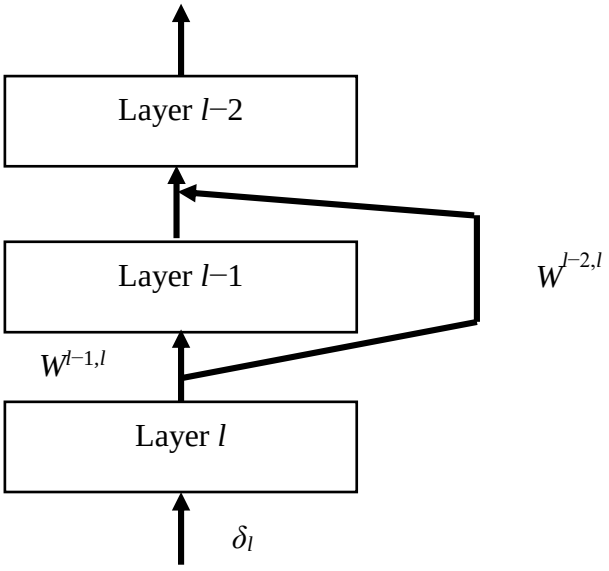

(b)

Figure 4.3: (a) Forward flow (b) Backward Flow

4.2 Proposed DR-ResNet+ Model

Figure 4.4 shows the overall architecture of the proposed DR-ResNet+ model for detection of Diabetic Retinopathy. The data is fed to the input with zero padding. After performing the convolution, batch normalization is applied before adding nonlinearity through an activation function ReLu. To reduce the dimensions, Max pooling is done prior to the residual blocks. After average pooling, the output is flattened up, and forwarded to the dense, fully connected artificial neural network.

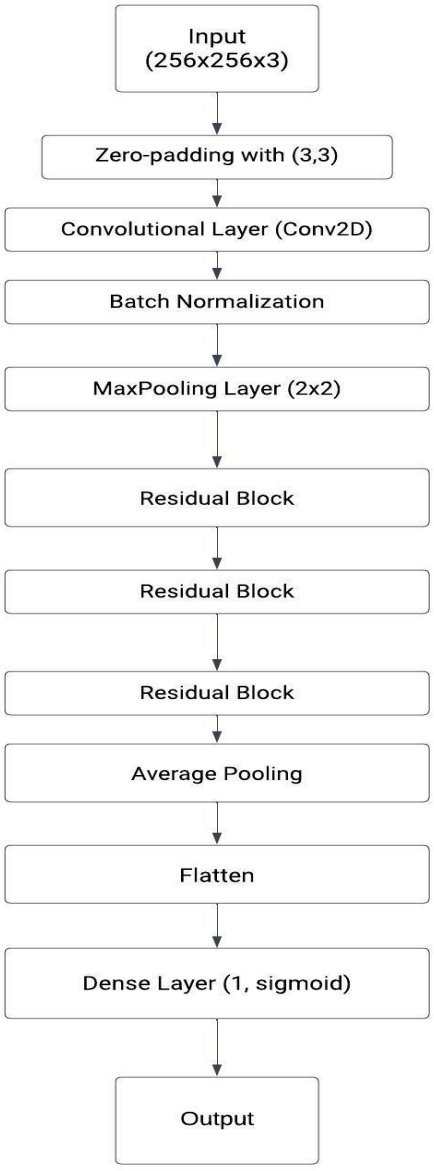

Figure 4.4: Proposed DR-ResNet+ Model for detection of Diabetic Retinopathy

The architectural design for the detection of Diabetic Retinopathy (DR) entails a comprehensive sequence of layers aimed at effectively discerning between images with and without DR. The initial input comprises images with dimensions of 256x256 pixels and three color channels. To prepare the input for subsequent processing, zero-padding is applied with a (3, 3) kernel, setting the stage for a Convolutional Layer (Conv2D) with 64 filters. This convolutional operation employs a kernel size of (7, 7) and is activated using Rectified Linear Unit (ReLU) activation.

Following the convolutional layer, batch normalization is performed to normalize the activations, and an additional ReLU activation function is applied for enhanced non-linearity. Max-pooling is then employed with a 2x2 window to down-sample the spatial dimensions of the feature maps.

The model integrates residual blocks to capture intricate hierarchical features crucial for effective image classification. In Stage 2, a residual block consists of three convolutional layers with filter sizes [64, 64, 256], supplemented by Identity Blocks 1 and 2. Similarly, both Stage 3 and Stage 4 incorporate their respective residual blocks with increasing filter sizes ([128, 128, 512] and [256, 256, 1024]). Each stage is accompanied by Identity Blocks to promote feature reuse and facilitate gradient flow during training.

To further streamline the representation, an average pooling layer with a 2x2 window is introduced, contributing to the reduction of spatial dimensions. The flattened output is then channelled into a dense layer housing a single neuron. The activation function employed in this final layer is the sigmoid function, facilitating binary classification and softmax function, facilitating the multi class classification. This meticulously crafted architecture aims to capture and distill pertinent features instrumental in distinguishing between images depicting Diabetic Retinopathy and those that do not.

The full architecture of the DR-ResNet+ model, which is developed for the purpose of identifying and classifying the diabetic retinopathy, is shown in Figure 4.5. Prior to getting into the convolutional layer, the input data passes through a process called zero padding. Next, batch normalization is applied, which introduces nonlinearity via the use of the ReLu activation function. This comes after the convolution algorithm.

Maximum pooling is then used to reduce the dimensionality of the data before it is entered into the residual blocks. After the pooling results have been averaged, the output is flattened and then sent to an artificial neural network that is dense and completely linked [353].

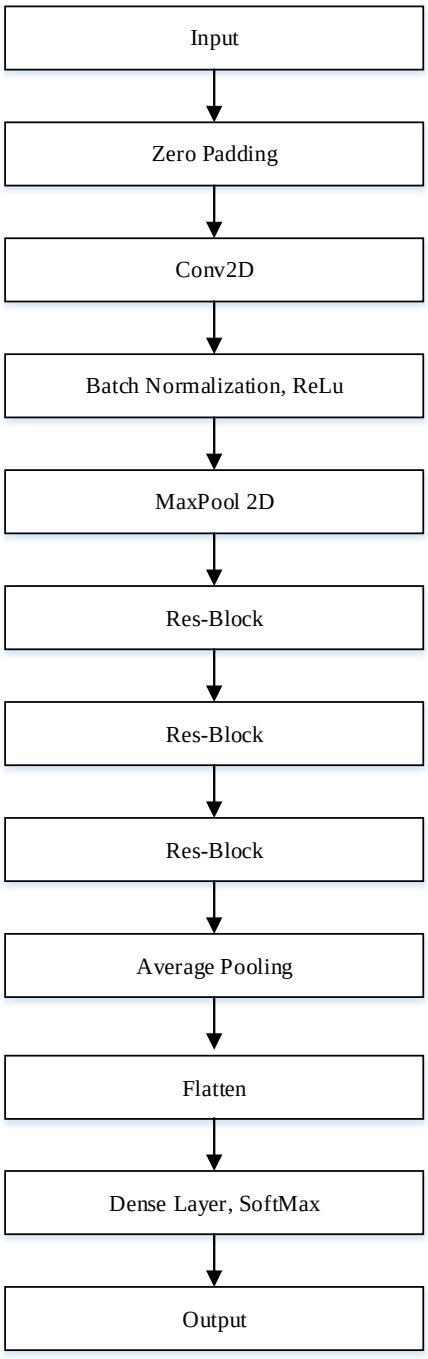

Figure 4.5: Proposed DR-ResNet+ Model for Classifying the Diabetic Retinopathy

All the blocks of the proposed model have a series of blocks within them. The Res-block itself has a convolution block first, followed by two identity blocks as shown in Fig. 4.6.

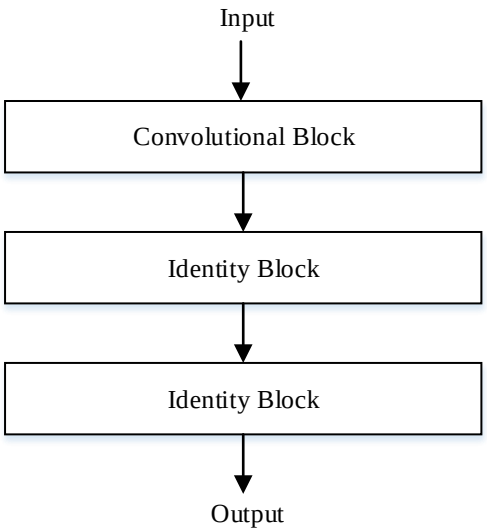

Figure 4.6: Res-Block

In the convolutional Block, as shown in Fig. 4.7, the input is fed to the main path and short path. The main path goes through the conv2D, max pooling, batch normalization with ReLu, then another convolution 2D, batch normalization with ReLu, another con2D, and then batch normalization. Whereas in the short path input is fed to con2D, the max pooling, batch Normalization block. The outputs obtained from these two different paths are added and then applied to the ReLu. Another block in ResNet is an identity block (batch Norm, conv2D, batch norm) in which input is directly fed to the short path, and then the results from the main and short path are added.

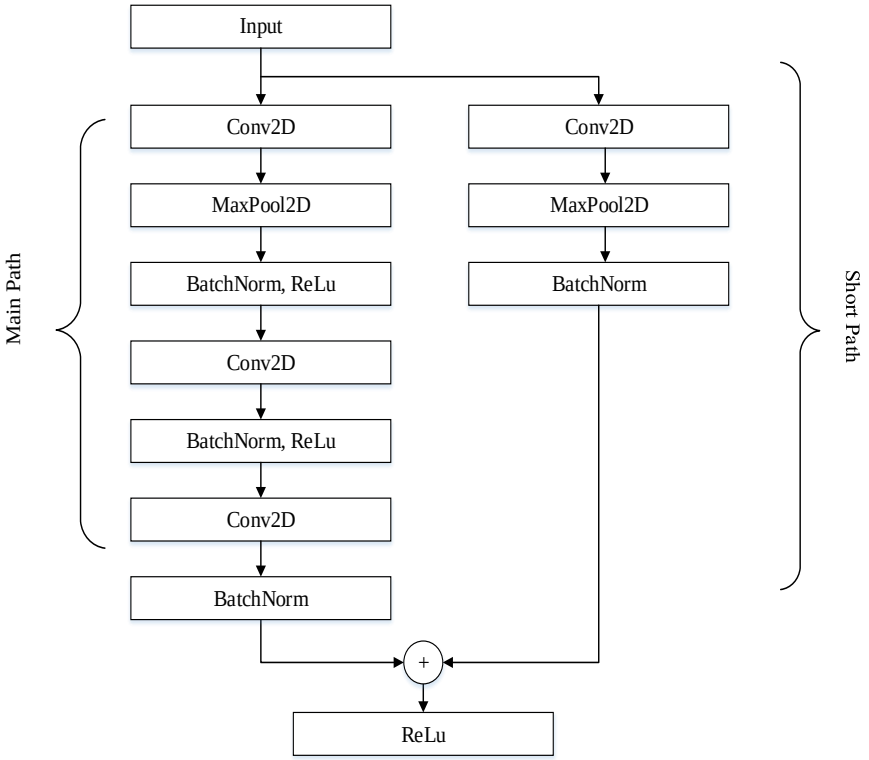

(a)

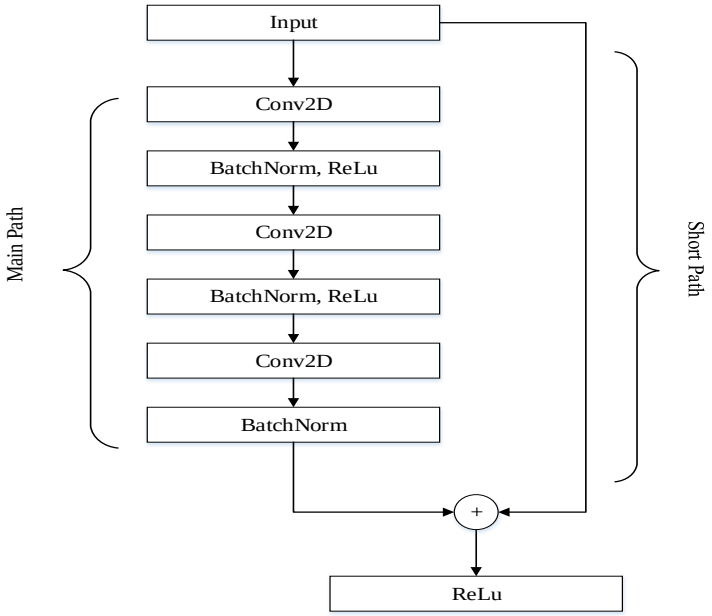

(b)

Figure 4.7: (a) Convolutional Block **(b)** Identity Block

The various steps involved in training the DR- ResNet+ model for diabetic retinopathy classification are enlisted in Table 4.1 as a proposed methodology.

Table 4.1: Proposed Methodology for Categorization of Retinal Images using DR-ResNet+

Steps	Description
Preparation of Data	Get the dataset and divide it into the three categories of training, validation, and testing. The validation set and test set are used to assess the model's performance on new, unseen data, respectively. The training set is used to train the model, the validation set to assess its accuracy and to optimise the hyperparameters.
Data enhancement	To enhance the model's resilience, data augmentation techniques are employed to expand the size of the training dataset. This facilitates the generation of supplementary images from the pre-existing dataset.
Preprocessing of Data	Prior to model training, preprocessing of photos is carried out, which commonly involves resizing, normalizing the pixel values within a specific range and transforming the images to a standardized format suitable for deep learning model processing.
Extraction of Features	Each preprocessed image is fed through the convolutional layers of the proposed DR-ResNet+ model in order to extract features. The model can learn to recognize the distinctive aspects of diabetic retinopathy by extracting these properties, which enables it to precisely diagnose and grade the severity of the condition.
Classification	The feature maps that are produced after feature extraction are flattened and sent through a fully linked layer. The final output scores for each of the five DR severity levels (0, 1, 2, 3, 4) are calculated by this layer. Using the softmax activation function in the output layer, these scores are then normalised into a probability distribution across the severity levels. Using the sigmoid for binary one.
Changing the Final Layer	The DR-ResNet+ model is tailored to classify diabetic retinopathy, and the network's final layer is changed to correspond to the number of necessary output classifications. Since there are five different severity levels of diabetic retinopathy in this case (0, 1, 2, 3, 4), the network's final layer must include five output nodes, one for each severity level, to allow for correct grading and categorization of diabetic retinopathy.
Model training	The DR-ResNet+ model is trained on a vast set of retinal images through backpropagation and stochastic gradient descent (SGD) optimization.

Model testing	To determine its accuracy, the DR-ResNet+ model is tested on a distinct validation dataset, and its precision, recall, F1 score, and other performance parameters are evaluated.
Hyperparameter tuning	To achieve the highest performance on the validation set, the hyperparameters such as learning rate, batch size, and number of epochs are adjusted.
Training	The model is trained with the appropriate hyperparameter values in the training set to optimize the model's performance.
Validation	After tuning the hyperparameters, the validity of the model is checked on the validation dataset.
Testing	To assess the model's generalizability, it is tested on the test data set. This involves evaluating the model's performance on new, unseen data and determining its accuracy in predicting the severity of DR.
Performance Assessment	To assess the trained model performance in identifying diabetic retinopathy, compute its accuracy, precision, recall, F1-score, and AUC-ROC.
Maintaining the Model	After training and validating the model, it is saved for future deployment and to ensure that the model's performance can be replicated and compared to other models or benchmarks in the future.

The architecture of the ResNet+ presents layers, parameters, connections, output, and a convolutional neural network utilized to classify diabetic retinopathy by dividing it into multiple layers. The architecture used is DR-ResNet+, a kind of residual neural network that enables the training of very deep networks. With 3 color channels, an image size of 256×256, and a batch size of none, the input layer has the form (None, 256, 256, 3). The zero-padding layer enlarges the input image to a size of 262×262 by surrounding it with zeros. The conv1 layer conducts the first convolution operation with 64 filters of size 7×7 and a stride of 2, resulting in an output shape of (None, 128, 128, 64). The Batch Normalization layer is used to normalize the output of the convolutional layer, which helps in enhancing the training process. Furthermore, the ReLU activation function is used to normalize the output of the Batch Normalization layer within the activation layer. The result of a max-pooling operation with a pool size of 3×3 and a stride of 2 is (None, 63, 63, 64) for the max_pooling2d layer. A Batch Normalization layer, a ReLU activation layer, two convolutional layers with 64 filters, and a 3×3 kernel size make up the ResNet block. The output of the first convolutional layer is transmitted via a Batch Normalization layer, then through another ResNet block

composed of one convolutional layer with 256 filters and a 1×1 kernel size. After the output of the max-pooling2d layer, a second convolutional layer with 256 filters and a 1×1 kernel size is applied. The next layer is referred to as Batch Normalization. The outputs of these two paths are then combined. The aforementioned processes are repeated four times, resulting in four ResNet blocks, each composed of two identity blocks and one convolutional block. The last layer, a global average pooling layer, uses the spatial average of the output tensor to produce a tensor of form (None, 256). The probability that the input image has diabetic retinopathy is represented by the output of this tensor, which has a range of 0 to 1. Then, this tensor is fed into a layer that is fully connected and has one neuron with a sigmoid activation function. The model has 4,987,525 total parameters, of which 4,967,685 can be trained.

4.2.1 DR-ResNet+ Methodological Elaboration

The proposed DR-ResNet+ architecture is meticulously designed to address the complex task of diabetic retinopathy classification. The detail description of each component is as follows:

1. **Input Layer (input_1)**
    - Shape: (None, 256, 256, 3)
    - Rationale: This layer accommodates varying batch sizes and RGB color images with dimensions of 256x256 pixels.
2. **Zero Padding Layer (zero_padding2d)**
    - Padding: (None, 262, 262, 3)
    - Rationale: Zero-padding enlarges the input image to 262x262, ensuring that spatial information is preserved during convolution.
3. **Convolutional Layer (conv1)**
    - Filters: 64
    - Kernel Size: 7x7
    - Stride: 2
    - Output Shape: (None, 128, 128, 64)
    - Rationale: This layer extracts low-level features from the input image while reducing spatial dimensions.

4. **Batch Normalization Layer (bn_conv1)**:
    - Output Shape: (None, 128, 128, 64)
    - Rationale: Batch normalization stabilizes training by normalizing activations, enhancing convergence and mitigating overfitting.
5. **Activation Layer (ReLU)**
    - Output Shape: (None, 128, 128, 64)
    - Rationale: The Rectified Linear Unit (ReLU) introduces non-linearity, enabling the model to learn complex patterns.
6. **Max Pooling Layer (max_pooling2d)**
    - Pool Size: 3x3
    - Stride: 2
    - Output Shape: (None, 63, 63, 64)
    - Rationale: Max pooling reduces spatial dimensions while retaining essential features, promoting translation invariance.
7. **ResNet Blocks (res_2_conv_a)**
    - Explanation: ResNet blocks are pivotal to our architecture. They comprise Convolutional Blocks and Identity Blocks.
    - Convolutional Block (res_2_conv_a)
        - Input Shape: (None, 63, 63, 64)
        - Configuration: Conv2D, Batch Normalization, ReLU, Conv2D, Batch Normalization
        - Output Shape: (None, 31, 31, 64)
    - Identity Block (res_2_identity_1_a)
        - Input Shape: (None, 31, 31, 64)
        - Configuration: Conv2D, Batch Normalization
        - Output Shape: (None, 31, 31, 256)
    - Rationale: These blocks mitigate the vanishing gradient problem, enabling training of very deep networks by using shortcut connections for gradient flow.

8. **Global Average Pooling Layer (Average_Pooling)**
    - Output Shape: (None, 3, 3, 1024)
    - Rationale: Global average pooling spatially averages feature maps, condensing information for classification while reducing overfitting.
9. **Flatten Layer (flatten)**
    - Output Shape: (None, 9216)
    - Explanation: Flattening the output prepares it for input into fully connected layers.
10. **Fully Connected Layer (Dense_final)**
    - Units: 5 (one for each DR severity level) and 2 for binary classification
    - Output Shape: (None, 5)
    - Rationale: This layer produces final output scores for classifying diabetic retinopathy severity levels.

4.2.1 Rationale behind the Design Choices

- **Residual Blocks**: ResNet blocks are adopted to counteract the vanishing gradient issue. Shortcut connections facilitate the flow of gradients during backpropagation, enabling training of deep networks.
- **Batch Normalization**: We incorporate batch normalization to enhance training stability and convergence by normalizing activations.
- **Global Average Pooling**: This layer reduces spatial dimensions while retaining crucial information, reducing the risk of overfitting and preparing data for classification.

CHAPTER 5
RESULTS AND DISCUSSION

This chapter provides a comprehensive analysis of the performance outcomes achieved with the proposed model, DR-ResNet+, using a variety of evaluation metrics. Results from simulations highlight the model's accuracy and reliability in identifying diabetic retinopathy. A comparative assessment follows, where the DR-ResNet+ model's effectiveness is benchmarked against traditional approaches to underscore improvements in diagnostic precision. The chapter discusses the model's potential implementation in real-world clinical practice, emphasizing its role in enhancing accessibility and effectiveness in diabetic retinopathy screening.

5.1 Performance Matrix

The effectiveness of a machine learning classification is evaluated using a confusion matrix. The confusion matrix provides a comparison that is based on matrices of actual and predicted values. Here, the DR is divided into five categories proliferative, no DR, mild, moderate, and severe. The confusion matrix for our classification problem would thus be a 5×5 matrix. The term "confusion matrix" refers to a matrix that has the dimensions N×N, where N is the total number of labels or classes. Understanding the concepts of true positive, true negative, false positive, and false negative is critical in data analysis and machine learning. Positive and negative numbers are used to assess prediction accuracy, and there are four major sorts of outcomes. A true positive is one when the predicted and actual values are both positive. On the other hand, it is referred to as a true negative when both values are negative. When the predicted value is positive even if the actual value is negative, this is referred to as a false positive or Type 1 error. When the predicted value is negative even if the actual value is positive, this is known as a false negative, or Type 2 error, and the confusion matrix for the same is shown in Figure 5.1.

<table>
<tr><th colspan="7">Predicted</th></tr>
<tr><td rowspan="6">Actual</td><td>Class</td><td>No DR</td><td>Mild</td><td>Moderate</td><td>Severe</td><td>Proliferative DR</td></tr>
<tr><td>No DR</td><td colspan="4" rowspan="4">TN</td><td rowspan="4">FP
(Type 1 Error)</td></tr>
<tr><td>Mild</td></tr>
<tr><td>Moderate</td></tr>
<tr><td>Severe</td></tr>
<tr><td>Proliferative</td><td colspan="4">FN (Type 2 Error)</td><td>TP</td></tr>
</table>

Figure 5.1: Basic Confusion Matrix

Accuracy is determined by dividing the number of correct positive predictions by the total number of positives. In other words, accuracy establishes the ratio of true positives to expected positives.

Recall is calculated by dividing true positive by true positive and false negative. Recall evaluates a model's propensity to predict successful outcomes.

The F1 score is determined by determining the harmonic mean of the values obtained for recall and accuracy. To get an individual's F1 score, the recall and accuracy scores are averaged together and then multiplied by the harmonic mean. The F1 score will be 0, not 0.5 if the accuracy and recall are both 0.

Deep learning models' categorization effectiveness may be evaluated using a variety of performance indicators [338]. Area under the curve (AUC), sensitivity, specificity, accuracy, and area under the receiver operating characteristic curve (ROC) are common metrics for deep learning models [339]. The percentage of aberrant pictures that are accurately identified as being aberrant is known as the image's sensitivity, while the percentage of normal pictures that are accurately recognized as being normal is known as the image's specificity. The AUC, a graph, illustrates how specificity and sensitivity are related. On the other hand, accuracy represents the proportion of images that were correctly classified.

5.2 Simulation Results

Figure 5.2(a) shows the loss curve of the proposed model during training and validation process over 100 epochs. It is clearly evident that the proposed model's loss decreases gradually over time, as its learning improves.

Fig. 5.2 (b) displays the proposed model's ROC curve that illustrates the model's true positive rate versus its false positive rate for different classification thresholds. The model has an area under the ROC curve (AUC) of 0.98, a high true positive rate, and a low false positive rate. It suggest that the proposed model has an excellent discrimination ability between the two classes.

The accuracy curve in Fig. 5.2 (c) and Fig. 5.2 (d) shows the proposed model's training and validation accuracy over 50 and 100 epochs, respectively. It is evident from Fig. 5.2 that the DR-ResNet+ model achieves a high accuracy of 98% over 50 epochs and maintain the same level of accuracy at 100 epochs which suggest that the proposed model is generalized and could maintain its performance over a longer training period. Further, it demonstrates that the proposed model's accuracy steadily increased over time and eventually stabilized at a high level. Thus, the model is capable to learn the features of the input data effectively and accurately classify the samples. The proposed model's loss value 0.5 indicates that the model minimizes the error between the predicted and actual outputs while training. Therefore, proposed DR-ResNet+ model is a highly effective model for classification tasks, with high accuracy, low loss, and excellent discrimination ability.

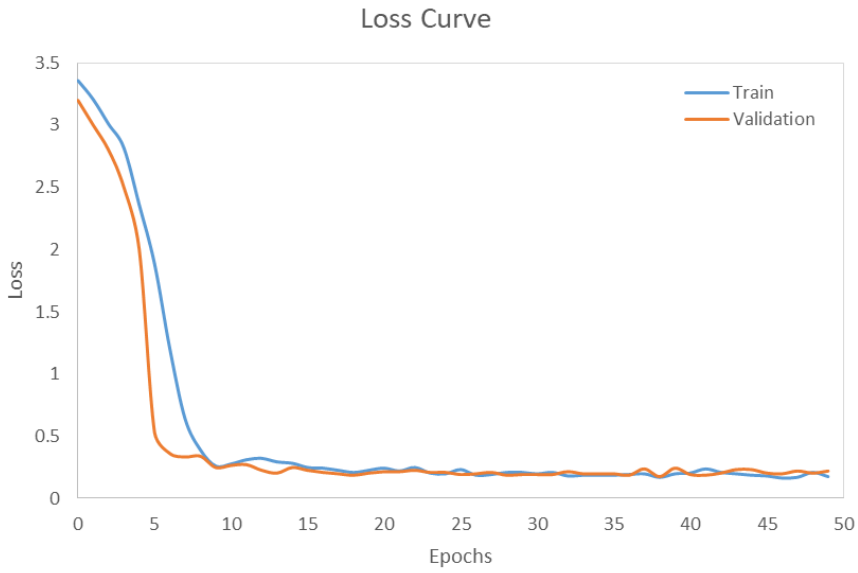
Loss Curve
Train
Validation
Loss
Epochs
3.5
3
2.5
2
1.5
1
0.5
0
0
5
10
15
20
25
30
35
40
45
50

(a)

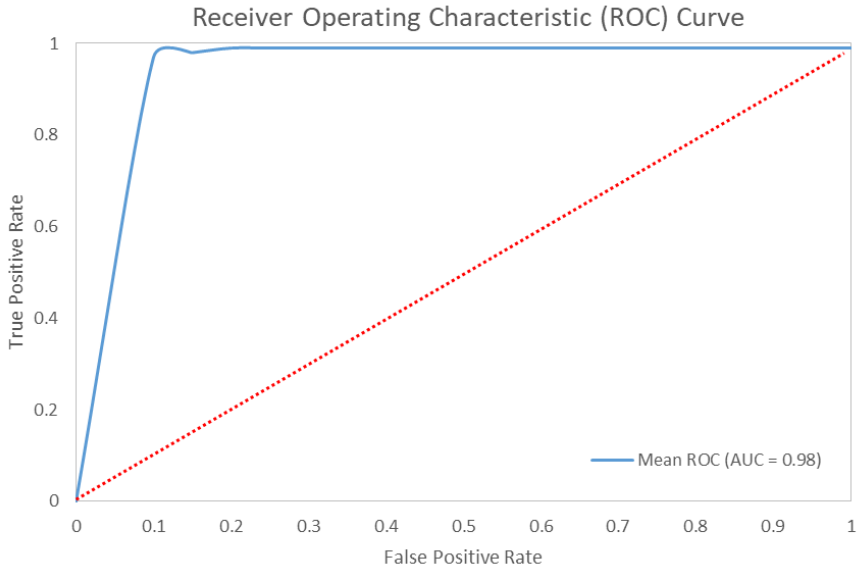
Receiver Operating Characteristic (ROC) Curve
True Positive Rate
False Positive Rate
Mean ROC (AUC = 0.98)
1
0.8
0.6
0.4
0.2
0
0
0.1
0.2
0.3
0.4
0.5
0.6
0.7
0.8
0.9
1

(b)

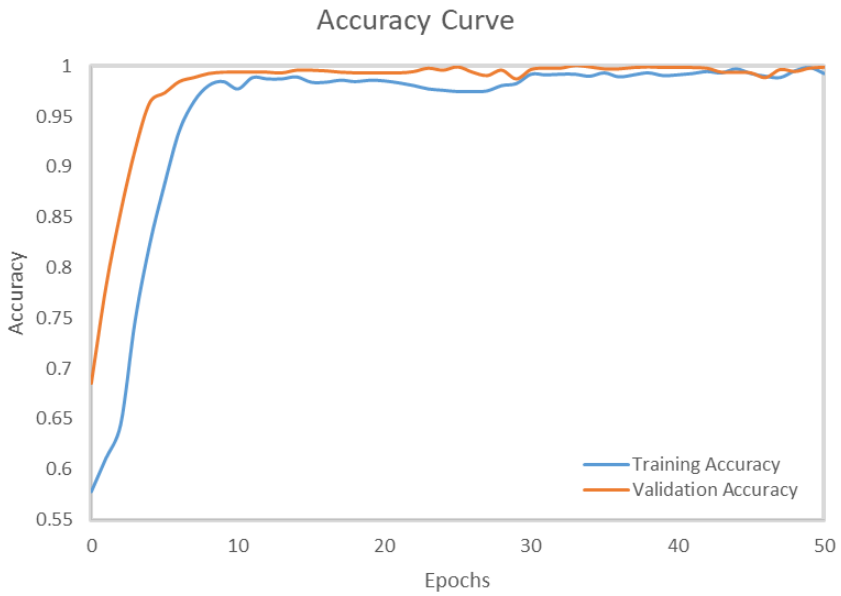

(c)

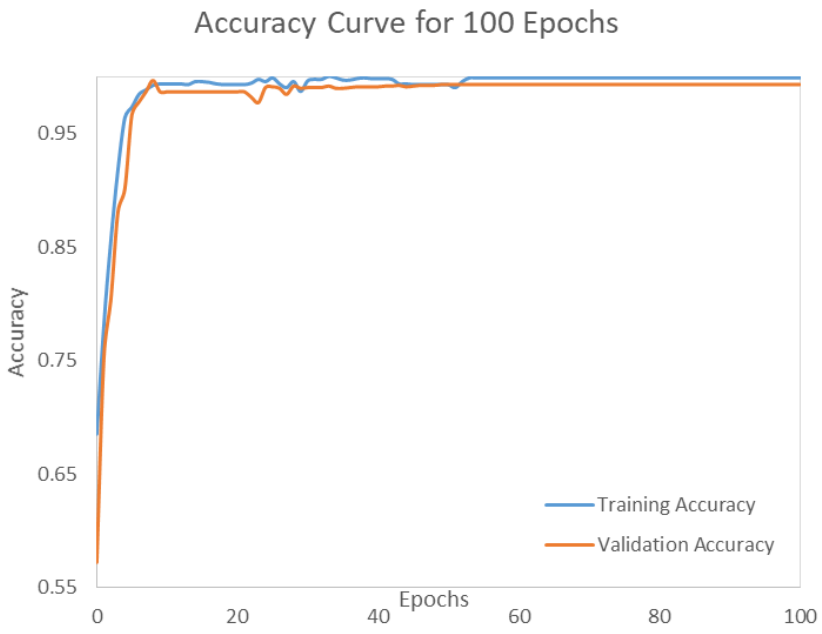

(d)

Figure 5.2: (a) the loss curve for the DR-ResNet+ model, (b) the receiver operating characteristic (ROC) curve for the DR-ResNet+ model, and (c) the accuracy curve for the DR-ResNet+ over 50 epochs model (d) the accuracy curve for the DR-ResNet+ over 100 epochs

The accuracy with which the suggested model can categorize the input data into the appropriate groups is shown by the confusion matrix in Figure 5.3(a). Along the diagonal, there are a disproportionately high number of properly categorized samples, suggesting that the model has high accuracy for each class. Fig. 5.3 (b) to Fig. 5.3 (f) shows the confusion matrix for no DR, Mild DR, Moderate DR, Severe DR, and Proliferative DR, respectively. It can be observed that for Proliferative DR using the aforementioned confusion matrix, TP = 1381. This is evident from the last column and final row which shows that only 1381 of the Proliferative were categorized properly.

FP = 9 + 21 + 94+ 13 = 47, except for the final row in the last column. It specifies that incorrectly classified proliferative include nine cases of no DR, twenty-one cases of mild DR, four cases of moderate DR, and thirteen cases of severe DR.

FN = 24, except for the last column in the final row, 6 of the Proliferative DR are mistakenly labeled as No DR, 10 of the Proliferative DR as Mild DR, 4 of the Proliferative DR as Moderate DR, and 4 of them as Severe DR

TN = 5573, Since it is not Proliferative and not even identified as Proliferative, the remaining classifications, with the exception of the final row and final column, can all be considered false negatives.

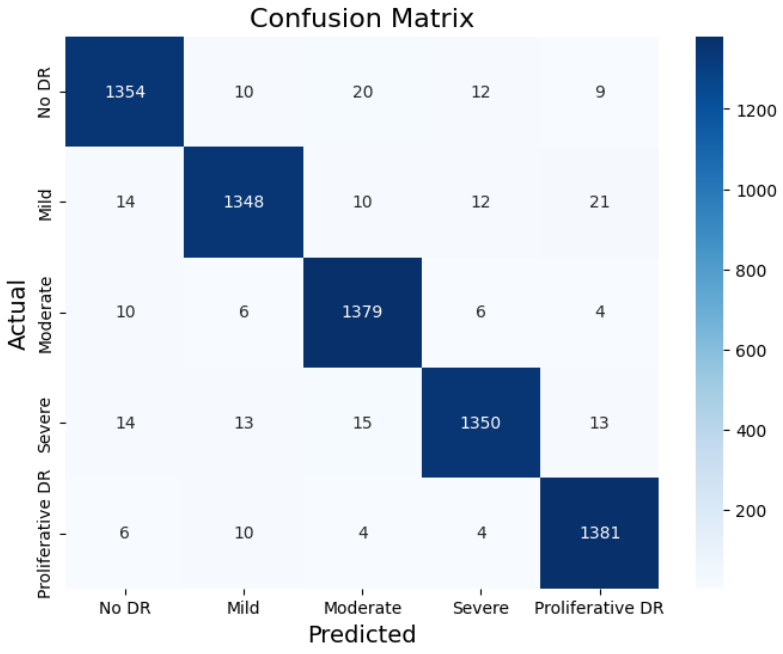

(a)

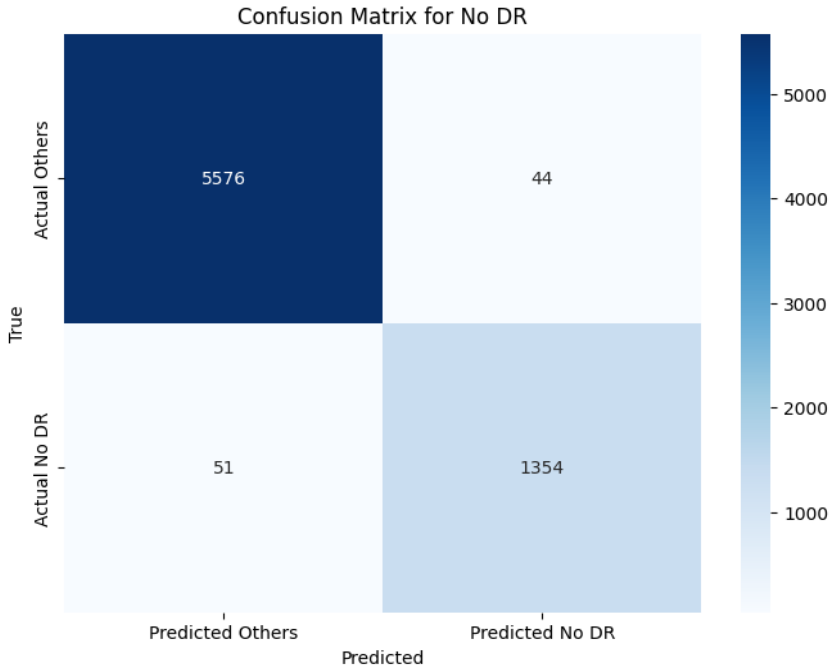
Confusion Matrix for No DR
Actual Others
Actual No DR
True
5576
44
51
1354
Predicted Others
Predicted No DR
Predicted
5000
4000
3000
2000
1000

(b)

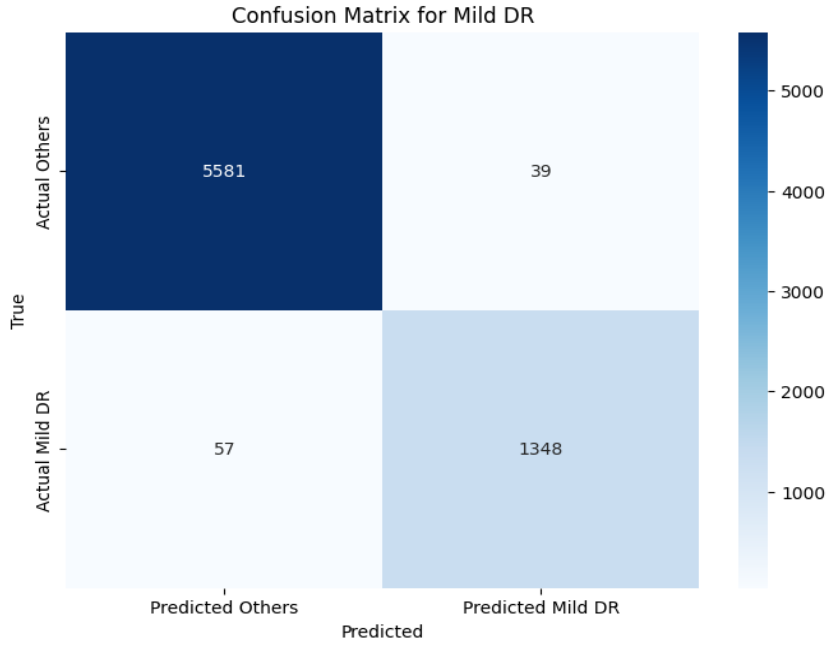
Confusion Matrix for Mild DR
Actual Others
Actual Mild DR
True
5581
39
57
1348
Predicted Others
Predicted Mild DR
Predicted
5000
4000
3000
2000
1000

(c)

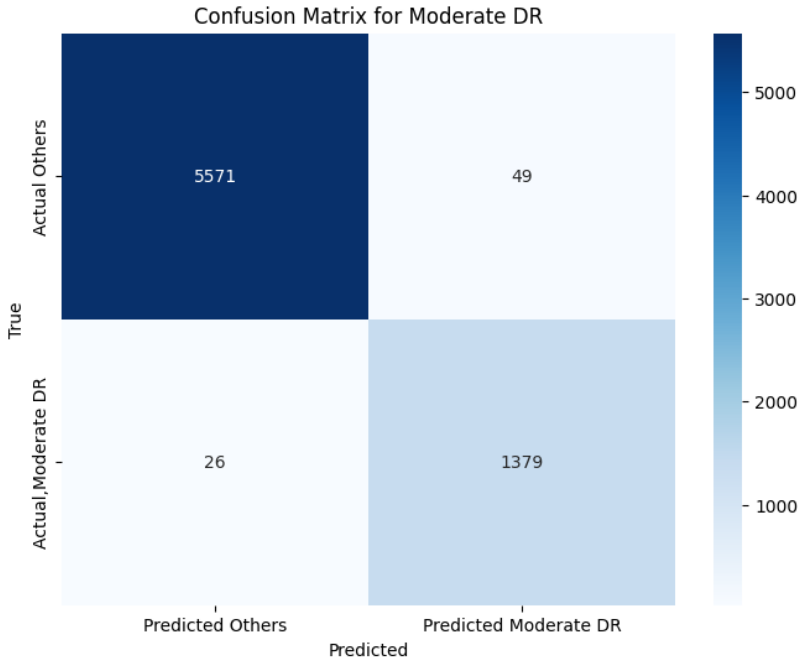
Confusion Matrix for Moderate DR
Actual Others
Actual,Moderate DR
True
5571
49
26
1379
Predicted Others
Predicted Moderate DR
Predicted
5000
4000
3000
2000
1000

(d)

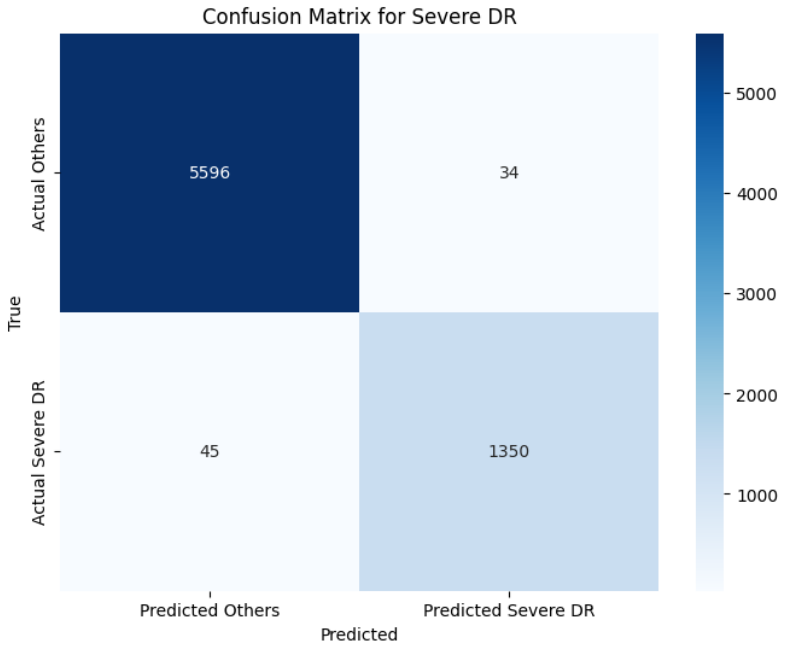
Confusion Matrix for Severe DR
Actual Others
Actual Severe DR
True
5596
34
45
1350
Predicted Others
Predicted Severe DR
Predicted
5000
4000
3000
2000
1000

(e)

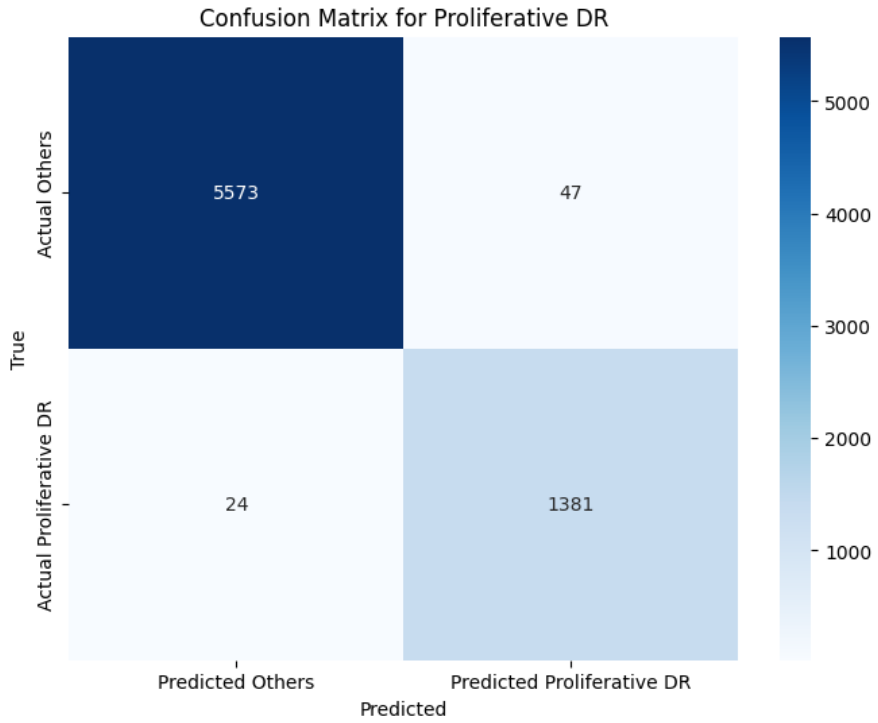

(f)

Figure 5.3: (a) The confusion matrix for the overall DR-ResNet+ model **(b)** confusion matrix for no DR **(c)** confusion matrix for Mild DR **(d)** confusion matrix for Moderate DR **(e)** confusion matrix for Severe DR **(f)** confusion matrix for Proliferative DR

Therefore, the accuracy, specificity, and sensitivity for 'Proliferative DR' can be calculated as follows:

$$Accuracy = A = \frac{TP + TN}{TP + TN + FP + FN}\ X\ 100 = 98.98\%$$

$$Sensitivity = B = \frac{TP}{TP + FN}\ X\ 100 = 98.29\%$$

$$Specificity = C = \frac{TN}{TN + FP}\ X\ 100 = 99.16\%$$

$$Precision = D = \frac{TP}{TP + FP}\ X\ 100 = 96.70\%$$

$$F1\ Score = \frac{2\ X\ (D\ X\ B)}{(D + B)} = 97.48\%$$

The effectiveness of the machine learning model in identifying “Proliferative DR” is evaluated utilizing a comprehensive set of performance indicators like accuracy, specificity, sensitivity, precision, and F1 score. In this work, a dataset of 1405 samples is used to test the model, and 1381 of these samples have “Proliferative DR” results that are positive. The proposed model is able to identify these samples with 98.98% accuracy. Similarly, the model is capable of correctly identifying negative instances i.e. the samples without “Proliferative DR” with a specificity of 99.16%. Further, the sensitivity of the proposed model is 98.29% which shows that the model is correctly identifying the vast majority of positive instances (those with “Proliferative DR”). Additionally, the precision of the model is calculated 96.70%, which shows that it correctly identified the majority of the samples classified as positive. The F1 score of the proposed model is 97.48%, which provides a sense of the overall performance of the model. The mean ROC AUC score of 0.98 for the multiclass classification of diabetic retinopathy demonstrates that it is capable of effectively differentiating between various disease severity levels. The efficiency of the proposed DR-ResNet+ model for categorizing diabetic retinopathy is shown in Table 5.1.

Table 5.1: Performance of the proposed ResNet+ model

Proposed Model	**Class**	**Accuracy**	**Specificity**	**Sensitivity/Recall**	**Precision**	**F1 score**
Proposed DR-ResNet+	No DR	0.9865	0.9922	0.9637	0.9685	0.9661
	Mild	0.9863	0.9931	0.9594	0.9719	0.9656
	Moderate	0.9893	0.9913	0.9815	0.9657	0.9735
	Severe	0.9888	0.994	0.9677	0.9754	0.9716
	Proliferative	0.9898	0.9916	0.9829	0.9670	0.9748

A number of performance indicators are taken into consideration to evaluate the effectiveness of the suggested model, including accuracy, specificity, sensitivity/recall, precision, and F1 score. For all classes, the proposed model produced high accuracy values ranging from 0.9863 to 0.9898. Additionally, all classes have high specificity values, ranging from 0.9913 to 0.994, showing that the model is effective at detecting real negatives. The model's sensitivity/recall values for the moderate and severe classes are marginally lower at 0.9594 and 0.9677, respectively. However, the model achieved

high sensitivity/recall values of 0.9815, 0.9829, and 0.9637 for the moderate, proliferative, and overall classification, respectively. For various classes the accuracy values, ranging from 0.9657 to 0.9754. This demonstrates the reliability of the model in locating positive samples. Similarly, high F1 score values for all classes ranging from 0.9656 to 0.9748 show the tradeoff between accuracy and recall.

The hyperparameter optimization procedure for a multiclass classification model trained on a dataset of diabetic retinopathy is shown in Table 5.2. For various combinations of hyperparameters, including epoch, batch size, learning rate, momentum, weight decay, batch normalization, dropout, data augmentation, optimizer, and activation function, the accuracy attained by the model is recorded in the table. It is evident that by using a lower batch size and raising the epoch improves accuracy using Adam optimizer with ReLU activation function and data augmentation. The model's accuracy varies from 63% to 99%, and certain hyperparameter values are more likely to overfit. Optimizing the functionality of the multiclass classification model for diabetic retinopathy depends critically on parameter adjustment. To find the most efficient set of hyperparameters, an intensive parameter optimization procedure is used in this work. Epoch, batch size, learning rate, momentum, weight decay, batch normalization, dropout, data augmentation, optimizer, and activation function were among the variables taken into account for optimization. A momentum of 0.9, batch normalization, and data augmentation techniques are consistently applied in all experiments to improve the model's functionality and capacity for generalization. To investigate the influence of each parameter range of values on the accuracy of the model, systematic variation is applied to each one. It has been observed during the optimization process that the accuracy of the model is significantly improved by reducing the batch size and by increasing the number of epochs. According to this result, smaller batch sizes improve generalization by decreasing the possibility of the model being stuck in local minima. In order to achieve high accuracy, the choice of optimizer and activation function is also very important. In the proposed method, the Adam optimizer with the ReLU activation function, one may improve the performance. Using data augmentation approaches, the model's resilience and generalizability are improved. The model grew more resistant to noise and variances in the test data by

adding variations and transformations to the training data, increasing its overall accuracy. In order to find the hyperparameter values that produced the greatest performance, a detailed examination of the data in Table 5.2 is performed to get the optimal balance between accuracy and overfitting. For future research to create a precise and dependable multiclass classification model for diabetic retinopathy, the results in Table 5.2 are an invaluable resource and one can choose the best set of hyperparameters to get the best model performance by using the insights gathered from the parameter optimization process.

Table 5.2: Results of a hyperparameter optimization

Epoch	Batch Size	Learning Rate	Weight Decay	Dropout	Optimizer	Activation Function	Accuracy Values	Median Accuracy	Variation
10	32	0.001	0.0001	0.2	Adam	ReLU	93, 86, 88, 87	88.5	± 2.69
10	128	0.0005	0.0001	0.3	SGD	LeakyReLU	77, 76, 75,78	76.5	± 1.11
10	256	0.0001	0.0005	0.4	RMSprop	ELU	73. 78,76, 68	72.5	± 3.37
10	512	0.00005	0.0005	0.5	Adam	ELU	65, 65, 75, 70	68.75	± 4.14
20	32	0.001	0.0001	0.2	Adam	ReLU	94 ,89, 88, 86	89.25	± 2.94
20	128	0.0005	0.0001	0.3	SGD	LeakyReLU	78, 76, 76,74	76	± 1.41
20	256	0.0001	0.0005	0.4	RMSprop	ELU	75, 78, 70,76	74.75	± 2.94
20	512	0.00005	0.0005	0.5	Adam	ELU	63, 62, 64, 68	64.25	± *2.27*
30	32	0.001	0.0001	0.2	Adam	ReLU	94, 89, 93, 94	92.5	± 2.06
30	128	0.0005	0.0001	0.3	SGD	LeakyReLU	75, 80, 84, 78	79.25	± 3.26
30	256	0.0001	0.0005	0.4	RMSprop	ELU	70, 74, 76, 87	76.25	± 6.29
30	512	0.00005	0.0005	0.5	Adam	ELU	66, 65, 60, 67	64.5	± 2.69
40	32	0.001	0.0001	0.2	Adam	ReLU	97, 96, 90,95	94.5	±2.69

40	128	0.0005	0.0001	0.3	SGD	LeakyReLU	86, 87, 89, 86	87	± 1.22
40	256	0.0001	0.0005	0.4	RMSprop	ELU	85, 86, 86, 89	86.5	± 1.5
40	512	0.00005	0.0005	0.5	Adam	ELU	76, 74, 78, 79	76.75	± 1.9
50	32	0.001	0.0001	0.2	Adam	ReLU	99. 100, 98, 99	98.7	± 0.49
50	128	0.0005	0.0001	0.3	SGD	LeakyReLU	86, 86, 84, 87	85.75	± 1.08
50	256	0.0001	0.0005	0.4	RMSprop	ELU	80, 76, 87, 79	80.5	± 4.03
50	512	0.00005	0.0005	0.5	Adam	ELU	76 , 74, 77, 76	75.75	± 1.08

5.3 Performance Evaluation of Proposed Model with Conventional Models

Conventional algorithms in DR detection and severity grading often rely on handcrafted features, rule-based systems, or traditional machine learning techniques. These approaches typically involve extracting specific image features, such as blood vessel characteristics, microaneurysm count, or lesion attributes, and utilizing classifiers or regression models to predict disease severity levels. While these algorithms have been widely used and have achieved some success, they may have limitations in handling complex image variations and capturing subtle patterns indicative of DR severity. In order to validate the model's effectiveness, its performance is compared to a variety of common techniques, including Support Vector Machines (SVMs), Random Forests, and traditional image processing procedures. These methods are both trained and implemented using the same dataset. The performance parameters considered include the area under the receiver operating characteristic curve (AUC-ROC), sensitivity, specificity, and accuracy. It has been observed that the proposed algorithms outperformed the conventional algorithms across various metrics. The proposed algorithm has demonstrated higher accuracy, sensitivity, and specificity in DR severity classification tasks. Furthermore, the AUC-ROC scores indicated superior discrimination abilities in identifying different severity levels of DR. The findings show

that the suggested algorithms may be able to predict DR severity more reliably and accurately. Additionally, qualitative evaluations demonstrated that the suggested method has the capacity to precisely detect DR severity indicators and capture fine-grained data, leading to more precise and informative segmentation and classification results compared to the conventional algorithms. The superior performance of the proposed algorithms can be attributed to their ability to automatically learn discriminative features directly from the data using deep learning architectures. The deep learning models excel in handling complex image variations and leveraging the hierarchical representation of features, which can be particularly advantageous in the context of DR severity classification.

Table 5.3 compares the DR-ResNet+ model to ResNet-8, ResNet34, Alexnet, GoogleNet, and VGG16. The table displays the performance metrics for each model, including accuracy, specificity, sensitivity, precision, and F1 score. The DR-ResNet+ model outperforms the other models in the comparison in terms of accuracy, specificity, sensitivity, precision, and F1 score.

Table 5.3: Comparison of DR-ResNet+ model with ResNet-8, ResNet34, Alexnet, GoogleNet and VGG16

Model Name	Accuracy Tested	Specificity Tested	Sensitivity Tested	Precision Tested	F1 score Tested	Ref.
ResNet-8	70	67	48	65	60	[340]
ResNet34	75	76	68	74	65	[341]
Alexnet	65	60	63	67	61	[342]
GoogleNet	67	62	76	60	79	[343]
VGG16	70	69	87	76	75	[344]
DR-ResNet+	98	99	98	96	97	Proposed

Figure 5.4 shows the comparison of the DR-ResNet+ model with five other models namely, ResNet-8 [340], ResNet34 [341], Alexnet [342], GoogleNet [343], VGG6 [344], in terms of accuracy. It is evident from the graph that the proposed DR-ResNet+ model's accuracy 25%, 30%, 32%, 45% and 47% high than ResNet34, ResNet-8, VGG16, GoogleNet and Alexnet, respectively.

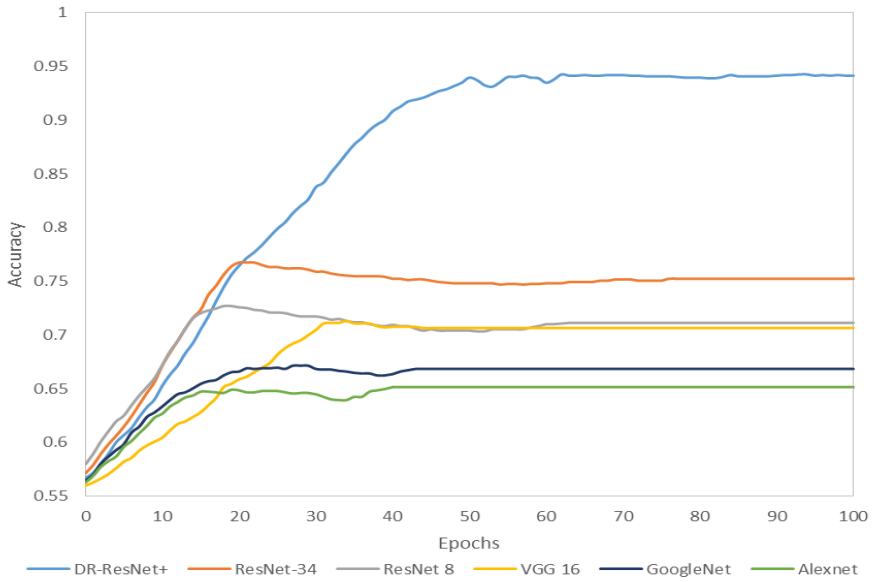

Figure 5.4: Comparison of DR-ResNet+ model with ResNet-8, ResNet34, Alexnet, GoogleNet and VGG16

Furthermore, the proposed model's accuracy is assessed using two unique datasets and three well-known diabetic retinopathy models: VGG16, GoogleNet, and AlexNet. These datasets are MESSIDOR [317] and IDRiD [308]. Figure 5.5 depicts the accuracy curve for the IDRiD dataset in relation to the number of epochs for DR severity categorization. The graph indicates that the proposed model achieves 95% accuracy over 5 epochs and approaches 99% accuracy as the epoch approaches 60. Fig. 5.6 depicts the accuracy curve for the MESSIDOR dataset. The recommended model outperforms other standard models on the MESSIDOR dataset, as it did on the IDRiD dataset. According to the graph, the recommended DR model use the MESSIDOR dataset and achieves 95% accuracy across 20 epochs. Furthermore, the model's accuracy increases with the number of epochs; after 80 epochs, the model achieves 99% accuracy. Based on the accuracy curves created with diverse datasets, the proposed model seems to be capable of correctly diagnosing DR severity levels across varied demographics and imaging circumstances. The consistent performance for both the IDRiD and MESSIDOR datasets further strengthens our claim for the robustness and generalizability of the proposed DR-ResNet+ model.

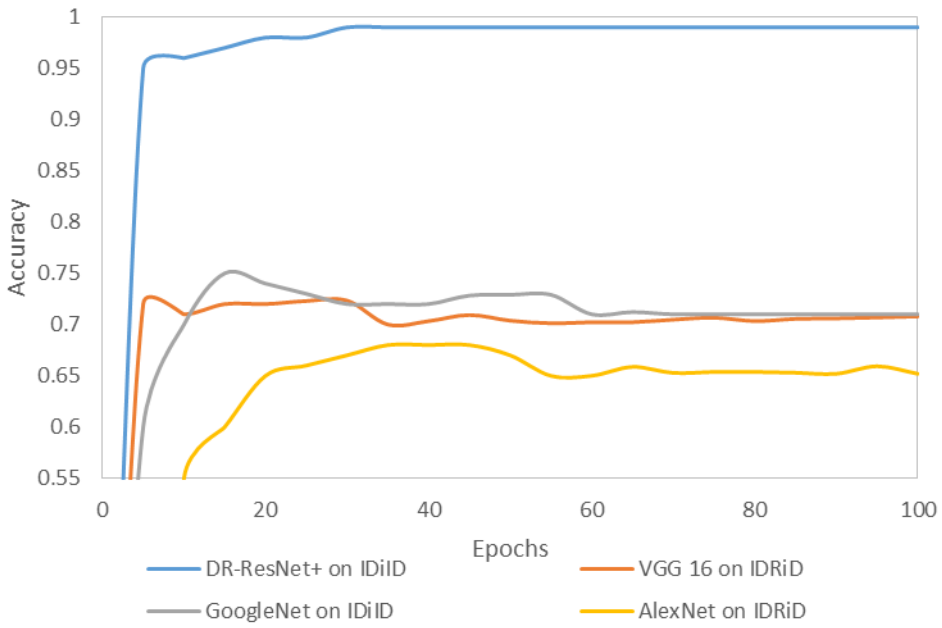

Figure 5.5: Accuracy curve for the IDRiD dataset

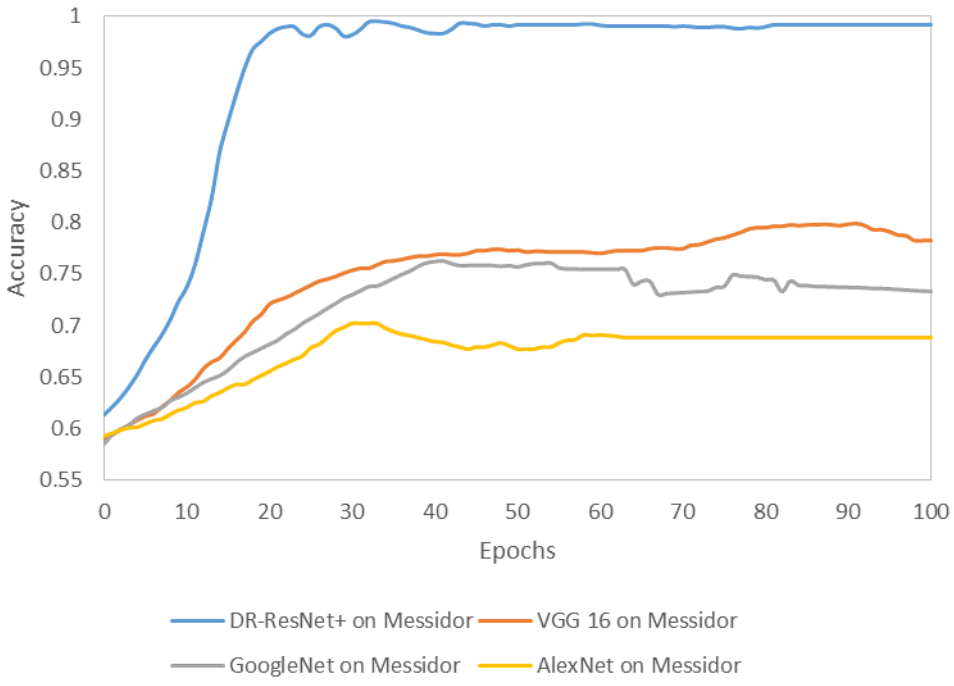

Figure 5.6: Accuracy curve for Messidor dataset

The simulated results are compared with the models presented in [345], [346], and [347] in order to verify the effectiveness of the suggested model. The models proposed in [345], [346], and [347] are referred as Model 1, Model 2, and Model 3, respectively.

The effectiveness of four different models for classifying and identifying diabetic retinopathy is compared with the proposed model as shown in Table 5.4. All these models are trained and tested with the publicly available Kaggle dataset using a high-performance graphics processor unit (GPU). It is evident from Table 5.4 that among all the models, the proposed model yields the highest degree of accuracy, specificity, precision, and F1-score, whereas Models 1 and Model 3 attain the highest levels of sensitivity. The F1-score of 97%, accuracy of 98%, specificity of 99%, sensitivity of 98%, and precision of 96% are accomplished by the proposed model. Moreover, the proposed DR-ResNet+ model saves training time by 98% as compared to the rest of the models.

Table 5.4: Comparison of the Proposed Model with existing Models

Parameters	**Model 1 [345]**	**Model 2 [346]**	**Model 3 [347]**	**Proposed Model (DR-ResNet+)**
Methodology used	Basic CNN	CNN with data augmentation	Parallel Classifiers and features learning using CNN	DR-ResNet+ with data augmentation
Dataset	Kaggle	Kaggle	Kaggle	Kaggle
Images Count	35,000	80,000	35,000	35,000
Classifier	CNN	CNN	CNN	DR-ResNet+
Accuracy	74%	75%	-	98%
Specificity	96%	-	96.37%	99%
Sensitivity	95%	95%	96.37%	98%
Precision	-	-	-	96%
F1-score	-	-	-	97%
Loss Function	0.35	0.20	0.15	0.05
Loss Interpretation	↑ (Under-fitting)	-	↓ (Over-fitting)	(Balanced)
Training Time (minutes)	120	90	60	15

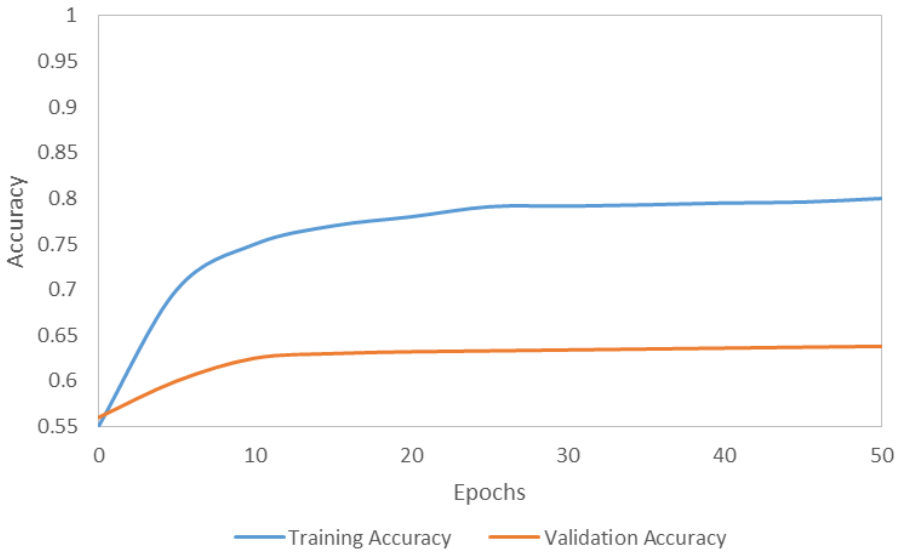

(a)

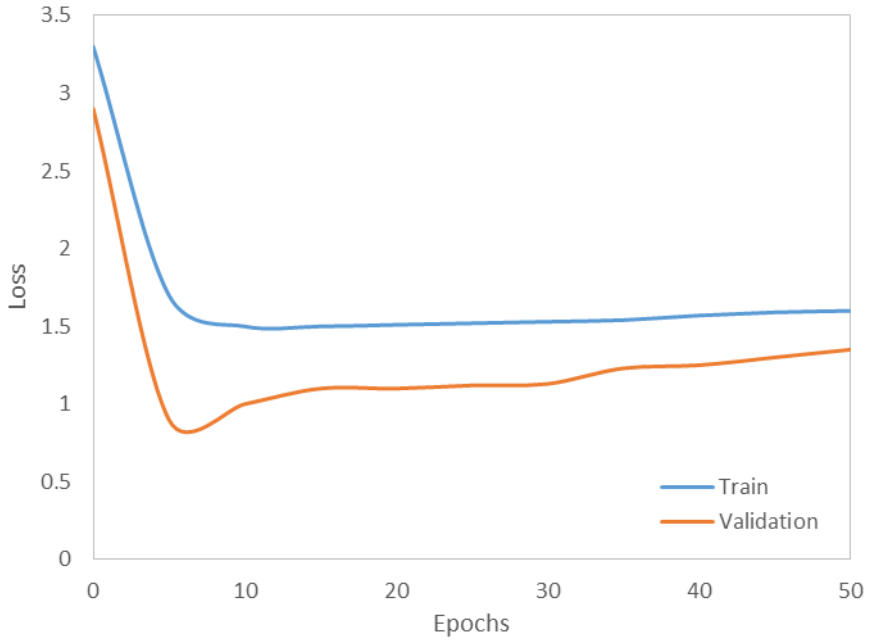

(b)

Figure 5.7 (a) Accuracy (b) Loss curve for Model-1

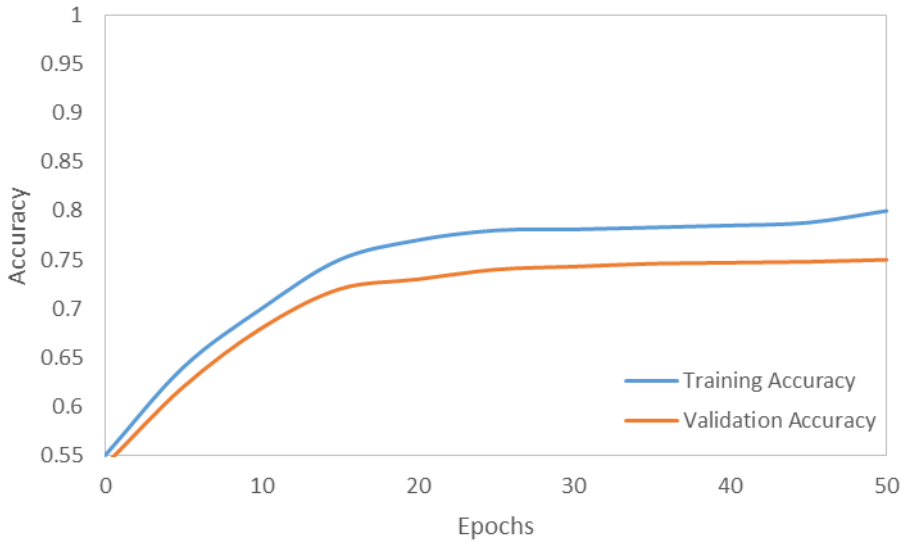

(a)

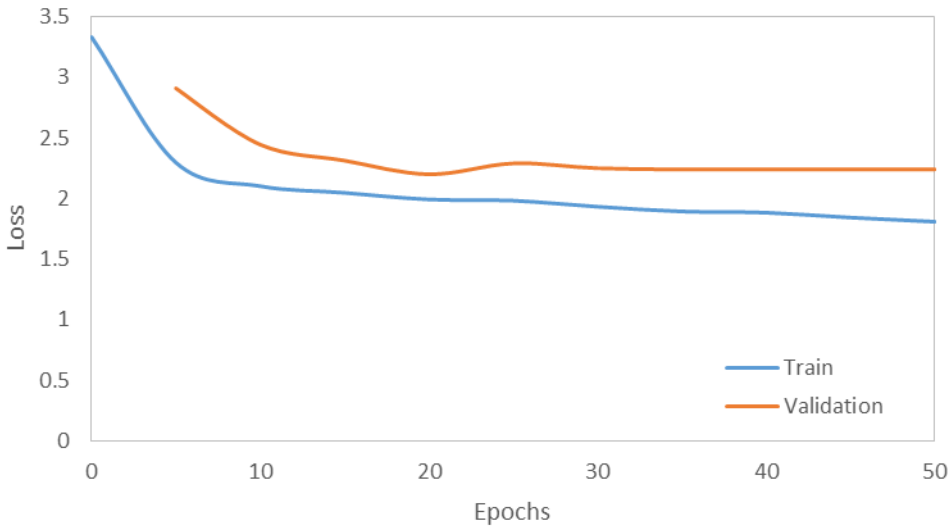

(b)

Figure 5.8: (a) Accuracy (b) Loss curve for Model-2

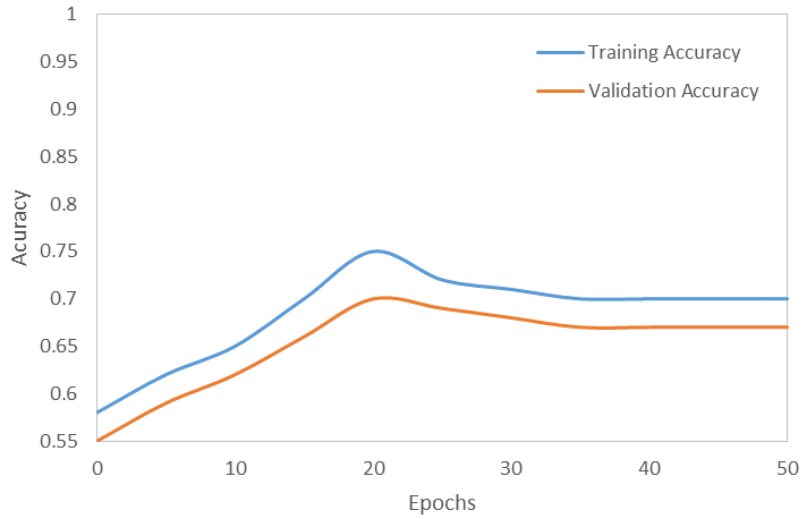

(a)

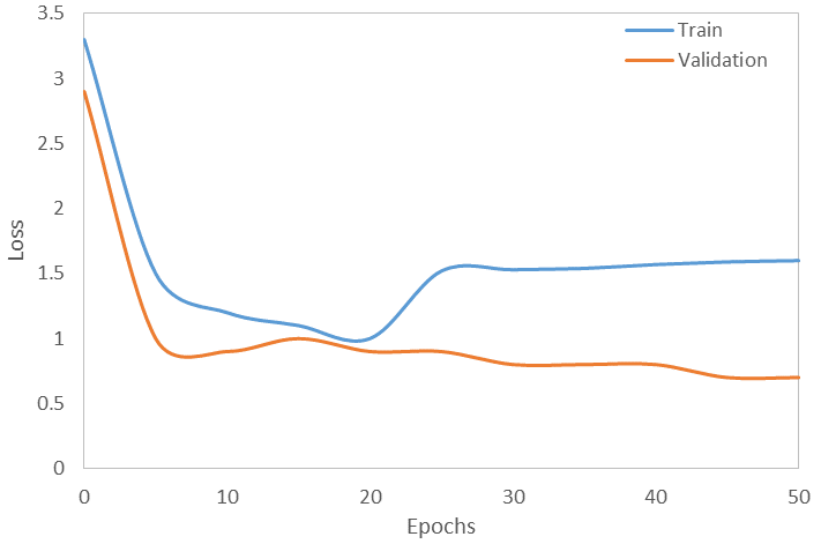

(b)

Figure 5.9: (a) Accuracy (b) loss curve for Model-3

The proposed model, Model 1, Model 2, and Model 3 accuracy and loss curves are illustrated from Fig. 5.7 to Fig. 5.9. Model 1 has a training accuracy of 80 and a validation accuracy of 63.75 throughout 50 epochs, as shown in Fig. 5.7 (a). The validation loss is 1, and the training loss is 1.6, as shown in Fig. 5.7 (b). According to Fig. 5.8 (a), Model-2 has a training accuracy of 70 and a validation accuracy of 65.8. The training and validation losses are 2 and 1.8, respectively, as shown in Fig. 5.8 (b).

According to Fig. 5.9 (a), the training and validation accuracies for Model 3 are 80 and 75, respectively, and the training and validation loss is 1.5 and 1. Figure 10 depicts the proposed DR-ResNet+ results, which may be used to compare the performance of these three models. Fig. 10(c) clearly indicates that the proposed model generates training and validation accuracy of 98 using the same dataset. Furthermore, Fig. 10(a) demonstrates that the training and validation losses are 0.2 and 0.25, respectively. The proposed model outperforms the previous three models in terms of overall accuracy and validation loss. This is due to its in-depth design, efficient regularization, and hyperparameter optimization. The proposed model's intricate design captures complex patterns, and techniques like dropout and batch normalization prevent overfitting. The careful data augmentation ensures robustness, and the use of ensemble methods broadens its learning scope. Task-specific adaptations further enhance its accuracy and reduce loss, making it the top-performing model among the options provided.

In Figure 5.10, the confusion matrix for DR-ResNet+ in binary classification provides insight into the model's performance. With 5600 true positives (TP) and 1400 true negatives (TN), the model demonstrates accurate identification of positive and negative instances. However, there are 5 false positives (FP) and 20 false negatives (FN), indicating instances where the model made incorrect predictions.

Moving to the comparisons in Figures 5.11 and 5.13, DR-ResNet+ stands out among other models. In terms of accuracy, it achieves an impressive 99.6%, surpassing logistic regression (65%), random forest (70%), SVM (75%), K-Nearest Neighbours (79%), and CNN (85%). Furthermore, the model exhibits exceptional sensitivity (99.6%), indicating its ability to correctly identify positive instances, outperforming other models like logistic regression (68%), random forest (56%), SVM (66%), K-Nearest Neighbours (56%), and CNN (79%). Additionally, DR-ResNet+ showcases high specificity (99%), highlighting its proficiency in correctly identifying negative instances compared to logistic regression (75%), random forest (75%), SVM (69%), K-Nearest Neighbours (76%), and CNN (81%).

In summary, the proposed DR-ResNet+ model excels in binary classification, demonstrating superior accuracy, sensitivity, and specificity compared to alternative models. These results suggest the model's effectiveness in accurately classifying

instances and its potential for applications where precise identification of positive and negative cases is crucial.

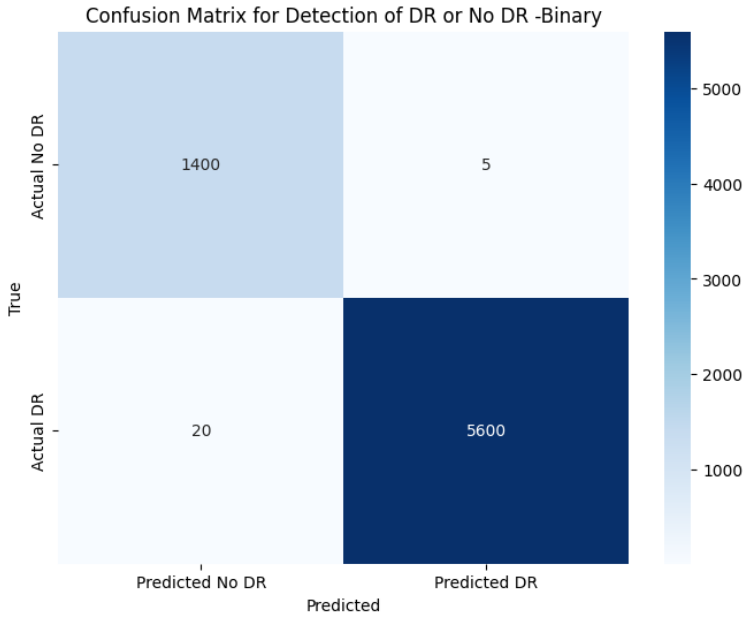

Figure 5.10: Confusion matrix for DR-ResNet+ Binary

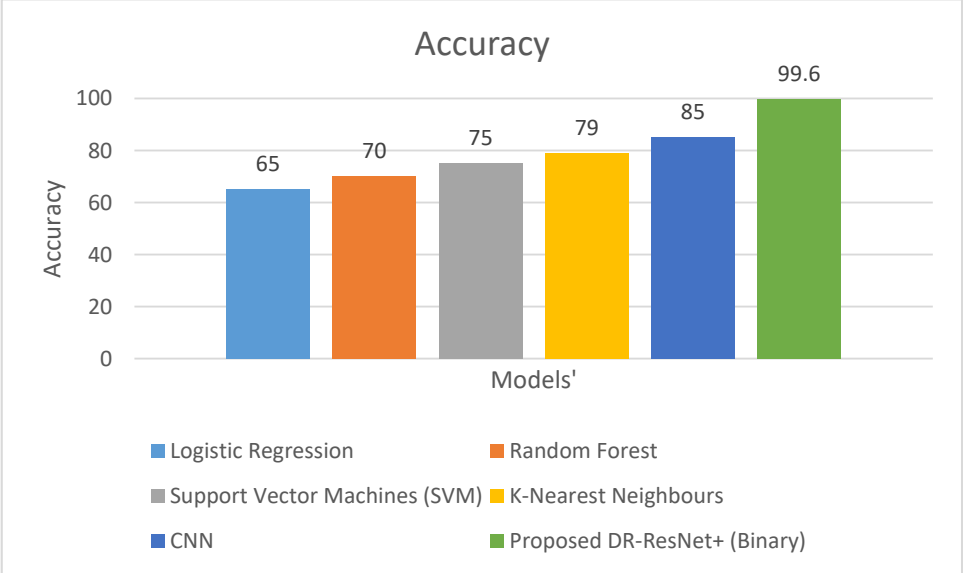

Figure 5.11: Comparison of DR-ResNet+ Accuracy (Binary) with other models

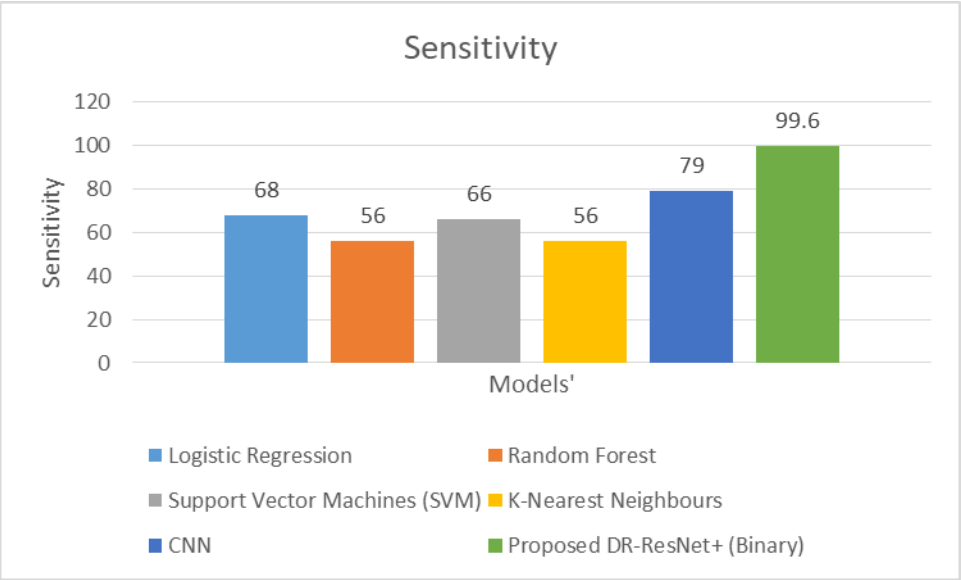

Figure 5.12: Comparison of DR-ResNet+ Sensitivity (Binary) with other models

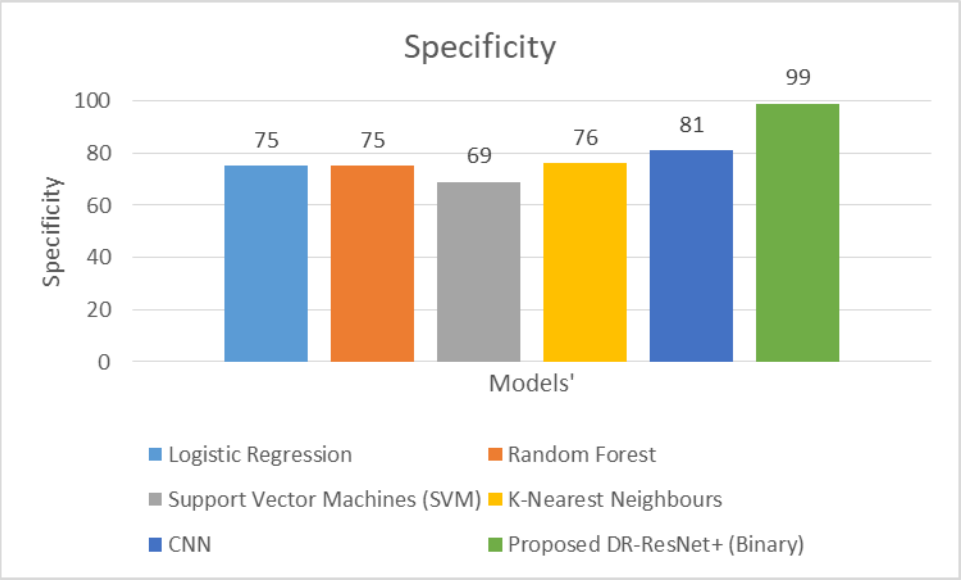

Figure 5.13: Comparison of DR-ResNet+ Specificity (Binary) with other models

Table 5.5: Comparison of DR-ResNet+ (Binary) with other models

Model Name	Accuracy	Accuracy [tested]	Sensitivity	Sensitivity [tested]	Specificity	Specificity [tested]	Ref
Logistic Regression	77	65	67	68	66	75	[348]
Random Forest	76	70	75	56	57	75	[349]
Support Vector Machines (SVM)	79	75	87	66	76	69	[350]
K-Nearest Neighbours	74	79	76	56	76	76	[351]
CNN	90	85	84	79	76	81	[352]
Proposed DR-ResNet+ (Binary)	99.6	99.6	99.6	99.6	99	99	-

Table 5.6: Comparison of severity level identified by experts and the proposed network

Image No.	Severity Level (Annotated)	Severity Level (by proposed model)
DR564	Mild	Mild
DR748	Moderate	Moderate
DR089	Mild	Mild
DR064	Proliferative	Proliferative
DR054	Proliferative	Proliferative
DR239	No DR	No DR
DR345	Mild	**No DR**
DR466	Mild	Mild
DR123	Mild	**Moderate**
DR235	Moderate	Moderate

In Table 5.6, a detailed examination of the diabetic retinopathy (DR) severity levels is presented, drawing comparisons between the annotations provided by domain expert

and the outcomes generated by the proposed model. The table captures the essence of the proposed work's focus on severity detection in fundus images and the subsequent alignment of results with expert-labelled images-SKIMS. An analysis of individual cases reveals specific discrepancies, notably in the instances of DR345 and DR123. The expert annotation for DR345 indicates mild DR, whereas the proposed network erroneously classifies it as normal i.e., No DR. Similarly, for DR123, characterized by mild DR according to experts, the proposed model misclassifies it as moderate. To validate the robustness and accuracy of the proposed model, rigorous experiments were conducted on fundus images, and the obtained results underwent meticulous verification by a domain expert. This meticulous validation process ensures the reliability of the severity level assessments, offering insights into potential areas for improvement in the proposed model's performance.

5.4 Real-world Implementation of DR-ResNet+ in Clinical Practice

The successful development and validation of DR-ResNet+ for diabetic retinopathy diagnosis opens the door to its potential integration into real-world clinical practice. In this section, Real world implementation challenges, system requirements, and integration are discussed for deploying DR-ResNet+ in clinical settings.

5.4.1 Challenges in Real-world Implementation

i. *Data Privacy and Security:* Patient data security and privacy are paramount. Compliance with data protection regulations, such as HIPAA in the United States, must be ensured.
ii. *Interoperability:* DR-ResNet+ should seamlessly integrate with existing Electronic Health Record (EHR) systems, Picture Archiving and Communication Systems (PACS), and other medical infrastructure.
iii. *Scalability:* The system should be capable of handling a high volume of retinal images generated in a clinical setting.

5.4.2 Practical Implications

i. *Early Detection and Intervention:* DR-ResNet+ can assist clinicians in early detection, enabling timely interventions and preventing vision loss in diabetic patients.
ii. *Reduced Workload:* Automation of the screening process reduces the workload on ophthalmologists, allowing them to focus on complex cases.

5.4.3 System Requirements

i. *Hardware: The* deployment requires robust hardware capable of processing large images efficiently. High-performance GPUs are recommended for real-time processing.
ii. *Software:* DR-ResNet+ software should be compatible with the hospital's IT infrastructure and EHR system.
iii. *Data Management:* An efficient data management system should be in place to handle the storage and retrieval of large image datasets.

5.4.4 Integration with Existing Medical Systems

i. *EHR Integration:* DR-ResNet+ should be seamlessly integrated into the EHR system, ensuring that results are readily available to clinicians during patient consultations.
ii. *PACS Compatibility:* Integration with PACS enables easy access to historical retinal images for longitudinal monitoring.
iii. *Clinical Decision Support:* DR-ResNet+ can serve as a clinical decision support tool, providing diagnostic recommendations to clinicians based on its predictions.

CHAPTER 6

CONCLUSION AND FUTURE SCOPE

6.1 Conclusion

This research embarked on a comprehensive exploration with the overarching aim of advancing the field of diabetic retinopathy (DR) detection and severity grading through the development and validation of a novel deep learning architecture. Each research objective was comprehensively addressed, leading to significant contributions in the field.

The primary objective was to create an algorithm for the detection of diabetic retinopathy using retinal images. The development of DR-ResNet+ has yielded an advanced algorithm for the effective detection of diabetic retinopathy (DR) from retinal images. Utilizing cutting-edge machine learning techniques, this model accurately identifies critical retinal features associated with DR, providing a robust and reliable solution for early-stage detection.

Building upon the initial objective, the second goal was to design an algorithm capable of classifying and grading retinal images for the detection of diabetic retinopathy. DR-ResNet+ was further refined to classify and grade DR severity levels, categorizing images from no DR to severe proliferative DR. This capability provides detailed insight into the disease's progression, allowing for targeted intervention and effective management strategies. The model's classification accuracy underscores its robustness in handling various DR severity levels.

To enhance clinical utility, the third objective focused on optimizing sensitivity, specificity, and accuracy of the proposed algorithm. Extensive optimization led to notable improvements in the model's performance metrics. DR-ResNet+ achieved a high level of sensitivity, specificity, and overall accuracy, ensuring reliable differentiation between healthy and DR-affected retinas. This optimized performance enhances the diagnostic utility of the model in real-world clinical settings.

The last objective sought to validate the proposed algorithms by comparing their performance with conventional algorithms. Through rigorous comparative analysis with well-known deep learning models like GoogleNet, VGG16, and Alexnet, DR-ResNet+ emerged as a frontrunner, emphasizing its efficacy in addressing the intricacies associated with DR diagnosis. The implementation of DR-ResNet+ resulted in a significant leap forward in the field of diabetic retinopathy diagnosis. The model's exceptional accuracy and robustness, as demonstrated by its performance metrics, position it as a state-of-the-art solution for automated diagnosis and severity grading. The model's overall accuracy of 98.98% signifies its ability to reliably identify diabetic retinopathy, while its high specificity 99.16% and sensitivity 98.29% underscore its capacity to differentiate between normal and abnormal retinal conditions. By comparing DR-ResNet+ with established deep learning models on the same dataset, it became evident that the proposed architecture outperforms its counterparts. The reduction in training time by 98% further solidifies its suitability for real-time clinical applications. Validation on external datasets, including Messidor and IDRiD, revealed the model's generalizability and robustness. The consistently superior performance across diverse datasets reinforces the reliability of DR-ResNet+ in real-world scenarios. The successful development and validation of DR-ResNet+ hold significant implications for clinical practice and patient care. The model's accuracy and efficiency make it a valuable tool. The ability of DR-ResNet+ to accurately categorize different severity levels of diabetic retinopathy facilitates early diagnosis, enabling timely medical interventions. This, in turn, has the potential to prevent or mitigate the progression of the disease, ultimately improving patient outcomes. The substantial reduction in training time enhances the feasibility of incorporating DR-ResNet+ into real-time clinical applications. This is particularly advantageous in busy healthcare settings where timely decision-making is crucial.

6.2 Future Scope

While DR-ResNet+ has achieved promising results, further advancements can enhance its utility and broaden its applicability. The future directions for this research include:

1. **Incorporating Additional Clinical Data**: Future studies could integrate patient demographics, medical history, laboratory results, and genetic markers to enhance the model's predictive value. Incorporating these clinical factors could enable a more comprehensive assessment, moving towards a holistic approach to DR diagnosis.

2. **Extension to Other Retinal Diseases**: Expanding DR-ResNet+ to detect and grade additional retinal diseases, such as age-related macular degeneration and glaucoma, could make it a versatile tool for comprehensive retinal disease screening, thus improving its clinical relevance.

3. **Real-Time Application and Optimization**: Efforts to further reduce processing time and optimize computational efficiency will make DR-ResNet+ more feasible for real-time diagnosis in busy clinical settings. Reducing latency in prediction could facilitate immediate diagnostic feedback during patient consultations.

4. **Development of a User-Friendly Clinical Interface**: Creating an intuitive interface for healthcare providers would streamline DR-ResNet+'s integration into clinical workflows. User-friendly software, potentially compatible with existing electronic health record (EHR) systems, would encourage widespread adoption and ease of use in healthcare environments.

5. **Validation through Clinical Trials**: To establish clinical efficacy, prospective clinical trials should be conducted to evaluate DR-ResNet+'s performance across diverse patient populations. This external validation would provide valuable insights into its real-world impact and reliability, supporting regulatory approval and eventual clinical deployment.

In conclusion, this research has successfully addressed the outlined objectives, culminating in the development and validation of DR-ResNet+, a powerful deep learning model for the automated diagnosis and severity grading of diabetic retinopathy. The model's exceptional performance, validated across multiple datasets, establishes it as a frontrunner in the field. As we look ahead, the integration of additional clinical parameters offers exciting prospects for further refinement, ensuring continued progress in the early detection and management of diabetic retinopathy. The journey undertaken in this research has not only expanded our understanding of diabetic retinopathy but has also contributed a practical and effective tool for the medical community. DR-ResNet+ stands as a testament to the potential of artificial intelligence in revolutionizing healthcare, paving the way for improved patient outcomes and more efficient clinical practices.

REFERENCES

[1] Bynum, W. F., & Porter, R. (Eds.). (1993). *Medicine and the five senses*. Cambridge University Press.

[2] Meister, M., & Berry, M. J. (1999). The neural code of the retina. *neuron*, *22*(3), 435-450.

[3] Sharma, S., Oliver-Fernandez, A., Liu, W., Buchholz, P., & Walt, J. (2005). The impact of diabetic retinopathy on health-related quality of life. *Current opinion in ophthalmology*, *16*(3), 155-159.

[4] *Eye Anatomy 1 Illustration*. (n.d.). Carlson Stock Art. https://www.carlsonstockart.com/photo/human-eye-anatomy-illustration-1/

[5] Cholkar, K., Dasari, S. R., Pal, D., & Mitra, A. K. (2013). Eye: Anatomy, physiology and barriers to drug delivery. In *Ocular transporters and receptors* (pp. 1-36). Woodhead publishing.

[6] Alipio, Z., Liao, W., Roemer, E. J., Waner, M., Fink, L. M., Ward, D. C., & Ma, Y. (2010). Reversal of hyperglycemia in diabetic mouse models using induced-pluripotent stem (iPS)-derived pancreatic β-like cells. *Proceedings of the National Academy of Sciences*, *107*(30), 13426-13431.

[7] Enes, P., Panserat, S., Kaushik, S., & Oliva-Teles, A. A. (2009). Nutritional regulation of hepatic glucose metabolism in fish. *Fish physiology and biochemistry*, *35*, 519-539.

[8] Lotfy, M., Adeghate, J., Kalasz, H., Singh, J., & Adeghate, E. (2017). Chronic complications of diabetes mellitus: a mini review. *Current diabetes reviews*, *13*(1), 3-10.

[9] McCaa, C. S. (1982). The eye and visual nervous system: anatomy, physiology and toxicology. *Environmental health perspectives*, *44*, 1-8.

[10] Nishida, T., & Saika, S. (2010). Cornea and sclera: anatomy and physiology. *Cornea*, *1*, 3-24.

[11] Remington, L. A., & Goodwin, D. (2004). *Clinical Anatomy of the Visual System E-Book: Clinical Anatomy of the Visual System E-Book*. Elsevier Health Sciences.

[12] Branchini, L. A., Adhi, M., Regatieri, C. V., Nandakumar, N., Liu, J. J., Laver, N., ... & Duker, J. S. (2013). Analysis of choroidal morphologic features and vasculature in healthy eyes using spectral-domain optical coherence tomography. *Ophthalmology*, *120*(9), 1901-1908.

[13] Bernstein, P. S., Li, B., Vachali, P. P., Gorusupudi, A., Shyam, R., Henriksen, B. S., & Nolan, J. M. (2016). Lutein, zeaxanthin, and meso-zeaxanthin: The basic and clinical science underlying carotenoid-based nutritional interventions against ocular disease. *Progress in retinal and eye research*, *50*, 34-66.

[14] Wildes, R. P. (1997). Iris recognition: an emerging biometric technology. *Proceedings of the IEEE*, *85*(9), 1348-1363.

[15] Ross, A. (2010). Iris recognition: The path forward. *Computer*, *43*(2), 30-35.

[16] Bill, A. N. D. E. R. S. (1975). Blood circulation and fluid dynamics in the eye. *Physiological reviews*, *55*(3), 383-417.

[17] Kolb, H. (2003). How the retina works: Much of the construction of an image takes place in the retina itself through the use of specialized neural circuits. *American scientist*, *91*(1), 28-35.

[18] Kolb, H. (2003). How the retina works: Much of the construction of an image takes place in the retina itself through the use of specialized neural circuits. *American scientist*, *91*(1), 28-35.

[19] Carter-Dawson, L. D., & Lavail, M. M. (1979). Rods and cones in the mouse retina. I. Structural analysis using light and electron microscopy. *Journal of Comparative Neurology*, *188*(2), 245-262.

[20] Thoreson, W. B., & Dacey, D. M. (2019). Diverse cell types, circuits, and mechanisms for color vision in the vertebrate retina. *Physiological reviews*.

[21] Provis, J. M., Dubis, A. M., Maddess, T., & Carroll, J. (2013). Adaptation of the central retina for high acuity vision: cones, the fovea and the avascular zone. *Progress in retinal and eye research*, *35*, 63-81.

[22] Hendee, W. R., & Wells, P. N. (1997). *The perception of visual information*. Springer Science & Business Media.

[23] Weng, J., Luo, J., Cheng, X., Jin, C., Zhou, X., Qu, J., ... & Liu, M. (2008). Deletion of G protein-coupled receptor 48 leads to ocular anterior segment dysgenesis (ASD) through down-regulation of Pitx2. *Proceedings of the National Academy of Sciences*, *105*(16), 6081-6086.

[24] Weng, Y., Liu, J., Jin, S., Guo, W., Liang, X., & Hu, Z. (2017). Nanotechnology-based strategies for treatment of ocular disease. *Acta pharmaceutica sinica B*, *7*(3), 281-291.

[25] Paunescu, L. A., Schuman, J. S., Price, L. L., Stark, P. C., Beaton, S., Ishikawa, H., ... & Fujimoto, J. G. (2004). Reproducibility of nerve fiber thickness, macular thickness, and optic nerve head measurements using StratusOCT. *Investigative ophthalmology & visual science*, *45*(6), 1716-1724.

[26] Jonas, J. B., Budde, W. M., & Panda-Jonas, S. (1999). Ophthalmoscopic evaluation of the optic nerve head. *Survey of ophthalmology*, *43*(4), 293-320.

[27] Shrier, E. M., Adam, C. R., Spund, B., Glazman, S., & Bodis-Wollner, I. (2012). Interocular asymmetry of foveal thickness in Parkinson disease. *Journal of ophthalmology*, *2012*.

[28] Rossi, E. A., & Roorda, A. (2010). The relationship between visual resolution and cone spacing in the human fovea. *Nature neuroscience*, *13*(2), 156-157.

[29] Dubis, A. M., Hansen, B. R., Cooper, R. F., Beringer, J., Dubra, A., & Carroll, J. (2012). Relationship between the foveal avascular zone and foveal pit morphology. *Investigative Ophthalmology & Visual Science*, *53*(3), 1628-1636.

[30] Provis, J. M., Dubis, A. M., Maddess, T., & Carroll, J. (2013). Adaptation of the central retina for high acuity vision: cones, the fovea and the avascular zone. *Progress in retinal and eye research*, *35*, 63-81.

[31] Varma, R., Skaf, M., & Barron, E. (1996). Retinal nerve fiber layer thickness in normal human eyes. *Ophthalmology*, *103*(12), 2114-2119.

[32] Straatsma, B. R., Landers, M. B., & Kreiger, A. E. (1968). The ora serrata in the adult human eye. *Archives of Ophthalmology*, *80*(1), 3-20.

[33] "Retina," *TheFreeDictionary.com*. https://medical-dictionary.thefreedictionary.com/Retina (accessed Aug. 01, 2023).

[34] Marmorstein, A. D. (2001). The polarity of the retinal pigment epithelium. *Traffic*, *2*(12), 867-872.

[35] Raviola, G. (1977). The structural basis of the blood-ocular barriers. *Experimental eye research*, *25*, 27-63.

[36] Sekaran, S., Foster, R. G., Lucas, R. J., & Hankins, M. W. (2003). Calcium imaging reveals a network of intrinsically light-sensitive inner-retinal neurons. *Current biology*, *13*(15), 1290-1298.

[37] Zrenner, E. (2002). Will retinal implants restore vision?. *Science*, *295*(5557), 1022-1025.

[38] Timberlake, G. T., Mainster, M. A., Peli, E., Augliere, R. A., Essock, E. A., & Arend, L. E. (1986). Reading with a macular scotoma. I. Retinal location of scotoma and fixation area. *Investigative ophthalmology & visual science*, *27*(7), 1137-1147.

[39] Schalch, W. (1992). Carotenoids in the retina—a review of their possible role in preventing or limiting damage caused by light and oxygen. *Free radicals and aging*, 280-298.

[40] Aquino, A. (2014). Establishing the macular grading grid by means of fovea centre detection using anatomical-based and visual-based features. *Computers in biology and medicine*, *55*, 61-73.

[41] Fairchild, M. D. (2013). *Color appearance models*. John Wiley & Sons.

[42] Quigley, H. A., & Green, W. R. (1979). The histology of human glaucoma cupping and optic nerve damage: clinicopathologic correlation in 21 eyes. *Ophthalmology*, *86*(10), 1803-1827.

[43] Auw-Haedrich, C., Staubach, F., & Witschel, H. (2002). Optic disk drusen. *Survey of ophthalmology*, *47*(6), 515-532.

[44] Rieke, F., & Baylor, D. A. (1998). Single-photon detection by rod cells of the retina. *Reviews of Modern Physics*, *70*(3), 1027.

[45] Fong, D. S., Aiello, L., Gardner, T. W., King, G. L., Blankenship, G., Cavallerano, J. D., ... & American Diabetes Association. (2003). Diabetic retinopathy. *Diabetes care*, *26*(suppl_1), s99-s102.

[46] Kollias, A. N., & Ulbig, M. W. (2010). Diabetic retinopathy: early diagnosis and effective treatment. *Deutsches Arzteblatt International*, *107*(5), 75.

[47] Aiello, L. P. (2002). The potential role of PKC β in diabetic retinopathy and macular edema. *Survey of ophthalmology*, *47*, S263-S269.

[48] Kollias, A. N., & Ulbig, M. W. (2010). Diabetic retinopathy: early diagnosis and effective treatment. *Deutsches Arzteblatt International*, *107*(5), 75.

[49] Diabetic Retinopathy - First Eye Care Irving, *First Eye Care Irving*. https://firsteyecareirving.com/eye-and-vision-health/eye-diseases/diabetic-retinopathy/ (accessed Aug. 01, 2023).

[50] Johnson, M. W. (2009). Etiology and treatment of macular edema. *American journal of ophthalmology*, *147*(1), 11-21.

[51] Suriyasekeran, K., Santhanamahalingam, S., & Duraisamy, M. (2021). Algorithms for diagnosis of diabetic retinopathy and diabetic macula edema-a review. *Diabetes: from Research to Clinical Practice: Volume 4*, 357-373.

[52] Kempen, J. H., Sugar, E. A., Jaffe, G. J., Acharya, N. R., Dunn, J. P., Elner, S. G., ... & Multicenter Uveitis Steroid Treatment (MUST) Trial Research Group. (2013).

Fluorescein angiography versus optical coherence tomography for diagnosis of uveitic macular edema. *Ophthalmology*, *120*(9), 1852-1859.

[53] "Diabetic macular edema," *Mayo Clinic*. https://www.mayoclinic.org/diseases-conditions/diabetic-retinopathy/multimedia/diabetic-macular-edema/img-20124558 (accessed Aug. 01, 2023).

[54] Parmeggiani, F., Romano, M. R., Costagliola, C., Semeraro, F., Incorvaia, C., D'Angelo, S., ... & Sebastiani, A. (2012). Mechanism of inflammation in age-related macular degeneration. *Mediators of inflammation*, *2012*.

[55] Wang, M., Munch, I. C., Hasler, P. W., Prünte, C., & Larsen, M. (2008). Central serous chorioretinopathy. *Acta ophthalmologica*, *86*(2), 126-145.

[56] Bhutto, I., & Lutty, G. (2012). Understanding age-related macular degeneration (AMD): relationships between the photoreceptor/retinal pigment epithelium/Bruch's membrane/choriocapillaris complex. *Molecular aspects of medicine*, *33*(4), 295-317.

[57] Schmidt-Erfurth, U., & Hasan, T. (2000). Mechanisms of action of photodynamic therapy with verteporfin for the treatment of age-related macular degeneration. *Survey of ophthalmology*, *45*(3), 195-214.

[58] "Macular Degeneration," *Centre for Sight UK Laser Eye Surgery and Vision Correction*. https://www.centreforsight.com/eye-conditions/macular-degeneration (accessed Aug. 01, 2023).

[59] Richa, S., & Yazbek, J. C. (2010). Ocular adverse effects of common psychotropic agents: a review. *CNS drugs*, *24*, 501-526.

[60] Barkhordar, Y. THE EFFECTS OF VISUAL DEFICIENCIES ON THE TASK OF TRANSLATION.

[61] Beebe, D. C., Holekamp, N. M., & Shui, Y. B. (2010). Oxidative damage and the prevention of age-related cataracts. *Ophthalmic research*, *44*(3), 155-165.

[62] J. Hann, “Causes of Early Onset Cataracts - Eastside Eye,” *Eastside Eye*, Feb. 28, 2021. https://www.eastsideeye.com.au/2021/03/01/causes-of-early-onset-cataracts/ (accessed Aug. 01, 2023).

[63] Margo, C. E., & Harman, L. E. (2023). Conjunctivitis: A Primer on Conjunctival Biopsy and Approach to Histopathologic Diagnosis. *Advances in Anatomic Pathology*, 10-1097.

[64] Cronau, H., Kankanala, R. R., & Mauger, T. (2010). Diagnosis and management of red eye in primary care. *American family physician*, *81*(2), 137-144.

[65] “Conjunctivitis: open your eyes to the facts!,” *WebMed Pharmacy - FREE next day UK delivery*, Oct. 19, 2017. https://webmedpharmacy.co.uk/blog/2017/10/conjunctivitis-causes-and-treatment (accessed Aug. 01, 2023).

[66] Bhowmik, D., Kumar, K. S., Deb, L., Paswan, S., & Dutta, A. S. (2012). Glaucoma-A Eye Disorder Its Causes, Risk Factor, Prevention and Medication. *The Pharma Innovation*, *1*(1, Part A), 66.

[67] Hou, R., Zhang, Z., Yang, D., Wang, H., Chen, W., Li, Z., ... & Wang, N. (2016). Intracranial pressure (ICP) and optic nerve subarachnoid space pressure (ONSP) correlation in the optic nerve chamber: the Beijing Intracranial and Intraocular Pressure (iCOP) study. *brain research*, *1635*, 201-208.

[68] Sampaolesi, R., Sampaolesi, J. R., & Zárate, J. (2013). *The Glaucomas: Volume II-Open angle glaucoma and angle closure glaucoma* (Vol. 2). Springer Science & Business Media.

[69] T. E. Experts, “7 Facts You Should Know About Glaucoma,” *True Eye Experts*, Jan. 29, 2014. https://trueeye.com/7-facts-you-should-know-about-glaucoma/ (accessed Aug. 01, 2023).

[70] Vallabha, D., Dorairaj, R., Namuduri, K., & Thompson, H. (2004, November). Automated detection and classification of vascular abnormalities in diabetic retinopathy. In *Conference Record of the Thirty-Eighth Asilomar Conference on Signals, Systems and Computers, 2004.* (Vol. 2, pp. 1625-1629). IEEE.

[71] Matsunaga, D. R., Yi, J. J., De Koo, L. O., Ameri, H., Puliafito, C. A., & Kashani, A. H. (2015). Optical coherence tomography angiography of diabetic retinopathy in human subjects. *Ophthalmic Surgery, Lasers and Imaging Retina*, *46*(8), 796-805.

[72] Mustafa, W. A., Abdul-Nasir, A. S., & Yazid, H. (2018, June). Diabetic retinopathy (DR) on retinal image: A pilot study. In *Journal of Physics: Conference Series* (Vol. 1019, No. 1, p. 012021). IOP Publishing.

[73] Silvia, R. C., & Vijayalakshmi, R. (2013, February). Detection of Non-Proliferative Diabetic Retinopathy in fundus images of the human retina. In *2013 International Conference on Information Communication and Embedded Systems (ICICES)* (pp. 978-983). IEEE.

[74] Cai, J., & Boulton, M. (2002). The pathogenesis of diabetic retinopathy: old concepts and new questions. *Eye*, *16*(3), 242-260.

[75] "Non Proliferative Diabetic Retinopathy," https://eyepatient.net/Home/articledetail/non-proliferative-diabetic-retinopathy-181 (accessed Aug. 01, 2023).

[76] *Diabetic Retinopathy | Houston Retina Associates | Houston Texas*. https://www.hretina.com/patient-resources/retinal-conditions/diabetic-retinopathy (accessed Aug. 01, 2023).

[77] M. Abdullah, M. M. Fraz, and S. A. Barman, "Localization and segmentation of optic disc in retinal images using circular Hough transform and grow-cut algorithm," *PeerJ*, May 10, 2016. https://peerj.com/articles/2003 (accessed Aug. 01, 2023).

[78] Venkataraman, S. T., Flanagan, J. G., & Hudson, C. (2010). Vascular reactivity of optic nerve head and retinal blood vessels in glaucoma—a review. *Microcirculation*, *17*(7), 568-581.

[79] Cogan, D. G., Toussaint, D., & Kuwabara, T. (1961). Retinal vascular patterns: IV. Diabetic retinopathy. *Archives of ophthalmology*, *66*(3), 366-378.

[80] De Carlo, T. E., Chin, A. T., Bonini Filho, M. A., Adhi, M., Branchini, L., Salz, D. A., ... & Waheed, N. K. (2015). Detection of microvascular changes in eyes of patients with diabetes but not clinical diabetic retinopathy using optical coherence tomography angiography. *Retina*, *35*(11), 2364-2370.

[81] Augustin, A. J. (Ed.). (2015). *Intravitreal Steroids* (No. 12023). Springer International Publishing.

[82] Akram, M. U., Khalid, S., & Khan, S. A. (2013). Identification and classification of microaneurysms for early detection of diabetic retinopathy. *Pattern recognition*, *46*(1), 107-116.

[83] Faust, O., Acharya U, R., Ng, E. Y. K., Ng, K. H., & Suri, J. S. (2012). Algorithms for the automated detection of diabetic retinopathy using digital fundus images: a review. *Journal of medical systems*, *36*, 145-157.

[84] Verma, S. B., & Yadav, A. K. (2019). Detection of hard exudates in retinopathy images. *ADCAIJ: Advances in Distributed Computing and Artificial Intelligence Journal*, *8*(4), 41-48.

[85] Zhang, S. X., Ma, J. H., Bhatta, M., Fliesler, S. J., & Wang, J. J. (2015). The unfolded protein response in retinal vascular diseases: implications and therapeutic potential beyond protein folding. *Progress in Retinal and eye Research*, *45*, 111-131.

[86] L. Biscaldi, "Discontinuing Treatments for Diabetic Retinopathy May Increase Neovascularization," Ophthalmology Advisor, Jul. 20, 2021. https://www.ophthalmologyadvisor.com/topics/systemic-ophthalmology/diabetic-retinopathy-neovascularization-panretinal-laser-photocoagulation-antivegf-pride-study-follow-up/ (accessed Aug. 01, 2023).

[87] Taylor, H. R., & Keeffe, J. E. (2001). World blindness: a 21st century perspective. *British journal of ophthalmology*, *85*(3), 261-266.

[88] Cunha-Vaz, J. G. (2011). *Diabetic retinopathy*. World Scientific.

[89] Bruce, B. B., Lamirel, C., Biousse, V., Ward, A., Heilpern, K. L., Newman, N. J., & Wright, D. W. (2011). Feasibility of nonmydriatic ocular fundus photography in the emergency department: phase I of the FOTO-ED study. *Academic Emergency Medicine*, *18*(9), 928-933.

[90] Spaide, R. F., Klancnik, J. M., & Cooney, M. J. (2015). Retinal vascular layers imaged by fluorescein angiography and optical coherence tomography angiography. *JAMA ophthalmology*, *133*(1), 45-50.

[91] Aumann, S., Donner, S., Fischer, J., & Müller, F. (2019). Optical coherence tomography (OCT): principle and technical realization. *High resolution imaging in microscopy and ophthalmology: new frontiers in biomedical optics*, 59-85.

[92] Dong, Z. M., Wollstein, G., Wang, B., & Schuman, J. S. (2017). Adaptive optics optical coherence tomography in glaucoma. *Progress in retinal and eye research*, *57*, 76-88.

[93] Bennett, T. J., & Barry, C. J. (2009). Ophthalmic imaging today: an ophthalmic photographer's viewpoint–a review. *Clinical & experimental ophthalmology*, *37*(1), 2-13.

[94] Alabboud, I., Muyo, G., Gorman, A., Mordant, D., McNaught, A., Petres, C., ... & Harvey, A. R. (2007, June). New spectral imaging techniques for blood oximetry in the retina. In *European Conference on Biomedical Optics* (p. 6631_22). Optica Publishing Group.

[95] Schmitz-Valckenberg, S., Holz, F. G., Bird, A. C., & Spaide, R. F. (2008). Fundus autofluorescence imaging: review and perspectives. *Retina*, *28*(3), 385-409.

[96] Shoughy, S. S., Arevalo, J. F., & Kozak, I. (2015). Update on wide-and ultra-widefield retinal imaging. *Indian Journal of Ophthalmology*, *63*(7), 575.

[97] Morello, C. M. (2007). Etiology and natural history of diabetic retinopathy: an overview. *American Journal of Health-System Pharmacy*, *64*(17_Supplement_12), S3-S7.

[98] Coyne, K. S., Margolis, M. K., Kennedy-Martin, T., Baker, T. M., Klein, R., Paul, M. D., & Revicki, D. A. (2004). The impact of diabetic retinopathy: perspectives from patient focus groups. *Family practice*, *21*(4), 447-453.

[99] Sendrowski, D. P., & Bronstein, M. A. (2010). Current treatment for vitreous floaters. *Optometry-Journal of the American Optometric Association*, *81*(3), 157-161.

[100] Khairallah, H., Alazzawi, L., & Sarhan, N. (2019). Mobile Smart Screening and Remote Monitoring for Vision Loss Diseases. *Eye*, *8*(10).

[101] Gordon, R., & Chatfield, R. K. (1969). Pits in the optic disc associated with macular degeneration. *The British Journal of Ophthalmology*, *53*(7), 481.

[102] Klein, R., Klein, B. E., & Moss, S. E. (1992). Epidemiology of proliferative diabetic retinopathy. *Diabetes care*, *15*(12), 1875-1891.

[103] Feldman-Billard, S., Larger, É., & Massin, P. (2018). Early worsening of diabetic retinopathy after rapid improvement of blood glucose control in patients with diabetes. *Diabetes & metabolism*, *44*(1), 4-14.

[104] Yau, J. W., Rogers, S. L., Kawasaki, R., Lamoureux, E. L., Kowalski, J. W., Bek, T., ... & Meta-Analysis for Eye Disease (META-EYE) Study Group. (2012). Global prevalence and major risk factors of diabetic retinopathy. *Diabetes care*, *35*(3), 556-564.

[105] Fruchart, J. C., Sacks, F., Hermans, M. P., Assmann, G., Brown, W. V., Ceska, R., ... & Residual Risk Reduction Initiative. (2008). The Residual Risk Reduction Initiative: a call to action to reduce residual vascular risk in patients with dyslipidemia. *The American journal of cardiology*, *102*(10), 1K-34K.

[106] Fong, D. S., Aiello, L., Gardner, T. W., King, G. L., Blankenship, G., Cavallerano, J. D., ... & American Diabetes Association. (2003). Diabetic retinopathy. *Diabetes care*, *26*(suppl_1), s99-s102.

[107] Morrison, J. L., Hodgson, L. A., Lim, L. L., & Al-Qureshi, S. (2016). Diabetic retinopathy in pregnancy: a review. *Clinical & experimental ophthalmology*, *44*(4), 321-334.

[108] Yau, J. W., Rogers, S. L., Kawasaki, R., Lamoureux, E. L., Kowalski, J. W., Bek, T., ... & Meta-Analysis for Eye Disease (META-EYE) Study Group. (2012). Global prevalence and major risk factors of diabetic retinopathy. *Diabetes care*, *35*(3), 556-564.

[109] Chang, S. A. (2012). Smoking and type 2 diabetes mellitus. *Diabetes & metabolism journal*, *36*(6), 399-403.

[110] Zhang, J., Wang, Y., Li, L., Zhang, R., Guo, R., Li, H., ... & Liu, F. (2018). Diabetic retinopathy may predict the renal outcomes of patients with diabetic nephropathy. *Renal failure*, *40*(1), 243-251.

[111] Fowler, M. J. (2008). Microvascular and macrovascular complications of diabetes. *Clinical diabetes*, *26*(2), 77-82.

[112] Wu, M. Y., Yiang, G. T., Lai, T. T., & Li, C. J. (2018). The oxidative stress and mitochondrial dysfunction during the pathogenesis of diabetic retinopathy. *Oxidative Medicine and Cellular Longevity*, *2018*.

[113] Chan, W. C., Lim, L. T., Quinn, M. J., Knox, F. A., McCance, D., & Best, R. M. (2004). Management and outcome of sight-threatening diabetic retinopathy in pregnancy. *Eye*, *18*(8), 826-832.

[114] Saxena, S., Jalali, S., Verma, L., & Pathengay, A. (2003). Management of vitreous haemorrhage. *Indian Journal of Ophthalmology*, *51*(2), 189-196.

[115] Gariano, R. F., & Kim, C. H. (2004). Evaluation and management of suspected retinal detachment. *American family physician*, *69*(7), 1691-1699.

[116] Olmos, L. C., & Lee, R. K. (2011). Medical and surgical treatment of neovascular glaucoma. *International ophthalmology clinics*, *51*(3), 27.

[117] Martins, B., Amorim, M., Reis, F., Ambrósio, A. F., & Fernandes, R. (2020). Extracellular vesicles and MicroRNA: putative role in diagnosis and treatment of diabetic retinopathy. *Antioxidants*, *9*(8), 705.

[118] Rucker, J. C., & Tomsak, R. L. (2005). Binocular diplopia: a practical approach. *The neurologist*, *11*(2), 98-110.

[119] Coyne, K. S., Margolis, M. K., Kennedy-Martin, T., Baker, T. M., Klein, R., Paul, M. D., & Revicki, D. A. (2004). The impact of diabetic retinopathy: perspectives from patient focus groups. *Family practice*, *21*(4), 447-453.

[120] Li, X., Zarbin, M. A., & Bhagat, N. (2017). Anti-vascular endothelial growth factor injections: the new standard of care in proliferative diabetic retinopathy?. *Management of Diabetic Retinopathy*, *60*, 131-142.

[121] Neufeld, G., Cohen, T., Gengrinovitch, S., & Poltorak, Z. (1999). Vascular endothelial growth factor (VEGF) and its receptors. *The FASEB journal*, *13*(1), 9-22.

[122] Dugel, P. U., Bandello, F., & Loewenstein, A. (2015). Dexamethasone intravitreal implant in the treatment of diabetic macular edema. *Clinical Ophthalmology*, 1321-1335.

[123] Evans, J. R., Michelessi, M., & Virgili, G. (2014). Laser photocoagulation for proliferative diabetic retinopathy. *Cochrane Database of Systematic Reviews*, (11).

[124] Ho, T., Smiddy, W. E., & Flynn Jr, H. W. (1992). Vitrectomy in the management of diabetic eye disease. *Survey of ophthalmology*, *37*(3), 190-202.

[125] Stefánsson, E. (2009). Physiology of vitreous surgery. *Graefe's archive for clinical and experimental ophthalmology*, *247*, 147-163.

[126] Reddy, S. V., & Husain, D. (2018, January). Panretinal photocoagulation: a review of complications. In *Seminars in ophthalmology* (Vol. 33, No. 1, pp. 83-88). Taylor & Francis.

[127] Diabetic Retinopathy Clinical Research Network. (2008). A randomized trial comparing intravitreal triamcinolone acetonide and focal/grid photocoagulation for diabetic macular edema. *Ophthalmology*, *115*(9), 1447-1459.

[128] Bandello, F., Lattanzio, R., Zucchiatti, I., & Del Turco, C. (2013). Pathophysiology and treatment of diabetic retinopathy. *Acta diabetologica*, *50*, 1-20.

[129] Gulshan, V., Peng, L., Coram, M., Stumpe, M. C., Wu, D., Narayanaswamy, A., ... & Webster, D. R. (2016). Development and validation of a deep learning algorithm for detection of diabetic retinopathy in retinal fundus photographs. *jama*, *316*(22), 2402-2410.

[130] Islam, M. M., Yang, H. C., Poly, T. N., Jian, W. S., & Li, Y. C. J. (2020). Deep learning algorithms for detection of diabetic retinopathy in retinal fundus photographs: A systematic review and meta-analysis. *Computer Methods and Programs in Biomedicine*, *191*, 105320.

[131] Cai, C. J., Winter, S., Steiner, D., Wilcox, L., & Terry, M. (2019). " Hello AI": uncovering the onboarding needs of medical practitioners for human-AI collaborative decision-making. *Proceedings of the ACM on Human-computer Interaction*, *3*(CSCW), 1-24.

[132] Schmidt-Erfurth, U., Sadeghipour, A., Gerendas, B. S., Waldstein, S. M., & Bogunović, H. (2018). Artificial intelligence in retina. *Progress in retinal and eye research*, *67*, 1-29.

[133] Abràmoff, M. D., Garvin, M. K., & Sonka, M. (2010). Retinal imaging and image analysis. *IEEE reviews in biomedical engineering*, *3*, 169-208.

[134] Gaube, S., Suresh, H., Raue, M., Merritt, A., Berkowitz, S. J., Lermer, E., ... & Ghassemi, M. (2021). Do as AI say: susceptibility in deployment of clinical decision-aids. *NPJ digital medicine*, *4*(1), 31.

[135] Varghese, F., Bukhari, A. B., Malhotra, R., & De, A. (2014). IHC Profiler: an open source plugin for the quantitative evaluation and automated scoring of immunohistochemistry images of human tissue samples. *PloS one*, *9*(5), e96801.

[136] Orlando, J. I., Fu, H., Breda, J. B., Van Keer, K., Bathula, D. R., Diaz-Pinto, A., ... & Bogunović, H. (2020). Refuge challenge: A unified framework for evaluating automated methods for glaucoma assessment from fundus photographs. *Medical image analysis*, *59*, 101570.

[137] Galdran, A., Chelbi, J., Kobi, R., Dolz, J., Lombaert, H., Ben Ayed, I., & Chakor, H. (2020). Non-uniform label smoothing for diabetic retinopathy grading from retinal fundus images with deep neural networks. *Translational Vision Science & Technology*, *9*(2), 34-34.

[138] Hosny, A., Parmar, C., Quackenbush, J., Schwartz, L. H., & Aerts, H. J. (2018). Artificial intelligence in radiology. *Nature Reviews Cancer*, *18*(8), 500-510.

[139] Olsen, L., Saunders, R. S., & Yong, P. L. (Eds.). (2010). The healthcare imperative: lowering costs and improving outcomes: workshop series summary.

[140] Shin, Y., Yang, J., Lee, Y. H., & Kim, S. (2021). Artificial intelligence in musculoskeletal ultrasound imaging. *Ultrasonography*, *40*(1), 30.

[141] Anwar, S. M., Majid, M., Qayyum, A., Awais, M., Alnowami, M., & Khan, M. K. (2018). Medical image analysis using convolutional neural networks: a review. *Journal of medical systems*, *42*, 1-13.

[142] Basith, S., Manavalan, B., Hwan Shin, T., & Lee, G. (2020). Machine intelligence in peptide therapeutics: A next-generation tool for rapid disease screening. *Medicinal research reviews*, *40*(4), 1276-1314.

[143] Thanh Noi, P., & Kappas, M. (2017). Comparison of random forest, k-nearest neighbor, and support vector machine classifiers for land cover classification using Sentinel-2 imagery. *Sensors*, *18*(1), 18.

[144] Trucco, E., Ruggeri, A., Karnowski, T., Giancardo, L., Chaum, E., Hubschman, J. P., ... & Dhillon, B. (2013). Validating retinal fundus image analysis algorithms: issues and a proposal. *Investigative ophthalmology & visual science*, *54*(5), 3546-3559.

[145] Liu, Y. Y., Chen, M., Ishikawa, H., Wollstein, G., Schuman, J. S., & Rehg, J. M. (2011). Automated macular pathology diagnosis in retinal OCT images using multi-scale spatial pyramid and local binary patterns in texture and shape encoding. *Medical image analysis*, *15*(5), 748-759.

[146] Javaid, M., Haleem, A., Singh, R. P., Suman, R., & Rab, S. (2022). Significance of machine learning in healthcare: Features, pillars and applications. *International Journal of Intelligent Networks*, *3*, 58-73.

[147] Jamshidi, M., Lalbakhsh, A., Talla, J., Peroutka, Z., Hadjilooei, F., Lalbakhsh, P., ... & Mohyuddin, W. (2020). Artificial intelligence and COVID-19: deep learning approaches for diagnosis and treatment. *Ieee Access*, *8*, 109581-109595.

[148] López, C. (2023). Artificial intelligence and advanced materials. *Advanced Materials*, *35*(23), 2208683.

[149] Ting, D. S., Peng, L., Varadarajan, A. V., Keane, P. A., Burlina, P. M., Chiang, M. F., ... & Wong, T. Y. (2019). Deep learning in ophthalmology: the technical and clinical considerations. *Progress in retinal and eye research*, *72*, 100759.

[150] Raghavendra, U., Fujita, H., Bhandary, S. V., Gudigar, A., Tan, J. H., & Acharya, U. R. (2018). Deep convolution neural network for accurate diagnosis of glaucoma using digital fundus images. *Information Sciences*, *441*, 41-49.

[151] Goldenberg, S. L., Nir, G., & Salcudean, S. E. (2019). A new era: artificial intelligence and machine learning in prostate cancer. *Nature Reviews Urology*, *16*(7), 391-403.

[152] Sarker, I. H. (2021). Deep learning: a comprehensive overview on techniques, taxonomy, applications and research directions. *SN Computer Science*, *2*(6), 420.

[153] Rasheed, K., Qayyum, A., Ghaly, M., Al-Fuqaha, A., Razi, A., & Qadir, J. (2022). Explainable, trustworthy, and ethical machine learning for healthcare: A survey. *Computers in Biology and Medicine*, 106043.

[154] Balyen, L., & Peto, T. (2019). Promising artificial intelligence-machine learning-deep learning algorithms in ophthalmology. *The Asia-Pacific Journal of Ophthalmology*, *8*(3), 264-272.

[155] Seeja, R. D., & Suresh, A. (2019). Deep learning based skin lesion segmentation and classification of melanoma using support vector machine (SVM). *Asian Pacific journal of cancer prevention: APJCP*, *20*(5), 1555.

[156] Sarki, R., Ahmed, K., Wang, H., & Zhang, Y. (2020). Automated detection of mild and multi-class diabetic eye diseases using deep learning. *Health Information Science and Systems*, *8*(1), 32.

[157] Yu, Z., Chen, H., Liu, J., You, J., Leung, H., & Han, G. (2015). Hybrid $ k $-nearest neighbor classifier. *IEEE transactions on cybernetics*, *46*(6), 1263-1275.

[158] Bosale, A. A. (2024). Detection and Classification of Diabetic Retinopathy using Deep Learning Algorithms for Segmentation to Facilitate Referral Recommendation for Test and Treatment Prediction. arXiv preprint arXiv:2401.02759.

[159] Dhibi, K., Mansouri, M., Abodayeh, K., Bouzrara, K., Nounou, H., & Nounou, M. (2022). Interval-Valued Reduced Ensemble Learning Based Fault Detection and Diagnosis Techniques for Uncertain Grid-Connected PV Systems. *IEEE Access*, *10*, 47673-47686.

[160] Salamat, N., Missen, M. M. S., & Rashid, A. (2019). Diabetic retinopathy techniques in retinal images: A review. *Artificial intelligence in medicine*, *97*, 168-188.

[161] Gonzalez, R. C. (2009). *Digital image processing*. Pearson education india.

[162] Tan, L., & Jiang, J. (2019). Image processing basics. *Digital signal processing*, 649-726.

[163] Niemeijer, M., Van Ginneken, B., Staal, J., Suttorp-Schulten, M. S., & Abràmoff, M. D. (2005). Automatic detection of red lesions in digital color fundus photographs. *IEEE Transactions on medical imaging*, *24*(5), 584-592.

[164] Hoover, A., & Goldbaum, M. (2003). Locating the optic nerve in a retinal image using the fuzzy convergence of the blood vessels. *IEEE transactions on medical imaging*, *22*(8), 951-958.

[165] Joshi, S., & Karule, P. T. (2012). Retinal blood vessel segmentation. *International Journal of Engineering and Innovative Technology (IJEIT)*, *1*(3), 175-178.

[166] Walter, T., Massin, P., Erginay, A., Ordonez, R., Jeulin, C., & Klein, J. C. (2007). Automatic detection of microaneurysms in color fundus images. *Medical image analysis*, *11*(6), 555-566.

[167] Antal, B., & Hajdu, A. (2012). Improving microaneurysm detection using an optimally selected subset of candidate extractors and preprocessing methods. *Pattern recognition*, *45*(1), 264-270.

[168] Fraz, M. M., Remagnino, P., Hoppe, A., Uyyanonvara, B., Rudnicka, A. R., Owen, C. G., & Barman, S. A. (2012). An ensemble classification-based approach applied to retinal blood vessel segmentation. *IEEE Transactions on Biomedical Engineering*, *59*(9), 2538-2548.

[169] Staal, J., Abràmoff, M. D., Niemeijer, M., Viergever, M. A., & Van Ginneken, B. (2004). Ridge-based vessel segmentation in color images of the retina. *IEEE transactions on medical imaging*, *23*(4), 501-509.

[170] Marín, D., Aquino, A., Gegúndez-Arias, M. E., & Bravo, J. M. (2010). A new supervised method for blood vessel segmentation in retinal images by using gray-level and moment invariants-based features. *IEEE Transactions on medical imaging*, *30*(1), 146-158.

[171] Soares, J. V., Leandro, J. J., Cesar, R. M., Jelinek, H. F., & Cree, M. J. (2006). Retinal vessel segmentation using the 2-D Gabor wavelet and supervised classification. *IEEE Transactions on medical Imaging*, *25*(9), 1214-1222.

[172] Fraz, M. M., Remagnino, P., Hoppe, A., Uyyanonvara, B., Rudnicka, A. R., Owen, C. G., & Barman, S. A. (2012). Blood vessel segmentation methodologies in retinal images–a survey. *Computer methods and programs in biomedicine*, *108*(1), 407-433.

[173] Roychowdhury, S., Koozekanani, D. D., & Parhi, K. K. (2014). Blood vessel segmentation of fundus images by major vessel extraction and subimage classification. *IEEE journal of biomedical and health informatics*, *19*(3), 1118-1128.

[174] Liskowski, P., & Krawiec, K. (2016). Segmenting retinal blood vessels with deep neural networks. *IEEE transactions on medical imaging*, *35*(11), 2369-2380.

[175] Ramlugun, G. S., Nagarajan, V. K., & Chakraborty, C. (2012). Small retinal vessels extraction towards proliferative diabetic retinopathy screening. *Expert Systems with Applications*, *39*(1), 1141-1146.

[176] Vasanthi, S., & Wahida Banu, R. S. D. (2014). Automatic segmentation and classification of hard exudates to detect macular edema in fundus images. *Journal of Theoretical & Applied Information Technology*, *66*(3).

[177] Franklin, S. W., & Rajan, S. E. (2014). Computerized screening of diabetic retinopathy employing blood vessel segmentation in retinal images. *biocybernetics and biomedical engineering*, *34*(2), 117-124.

[178] Rajput, Y. M., Manza, R. R., Deepali, R. D., Patwari, M. B., Saswade, M., & Deshpande, N. (2016). Design New Biorthogonal Wavelet Filter for Extraction of Blood Vessels and Calculate the Statistical Features. In *Information Systems Design and Intelligent Applications: Proceedings of Third International Conference INDIA 2016, Volume 1* (pp. 647-655). Springer India.

[179] Vlachos, M., & Dermatas, E. (2010). Multi-scale retinal vessel segmentation using line tracking. *Computerized Medical Imaging and Graphics*, *34*(3), 213-227.

[180] Nayebifar, B., & Moghaddam, H. A. (2013). A novel method for retinal vessel tracking using particle filters. *Computers in biology and medicine*, *43*(5), 541-548.

[181] Badsha, S., Reza, A. W., Tan, K. G., & Dimyati, K. (2013). A new blood vessel extraction technique using edge enhancement and object classification. *Journal of digital imaging*, *26*, 1107-1115.

[182] Akram, M. U., & Khan, S. A. (2013). Multilayered thresholding-based blood vessel segmentation for screening of diabetic retinopathy. *Engineering with computers*, *29*, 165-173.

[183] Sopharak, A., Uyyanonvara, B., & Barman, S. (2011). Automatic microaneurysm detection from non-dilated diabetic retinopathy retinal images using mathematical morphology methods. *IAENG International Journal of Computer Science*, *38*(3), 295-301.

[184] Saleh, M. D., & Eswaran, C. (2012). An automated decision-support system for non-proliferative diabetic retinopathy disease based on MAs and HAs detection. *Computer methods and programs in biomedicine*, *108*(1), 186-196.

[185] Zhang, B., Wu, X., You, J., Li, Q., & Karray, F. (2010). Detection of microaneurysms using multi-scale correlation coefficients. *Pattern recognition*, *43*(6), 2237-2248.

[186] Tavakoli, M., Shahri, R. P., Pourreza, H., Mehdizadeh, A., Banaee, T., & Toosi, M. H. B. (2013). A complementary method for automated detection of microaneurysms in fluorescein angiography fundus images to assess diabetic retinopathy. *Pattern Recognition*, *46*(10), 2740-2753.

[187] Lazar, Istvan, and Andras Hajdu. "Retinal microaneurysm detection through local rotating cross-section profile analysis." *IEEE transactions on medical imaging* 32.2 (2012): 400-407.

[188] Dupas, B., Walter, T., Erginay, A., Ordonez, R., Deb-Joardar, N., Gain, P., ... & Massin, P. (2010). Evaluation of automated fundus photograph analysis algorithms for detecting microaneurysms, haemorrhages and exudates, and of a computer-assisted diagnostic system for grading diabetic retinopathy. *Diabetes & metabolism*, *36*(3), 213-220.

[189] Antal, B., & Hajdu, A. (2012). An ensemble-based system for microaneurysm detection and diabetic retinopathy grading. *IEEE transactions on biomedical engineering*, *59*(6), 1720-1726.

[190] Pereira, C., Veiga, D., Mahdjoub, J., Guessoum, Z., Gonçalves, L., Ferreira, M., & Monteiro, J. (2014). Using a multi-agent system approach for microaneurysm detection in fundus images. *Artificial intelligence in medicine*, *60*(3), 179-188.

[191] Niemeijer, M., Van Ginneken, B., Staal, J., Suttorp-Schulten, M. S., & Abràmoff, M. D. (2005). Automatic detection of red lesions in digital color fundus photographs. *IEEE Transactions on medical imaging*, *24*(5), 584-592.

[192] Adal, K. M., Sidibé, D., Ali, S., Chaum, E., Karnowski, T. P., & Mériaudeau, F. (2014). Automated detection of microaneurysms using scale-adapted blob analysis and semi-supervised learning. *Computer methods and programs in biomedicine*, *114*(1), 1-10.

[193] Grisan, E., & Ruggeri, A. (2007, August). Segmentation of candidate dark lesions in fundus images based on local thresholding and pixel density. In *2007 29th Annual International Conference of the IEEE Engineering in Medicine and Biology Society* (pp. 6735-6738). IEEE.

[194] Harangi, B., & Hajdu, A. (2014). Automatic exudate detection by fusing multiple active contours and regionwise classification. *Computers in biology and medicine*, *54*, 156-171.

[195] Karegowda, A. G., Nasiha, A., Jayaram, M. A., & Manjunath, A. S. (2011). Exudates detection in retinal images using back propagation neural network. *International Journal of Computer Applications*, *25*(3), 25-31.

[196] Mookiah, M. R. K., Acharya, U. R., Chua, C. K., Min, L. C., Ng, E. Y. K., Mushrif, M. M., & Laude, A. (2013). Automated detection of optic disk in retinal fundus images using intuitionistic fuzzy histon segmentation. *Proceedings of the Institution of Mechanical Engineers, Part H: Journal of Engineering in Medicine*, *227*(1), 37-49.

[197] Mookiah, M. R. K., Acharya, U. R., Martis, R. J., Chua, C. K., Lim, C. M., Ng, E. Y. K., & Laude, A. (2013). Evolutionary algorithm based classifier parameter tuning for automatic diabetic retinopathy grading: A hybrid feature extraction approach. *Knowledge-based systems*, *39*, 9-22.

[198] Li, H., & Chutatape, O. (2004). Automated feature extraction in color retinal images by a model based approach. *IEEE Transactions on biomedical engineering*, *51*(2), 246-254.

[199] Sinthanayothin, C., Kongbunkiat, V., Phoojaruenchanachai, S., & Singalavanija, A. (2003, September). Automated screening system for diabetic retinopathy. In *3rd International Symposium on Image and Signal Processing and Analysis, 2003. ISPA 2003. Proceedings of the* (Vol. 2, pp. 915-920). IEEE.

[200] Osareh, A., Shadgar, B., & Markham, R. (2009). A computational-intelligence-based approach for detection of exudates in diabetic retinopathy images. *IEEE Transactions on Information Technology in Biomedicine*, *13*(4), 535-545.

[201] Sánchez, C. I., García, M., Mayo, A., López, M. I., & Hornero, R. (2009). Retinal image analysis based on mixture models to detect hard exudates. *Medical Image Analysis*, *13*(4), 650-658.

[202] Agurto, C., Murray, V., Barriga, E., Murillo, S., Pattichis, M., Davis, H., ... & Soliz, P. (2010). Multiscale AM-FM methods for diabetic retinopathy lesion detection. *IEEE transactions on medical imaging*, *29*(2), 502-512.

[203] Ali, S., Sidibé, D., Adal, K. M., Giancardo, L., Chaum, E., Karnowski, T. P., & Mériaudeau, F. (2013). Statistical atlas based exudate segmentation. *Computerized Medical Imaging and Graphics*, *37*(5-6), 358-368.

[204] Welfer, D., Scharcanski, J., & Marinho, D. R. (2010). A coarse-to-fine strategy for automatically detecting exudates in color eye fundus images. *computerized medical imaging and graphics*, *34*(3), 228-235.

[205] Fathi, A., & Naghsh-Nilchi, A. R. (2013). Automatic wavelet-based retinal blood vessels segmentation and vessel diameter estimation. *Biomedical Signal Processing and Control*, *8*(1), 71-80.

[206] Giancardo, L., Meriaudeau, F., Karnowski, T. P., Li, Y., Garg, S., Tobin Jr, K. W., & Chaum, E. (2012). Exudate-based diabetic macular edema detection in fundus images using publicly available datasets. *Medical image analysis*, *16*(1), 216-226.

[207] Jaafar, H. F., Nandi, A. K., & Al-Nuaimy, W. (2010, August). Detection of exudates in retinal images using a pure splitting technique. In *2010 Annual International Conference of the IEEE Engineering in Medicine and Biology* (pp. 6745-6748). IEEE.

[208] Harangi, B., Lazar, I., & Hajdu, A. (2012, August). Automatic exudate detection using active contour model and regionwise classification. In *2012 Annual International Conference of the IEEE Engineering in Medicine and Biology Society* (pp. 5951-5954). IEEE.

[209] Akram, M. U., & Khan, S. A. (2013). Multilayered thresholding-based blood vessel segmentation for screening of diabetic retinopathy. *Engineering with computers*, *29*, 165-173.

[210] Reza, A. W., Eswaran, C., & Dimyati, K. (2011). Diagnosis of diabetic retinopathy: automatic extraction of optic disc and exudates from retinal images using marker-controlled watershed transformation. *Journal of medical systems*, *35*, 1491-1501.

[211] Muramatsu, C., Nakagawa, T., Sawada, A., Hatanaka, Y., Hara, T., Yamamoto, T., & Fujita, H. (2011). Automated segmentation of optic disc region on retinal fundus photographs: Comparison of contour modeling and pixel classification methods. *Computer methods and programs in biomedicine*, *101*(1), 23-32.

[212] Aquino, A., Gegúndez-Arias, M. E., & Marín, D. (2010). Detecting the optic disc boundary in digital fundus images using morphological, edge detection, and feature extraction techniques. *IEEE transactions on medical imaging*, *29*(11), 1860-1869.

[213] Yu, H., Barriga, E. S., Agurto, C., Echegaray, S., Pattichis, M. S., Bauman, W., & Soliz, P. (2012). Fast localization and segmentation of optic disk in retinal images using directional matched filtering and level sets. *IEEE Transactions on information technology in biomedicine*, *16*(4), 644-657.

[214] Kavitha, G., & Ramakrishnan, S. (2010). An approach to identify optic disc in human retinal images using ant colony optimization method. *Journal of medical systems*, *34*, 809-813.

[215] Li, H., & Chutatape, O. (2004). Automated feature extraction in color retinal images by a model based approach. *IEEE Transactions on biomedical engineering*, *51*(2), 246-254.

[216] Youssif, A. A. H. A. R., Ghalwash, A. Z., & Ghoneim, A. A. S. A. R. (2007). Optic disc detection from normalized digital fundus images by means of a vessels' direction matched filter. *IEEE transactions on medical imaging*, *27*(1), 11-18.

[217] Walter, T., Klein, J. C., Massin, P., & Erginay, A. (2002). A contribution of image processing to the diagnosis of diabetic retinopathy-detection of exudates in color fundus images of the human retina. *IEEE transactions on medical imaging*, *21*(10), 1236-1243.

[218] Zhu, X., & Rangayyan, R. M. (2008, August). Detection of the optic disc in images of the retina using the Hough transform. In *2008 30th annual international conference of the IEEE engineering in medicine and biology society* (pp. 3546-3549). IEEE.

[219] Hajer, J., Kamel, H., & Noureddine, E. (2008, May). Localization of the optic disk in retinal image using the 'watersnake'. In *2008 International Conference on Computer and Communication Engineering* (pp. 947-951). IEEE.

[220] Chaudhuri, S., Chatterjee, S., Katz, N., Nelson, M., & Goldbaum, M. (1989). Detection of blood vessels in retinal images using two-dimensional matched filters. *IEEE Transactions on medical imaging*, *8*(3), 263-269.

[221] Li, Q., You, J., & Zhang, D. (2012). Vessel segmentation and width estimation in retinal images using multiscale production of matched filter responses. *Expert Systems with Applications*, *39*(9), 7600-7610.

[222] Aguirre-Ramos, H., Avina-Cervantes, J. G., Cruz-Aceves, I., Ruiz-Pinales, J., & Ledesma, S. (2018). Blood vessel segmentation in retinal fundus images using Gabor filters, fractional derivatives, and Expectation Maximization. *Applied Mathematics and Computation*, *339*, 568-587.

[223] Singh, N. P., & Srivastava, R. (2016). Retinal blood vessels segmentation by using Gumbel probability distribution function based matched filter. *Computer methods and programs in biomedicine*, *129*, 40-50.

[224] Mendonca, A. M., & Campilho, A. (2006). Segmentation of retinal blood vessels by combining the detection of centerlines and morphological reconstruction. *IEEE transactions on medical imaging*, *25*(9), 1200-1213.

[225] Cree, M. J., Cornforth, D., & Jelinek, H. F. (2005). Vessel segmentation and tracking using a two-dimensional model. *IVC New Zealand*, 345-350.

[226] A. F. Frangi, W. J. Niessen, K. L. Vincken and M. A. Viergever, "Multiscale vessel enhancement filtering," in International conference on medical image computing and computer-assisted intervention, 1998.

[227] Fathi, A., & Naghsh-Nilchi, A. R. (2013). Automatic wavelet-based retinal blood vessels segmentation and vessel diameter estimation. *Biomedical Signal Processing and Control*, *8*(1), 71-80.

[228] Ghoshal, R., Saha, A., & Das, S. (2019). An improved vessel extraction scheme from retinal fundus images. *Multimedia Tools and Applications*, *78*(18), 25221-25239.

[229] Morales, S., Engan, K., Naranjo, V., & Colomer, A. (2015). Retinal disease screening through local binary patterns. *IEEE journal of biomedical and health informatics*, *21*(1), 184-192.

[230] Dhiravidachelvi, E., Rajamani, V., & Manimegalai, C. T. (2019). GLCM-based detection and classification of microaneurysm in diabetic retinopathy fundus images. *International Journal of Advanced Intelligence Paradigms*, *14*(1-2), 55-69.

[231] Veiga, D., Martins, N., Ferreira, M., & Monteiro, J. (2018). Automatic microaneurysm detection using laws texture masks and support vector machines. *Computer Methods in Biomechanics and Biomedical Engineering: Imaging & Visualization*, *6*(4), 405-416.

[232] Agurto, C., Murray, V., Barriga, E., Murillo, S., Pattichis, M., Davis, H., ... & Soliz, P. (2010). Multiscale AM-FM methods for diabetic retinopathy lesion detection. *IEEE transactions on medical imaging*, *29*(2), 502-512.

[233] Vijayan, T., Sangeetha, M., Kumaravel, A., & Karthik, B. (2020). WITHDRAWN: Gabor filter and machine learning based diabetic retinopathy analysis and detection.

[234] Zhou, W., Wu, C., Chen, D., Wang, Z., Yi, Y., & Du, W. (2017). Automatic microaneurysms detection based on multifeature fusion dictionary learning. *Computational and Mathematical Methods in Medicine*, *2017*.

[235] Javidi, M., Pourreza, H. R., & Harati, A. (2017). Vessel segmentation and microaneurysm detection using discriminative dictionary learning and sparse representation. *Computer methods and programs in biomedicine*, *139*, 93-108.

[236] Shan, J., & Li, L. (2016, June). A deep learning method for microaneurysm detection in fundus images. In *2016 IEEE First International Conference on Connected Health: Applications, Systems and Engineering Technologies (CHASE)* (pp. 357-358). IEEE.

[237] Kumar, S., & Kumar, B. (2018, February). Diabetic retinopathy detection by extracting area and number of microaneurysm from colour fundus image. In *2018 5th International Conference on Signal Processing and Integrated Networks (SPIN)* (pp. 359-364). IEEE.

[238] Aljuhani, A. (2021). Machine learning approaches for combating distributed denial of service attacks in modern networking environments. *IEEE Access*, *9*, 42236-42264.

[239] Kumar, P., Chauhan, S., & Awasthi, L. K. (2023). Human Activity Recognition (HAR) Using Deep Learning: Review, Methodologies, Progress and Future Research Directions. *Archives of Computational Methods in Engineering*, 1-41.

[240] Mao, Q., Hu, F., & Hao, Q. (2018). Deep learning for intelligent wireless networks: A comprehensive survey. *IEEE Communications Surveys & Tutorials*, *20*(4), 2595-2621.

[241] Derwin, D. J., Selvi, S. T., Singh, O. J., & Shan, B. P. (2020). A novel automated system of discriminating Microaneurysms in fundus images. *Biomedical Signal Processing and Control*, *58*, 101839.

[242] Long, S., Chen, J., Hu, A., Liu, H., Chen, Z., & Zheng, D. (2020). Microaneurysms detection in color fundus images using machine learning based on directional local contrast. *Biomedical engineering online*, *19*(1), 1-23.

[243] Dharani, V., & Lavanya, R. (2018). Improved microaneurysm detection in fundus images for diagnosis of diabetic retinopathy. In *Advances in Signal Processing and Intelligent Recognition Systems: Proceedings of Third International Symposium on Signal Processing and Intelligent Recognition Systems (SIRS-2017), September 13-16, 2017, Manipal, India* (pp. 185-198). Springer International Publishing.

[244] Joshi, S., & Karule, P. T. (2020). Mathematical morphology for microaneurysm detection in fundus images. *European journal of ophthalmology*, *30*(5), 1135-1142.

[245] Colomer, A., Igual, J., & Naranjo, V. (2020). Detection of early signs of diabetic retinopathy based on textural and morphological information in fundus images. *Sensors*, *20*(4), 1005.

[246] Cao, W., Czarnek, N., Shan, J., & Li, L. (2018). Microaneurysm detection using principal component analysis and machine learning methods. *IEEE transactions on nanobioscience*, *17*(3), 191-198.

[247] Melo, T., Mendonça, A. M., & Campilho, A. (2020). Microaneurysm detection in color eye fundus images for diabetic retinopathy screening. *Computers in biology and medicine*, *126*, 103995.

[248] Du, J., Zou, B., Chen, C., Xu, Z., & Liu, Q. (2020). Automatic microaneurysm detection in fundus image based on local cross-section transformation and multi-feature fusion. *Computer Methods and Programs in Biomedicine*, *196*, 105687.

[249] Veiga D, Martins N, Ferreira M, Monteiro J (2018) Automatic microaneurysm detection using laws texture masks and support vector machines. Comput Methods Biomech Biomed Eng Imaging Vis 6(4):405–416

[250] Deepa, V., Sathish Kumar, C., & Susan Andrews, S. (2019). Automated detection of microaneurysms using Stockwell transform and statistical features. *IET Image Processing*, *13*(8), 1341-1348.

[251] Selcuk, T., & Alkan, A. (2019). Detection of microaneurysms using ant colony algorithm in the early diagnosis of diabetic retinopathy. *Medical hypotheses*, *129*, 109242.

[252] Pundikal, M., & Holi, M. S. (2022). Microaneurysms Detection Using Grey Wolf Optimizer and Modified K-Nearest Neighbor for Early Diagnosis of Diabetic Retinopathy. *International Journal of Intelligent Engineering & Systems*, *15*(1).

[253] Kumar, S., Adarsh, A., Kumar, B., & Singh, A. K. (2020). An automated early diabetic retinopathy detection through improved blood vessel and optic disc segmentation. *Optics & Laser Technology*, *121*, 105815.

[254] Eftekhari, N., Pourreza, H. R., Masoudi, M., Ghiasi-Shirazi, K., & Saeedi, E. (2019). Microaneurysm detection in fundus images using a two-step convolutional neural network. *Biomedical engineering online*, *18*, 1-16.

[255] Shan, J., & Li, L. (2016, June). A deep learning method for microaneurysm detection in fundus images. In *2016 IEEE First International Conference on Connected Health: Applications, Systems and Engineering Technologies (CHASE)* (pp. 357-358). IEEE.

[256] Zhang, X., Wu, J., Meng, M., Sun, Y., & Sun, W. (2021). Feature-transfer network and local background suppression for microaneurysm detection. *Machine Vision and Applications*, *32*, 1-13.

[257] Chudzik, P., Majumdar, S., Calivá, F., Al-Diri, B., & Hunter, A. (2018). Microaneurysm detection using fully convolutional neural networks. *Computer methods and programs in biomedicine*, *158*, 185-192.

[258] Deepa, R., & Narayanan, N. K. (2021, March). Retinal Microaneurysm Detection by CNN. In *IOP Conference Series: Materials Science and Engineering* (Vol. 1099, No. 1, p. 012057). IOP Publishing.

[259] Kou, C., Li, W., Liang, W., Yu, Z., & Hao, J. (2019). Microaneurysms segmentation with a U-Net based on recurrent residual convolutional neural network. *Journal of Medical Imaging*, *6*(2), 025008-025008.

[260] Qomariah, D., Nopember, I. T. S., Tjandrasa, H., & Fatichah, C. (2021). Segmentation of microaneurysms for early detection of diabetic retinopathy using MResUNet. *Int. J. Intell. Eng. Syst*, *14*, 359-373.

[261] Zhang, L., Feng, S., Duan, G., Li, Y., & Liu, G. (2019). Detection of microaneurysms in fundus images based on an attention mechanism. *Genes*, *10*(10), 817.

[262] Liao, Y., Xia, H., Song, S., & Li, H. (2021). Microaneurysm detection in fundus images based on a novel end-to-end convolutional neural network. *Biocybernetics and Biomedical Engineering*, *41*(2), 589-604.

[263] Liu, T., Chen, Y., Shen, H., Zhou, R., Zhang, M., Liu, T., & Liu, J. (2021). A novel diabetic retinopathy detection approach based on deep symmetric convolutional neural network. *IEEE Access*, *9*, 160552-160558.

[264] Gu, Y., Wang, X., Pan, J., & Zhou, Z. (2021). Diabetic retinopathy grading base on contrastive learning and semi-supervised learning. In *Bioinformatics Research and Applications: 17th International Symposium, ISBRA 2021, Shenzhen, China, November 26–28, 2021, Proceedings 17* (pp. 68-79). Springer International Publishing.

[265] Deepa, V., Kumar, C. S., & Andrews, S. S. (2021). Fusing dual-tree quaternion wavelet transform and local mesh based features for grading of diabetic retinopathy using extreme learning machine classifier. *International Journal of Imaging Systems and Technology*, *31*(3), 1625-1637.

[266] AlDahoul, N., Karim, H. A., Tan, M. J. T., Momo, M. A., & Fermin, J. L. (2021). Encoding retina image to words using ensemble of vision transformers for diabetic retinopathy grading. *F1000Research*, *10*(948), 948.

[267] Araujo, T., Aresta, G., Mendonça, L., Penas, S., Maia, C., Carneiro, Â., ... & Campilho, A. (2020). DR| GRADUATE: Uncertainty-aware deep learning-based

diabetic retinopathy grading in eye fundus images. *Medical Image Analysis*, *63*, 101715.

[268] Shi, L., & Zhang, J. (2021). Few-shot Learning Based on Multi-stage Transfer and Class-Balanced Loss for Diabetic Retinopathy Grading. *arXiv preprint arXiv:2109.11806*.

[269] AbdelMaksoud, E., Barakat, S., & Elmogy, M. (2020, October). Diabetic retinopathy grading based on a hybrid deep learning model. In *2020 International Conference on Data Analytics for Business and Industry: Way Towards a Sustainable Economy (ICDABI)* (pp. 1-6). IEEE.

[270] Yasin, S., Iqbal, N., Ali, T., Draz, U., Alqahtani, A., Irfan, M., ... & Wzorek, L. (2021). Severity grading and early retinopathy lesion detection through hybrid inception-ResNet architecture. *Sensors*, *21*(20), 6933.

[271] Eladawi, N., Elmogy, M., Ghazal, M., Fraiwan, L., Aboelfetouh, A., Riad, A., ... & El-Baz, A. (2019, December). Diabetic retinopathy grading using 3d multi-path convolutional neural network based on fusing features from octa scans, demographic, and clinical biomarkers. In *2019 IEEE International Conference on Imaging Systems and Techniques (IST)* (pp. 1-6). IEEE.

[272] Skariah, S. M., & Arun, K. S. (2021, January). A deep learning based approach for automated diabetic retinopathy detection and grading. In *2021 4th Biennial International Conference on Nascent Technologies in Engineering (ICNTE)* (pp. 1-6). IEEE.

[273] Yang, Y., Shang, F., Wu, B., Yang, D., Wang, L., Xu, Y., ... & Zhang, T. (2021). Robust collaborative learning of patch-level and image-level annotations for diabetic retinopathy grading from fundus image. *IEEE Transactions on Cybernetics*, *52*(11), 11407-11417.

[274] Zhao, Z., Zhang, K., Hao, X., Tian, J., Chua, M. C. H., Chen, L., & Xu, X. (2019, September). Bira-net: Bilinear attention net for diabetic retinopathy grading. In *2019 IEEE International Conference on Image Processing (ICIP)* (pp. 1385-1389). IEEE.

[275] Al-Turk, L., Wawrzynski, J., Wang, S., Krause, P., Saleh, G. M., Alsawadi, H., ... & Tang, H. L. (2022). Automated feature-based grading and progression analysis of diabetic retinopathy. *Eye*, *36*(3), 524-532.

[276] Gayathri, S., Gopi, V. P., & Palanisamy, P. (2021). Diabetic retinopathy classification based on multipath CNN and machine learning classifiers. *Physical and engineering sciences in medicine*, *44*(3), 639-653.

[277] Zhang, W., Zhong, J., Yang, S., Gao, Z., Hu, J., Chen, Y., & Yi, Z. (2019). Automated identification and grading system of diabetic retinopathy using deep neural networks. *Knowledge-Based Systems*, *175*, 12-25.

[278] Sun, R., Li, Y., Zhang, T., Mao, Z., Wu, F., & Zhang, Y. (2021). Lesion-aware transformers for diabetic retinopathy grading. In *Proceedings of the IEEE/CVF Conference on Computer Vision and Pattern Recognition* (pp. 10938-10947).

[279] Wu, Z., Shi, G., Chen, Y., Shi, F., Chen, X., Coatrieux, G., ... & Li, S. (2020). Coarse-to-fine classification for diabetic retinopathy grading using convolutional neural network. *Artificial Intelligence in Medicine*, *108*, 101936.

[280] Wang, X., Xu, M., Zhang, J., Jiang, L., & Li, L. (2021, May). Deep multi-task learning for diabetic retinopathy grading in fundus images. In *Proceedings of the AAAI Conference on Artificial Intelligence* (Vol. 35, No. 4, pp. 2826-2834).

[281] Yi, S. L., Yang, X. L., Wang, T. W., She, F. R., Xiong, X., & He, J. F. (2021). Diabetic retinopathy diagnosis based on RA-EfficientNet. *Applied Sciences*, *11*(22), 11035.

[282] Zhou, Y., Wang, B., Huang, L., Cui, S., & Shao, L. (2020). A benchmark for studying diabetic retinopathy: segmentation, grading, and transferability. *IEEE Transactions on Medical Imaging*, *40*(3), 818-828.

[283] Zhang, D., Bu, W., & Wu, X. (2017, August). Diabetic retinopathy classification using deeply supervised ResNet. In *2017 IEEE SmartWorld, Ubiquitous Intelligence & Computing, Advanced & Trusted Computed, Scalable Computing & Communications, Cloud & Big Data Computing, Internet of People and Smart*

City Innovation (SmartWorld/SCALCOM/UIC/ATC/CBDCom/IOP/SCI) (pp. 1-6). IEEE.

[284] Qummar, S., Khan, F. G., Shah, S., Khan, A., Shamshirband, S., Rehman, Z. U., ... & Jadoon, W. (2019). A deep learning ensemble approach for diabetic retinopathy detection. *Ieee Access*, *7*, 150530-150539.

[285] Xiao, Z., Zhang, Y., Wu, J., & Zhang, X. (2021, April). SE-MIDNet Based on Deep Learning for Diabetic Retinopathy Classification. In *2021 7th International Conference on Computing and Artificial Intelligence* (pp. 92-98).

[286] AbdelMaksoud, E., Barakat, S., & Elmogy, M. (2020). Diabetic retinopathy grading system based on transfer learning. *arXiv preprint arXiv:2012.12515*.

[287] Mukti, F. A., Eswaran, C., Hashim, N., Ching, H. C., & Ayoobkhan, M. U. A. (2018). An automated grading system for diabetic retinopathy using curvelet transform and hierarchical classification. *International Journal of Engineering & Technology*, *7*(2.15), 154-157.

[288] Luo, L., Xue, D., & Feng, X. (2020). Automatic diabetic retinopathy grading via self-knowledge distillation. *Electronics*, *9*(9), 1337.

[289] Sarwinda, D., Bustamam, A., & Wibisono, A. (2017, November). A complete modelling of Local Binary Pattern for detection of diabetic retinopathy. In *2017 1st international conference on informatics and computational sciences (ICICoS)* (pp. 7-10). IEEE.

[290] Nguyen, Q. H., Muthuraman, R., Singh, L., Sen, G., Tran, A. C., Nguyen, B. P., & Chua, M. (2020, January). Diabetic retinopathy detection using deep learning. In *Proceedings of the 4th international conference on machine learning and soft computing* (pp. 103-107).

[291] Kaggle. Diabetic Retinopathy Detection. https://www.kaggle.com/c/diabetic-retinopathy-detection. Accessed 24 April 2022.

[292] Wilkinson, C. P., Ferris III, F. L., Klein, R. E., Lee, P. P., Agardh, C. D., Davis, M., ... & Global Diabetic Retinopathy Project Group. (2003). Proposed

international clinical diabetic retinopathy and diabetic macular edema disease severity scales. Ophthalmology, 110(9), 1677-1682.

[293] Davis, M. D., Fisher, M. R., Gangnon, R. E., Barton, F., Aiello, L. M., Chew, E. Y., ... & Knatterud, G. L. (1998). Risk factors for high-risk proliferative diabetic retinopathy and severe visual loss: Early Treatment Diabetic Retinopathy Study Report# 18. Investigative ophthalmology & visual science, 39(2), 233-252.

[294] Porwal, P., Pachade, S., Kamble, R., Kokare, M., Deshmukh, G., Sahasrabuddhe, V., & Meriaudeau, F. (2018). Indian diabetic retinopathy image dataset (IDRiD): a database for diabetic retinopathy screening research. Data, 3(3), 25.

[295] Li, T.; Gao, Y.; Wang, K.; Guo, S.; Liu, H.; Kang, H. Diagnostic assessment of deep learning algorithms for diabetic retinopathy screening. Inf. Sci. 2019, 501, 511–522

[296] Noor-Ul-Huda, M.; Tehsin, S.; Ahmed, S.; Niazi, F.A.; Murtaza, Z. Retinal images benchmark for the detection of diabetic retinopathy and clinically significant macular edema (CSME). Biomed. Tech. Eng. 2018, 64, 297–307.

[297] Wei, Q.; Li, X.; Yu, W.; Zhang, X.; Zhang, Y.; Hu, B.; Mo, B.; Gong, D.; Chen, N.; Ding, D.; et al. Learn to Segment Retinal Lesions and Beyond. In Proceedings of the 2020 25th International Conference on Pattern Recognition (ICPR), Milan, Italy, 10–15 January 2021; pp. 7403–7410.

[298] Ali, A.; Qadri, S.; Mashwani, W.K.; Kumam, W.; Kumam, P.; Naeem, S.; Goktas, A.; Jamal, F.; Chesneau, C.; Anam, S.; et al. Machine Learning Based Automated Segmentation and Hybrid Feature Analysis for Diabetic Retinopathy Classification Using Fundus Image. Entropy 2020, 22, 567

[299] Benítez, V.E.C.; Matto, I.C.; Román, J.C.M.; Noguera, J.L.V.; García-Torres, M.; Ayala, J.; Pinto-Roa, D.P.; Gardel-Sotomayor, P.E.; Facon, J.; Grillo, S.A. Dataset from fundus images for the study of diabetic retinopathy. Data Brief. 2021, 36, 107068.

[300] Li, F.; Liu, Z.; Chen, H.; Jiang, M.; Zhang, X.; Wu, Z. Automatic Detection of Diabetic Retinopathy in Retinal Fundus Photographs Based on Deep Learning Algorithm. Transl. Vis. Sci. Technol. 2019, 8, 4.

[301] Li, T.; Gao, Y.; Wang, K.; Guo, S.; Liu, H.; Kang, H. Diagnostic assessment of deep learning algorithms for diabetic retinopathy screening. Inf Sci (Ny). 2019, 501, 511–22. DOI:10.1016/j.ins.2019.06.011

[302] ODIR-2019. Available online: https://odir2019.grand-challenge.org/ (accessed on 22 June 2021).

[303] Díaz, M.; Novo, J.; Cutrín, P.; Gómez-Ulla, F.; Penedo, M.G.; Ortega, M. Automatic segmentation of the foveal avascular zone in ophthalmological OCT-A images. PLoS ONE 2019, 14, e0212364.

[304] Ali, A.; Qadri, S.; Mashwani, W.K.; Kumam, W.; Kumam, P.; Naeem, S.; Goktas, A.; Jamal, F.; Chesneau, C.; Anam, S.; et al. Machine Learning Based Automated Segmentation and Hybrid Feature Analysis for Diabetic Retinopathy Classification Using Fundus Image. Entropy 2020, 22, 567.

[305] Kaggle.com. Available online: https://www.kaggle.com/c/aptos2019-blindness-detection (accessed on 23 May 2021).

[306] Abdulla, W.; Chalakkal, R.J. University of Auckland Diabetic Retinopathy (UoA-DR) Database-End User Licence Agreement. Available online: https://auckland.figshare.com/articles/journal_contribution/UoA-DR_Database_Info/5985208 (accessed on 28 May 2021).

[307] Gholami, P.; Roy, P.; Parthasarathy, M.K.; Lakshminarayanan, V. OCTID: Optical coherence tomography image database. Comput. Electr. Eng. 2020, 81, 106532.

[308] Porwal, P.; Pachade, S.; Kamble, R.; Kokare, M.; Deshmukh, G.; Sahasrabuddhe, V.; Meriaudeau, F. Indian diabetic retinopathy image dataset (IDRiD): A database for diabetic retinopathy screening research. Data 2018, 3, 25.

[309] Ting, D.S.W.; Cheung, C.Y.-L.; Lim, G.; Tan, G.S.W.; Quang, N.D.; Gan, A.; Hamzah, H.; Garcia-Franco, R.; Yeo, I.Y.S.; Lee, S.Y.; et al. Development and

Validation of a Deep Learning System for Diabetic Retinopathy and Related Eye Diseases Using Retinal Images From Multiethnic Populations With Diabetes. JAMA 2017, 318, 2211–2223.

[310] Rotterdam Ophthalmic Data Repository. re3data.org. Available online: https://www.re3data.org/repository/r3d (accessed on 22 June 2021)

[311] Takahashi, H.; Tampo, H.; Arai, Y.; Inoue, Y.; Kawashima, H. Applying artificial intelligence to disease staging: Deep learning for improved staging of diabetic retinopathy. PLoS ONE 2017, 12, e0179790

[312] Holm, S.; Russell, G.; Nourrit, V.; McLoughlin, N. DR HAGIS—A fundus image database for the automatic extraction of retinal surface vessels from diabetic patients. J. Med. Imaging 2017, 4, 014503

[313] People.duke.edu Website. Available online: http://people.duke.edu/~{}sf59/software.html (accessed on 26 May 2021).

[314] Kaggle.com. Available online: https://www.kaggle.com/c/diabetic-retinopathy-detection/data (accessed on 26 May 2021).

[315] Srinivasan, P.P.; Kim, L.; Mettu, P.S.; Cousins, S.W.; Comer, G.M.; Izatt, J.A.; Farsiu, S. Fully automated detection of diabetic macular edema and dry age-related macular degeneration from optical coherence tomography images. Biomed. Opt. Express 2014, 5, 3568–3577.

[316] Bala, M.P.; Vijayachitra, S. Early detection and classification of microaneurysms in retinal fundus images using sequential learning methods. Int. J. Biomed. Eng. Technol. 2014, 15, 128.

[317] Decencière, E.; Zhang, X.; Cazuguel, G.; Lay, B.; Cochener, B.; Trone, C.; Gain, P.; Ordóñez-Varela, J.-R.; Massin, P.; Erginay, A.; et al. Feedback on a publicly distributed image database: The MESSIDOR database. Image Anal. Ster. 2014, 33, 231.

[318] Alipour, S.H.M.; Rabbani, H.; Akhlaghi, M. A new combined method based on curvelet transform and morphological operators for automatic detection of foveal avascular zone. Signal Image Video Process. 2014, 8, 205–222

[319] Sevik, U.; Köse, C.; Berber, T.; Erdöl, H. Identification of suitable fundus images using automated quality assessment methods.J. Biomed. Opt. 2014, 19, 046006

[320] Pires, R.; Jelinek, H.F.; Wainer, J.; Valle, E.; Rocha, A. Advancing Bag-of-Visual-Words Representations for Lesion Classification in Retinal Images. PLoS ONE 2014, 9, e96814

[321] Hu, Q.; Abràmoff, M.D.; Garvin, M.K. Automated Separation of Binary Overlapping Trees in Low-Contrast Color Retinal Images. In Medical Image Computing and Computer-Assisted Intervention; Lecture Notes in Computer Science; Mori, K., Sakuma, I., Sato, Y., Barillot, C., Navab, N., Eds.; Springer: Berlin/Heidelberg, Germany, 2013; Volume 8150.

[322] Odstrcilik, J.; Kolar, R.; Budai, A.; Hornegger, J.; Jan, J.; Gazarek, J.; Kubena, T.; Cernosek, P.; Svoboda, O.; Angelopoulou, E. Retinal vessel segmentation by improved matched filtering: Evaluation on a new high-resolution fundus image database. IET Image Process. 2013, 7, 373–383.

[323] Somaraki, V.; Broadbent, D.; Coenen, F.; Harding, S. Finding Temporal Patterns in Noisy Longitudinal Data: A Study in Diabetic Retinopathy. In Advances in Data Mining. Applications and Theoretical Aspects; Springer: New York, NY, USA, 2010; Volume 6171, pp. 418–431.

[324] Decencière, E.; Cazuguel, G.; Zhang, X.; Thibault, G.; Klein, J.-C.; Meyer, F.; Marcotegui, B.; Quellec, G.; Lamard, M.; Danno, R.; et al. TeleOphta: Machine learning and image processing methods for teleophthalmology. IRBM 2013, 34, 196–203.

[325] Prentasic, P.; Loncaric, S.; Vatavuk, Z.; Bencic, G.; Subasic, M.; Petkovic´, T. Diabetic retinopathy image database(DRiDB): A new database for diabetic retinopathy screening programs research. In Proceedings of the 2013 8th

International Symposium on Image and Signal Processing and Analysis (ISPA), Trieste, Italy, 4–6 September 2013; pp. 711–716.

[326] Esmaeili, M.; Rabbani, H.; Dehnavi, A.; Dehghani, A. Automatic detection of exudates and optic disk in retinal images using curvelet transform. IET Image Process. 2012, 6, 1005–1013.

[327] Alipour, S.H.M.; Rabbani, H.; Akhlaghi, M. Diabetic Retinopathy Grading by Digital Curvelet Transform. Comput. Math. Methods Med. 2012, 2012, 1–11.

[328] Alipour, S.H.M.; Rabbani, H.; Akhlaghi, M.; Mehridehnavi, A.; Javanmard, S.H. Analysis of foveal avascular zone for grading of diabetic retinopathy severity based on curvelet transform. Graefe's Arch. Clin. Exp. Ophthalmol. 2012, 250, 1607–1614.

[329] Giancardo, L.; Meriaudeau, F.; Karnowski, T.P.; Li, Y.; Garg, S.; Tobin, K.W.; Chaum, E. Exudate-based diabetic macular edema detection in fundus images using publicly available datasets. Med. Image Anal. 2012, 16, 216–226.

[330] Hsieh, Y.-T.; Chuang, L.-M.; Jiang, Y.-D.; Chang, T.-J.; Yang, C.-M.; Yang, C.-H.; Chan, L.-W.; Kao, T.-Y.; Chen, T.-C.; Lin, H.-C.; et al. Application of deep learning image assessment software VeriSee™ for diabetic retinopathy screening. J. Formos. Med. Assoc. 2021, 120, 165–171.

[331] Kauppi, T.; Kalesnykiene, V.; Kamarainen, J.-K.; Lensu, L.; Sorri, I.; Raninen, A.; Voutilainen, R.; Uusitalo, H.; Kalviainen, H.; Pietila, J. The diaretdb1 diabetic retinopathy database and evaluation protocol. In Proceedings of the British Machine Vision Conference 2007, Coventry, UK, 10–13 September 2007; pp. 61–65.

[332] Kauppi, T.; Kalesnykiene, V.; Kamarainen, J.; Lensu, L.; Sorri, I. DIARETDB0: Evaluation Database and Methodology for Diabetic Retinopathy Algorithms. Mach Vis Pattern Recognit Res Group, Lappeenranta Univ Technol Finland. 2006, pp. 1–17. Available online: http://www.siue.edu/~{}sumbaug/RetinalProjectPapers/DiabeticRetinopathyImageDatabaseInformation.pdf (accessed on 25 May 2021).

[333] Drive-Grand Challenge Official Website. Available online: https://drive.grand-challenge.org/ (accessed on 23 May 2021).

[334] Alzubaidi, L., Zhang, J., Humaidi, A. J., Al-Dujaili, A., Duan, Y., Al-Shamma, O., ... & Farhan, L. (2021). Review of deep learning: Concepts, CNN architectures, challenges, applications, future directions. Journal of big Data, 8, 1-74.

[335] He, K., Zhang, X., Ren, S., & Sun, J. (2015). Deep residual learning for image recognition. arXiv preprint arXiv:1512.03385. Available at: https://arxiv.org/abs/1512.03385

[336] Zagoruyko, S., & Komodakis, N. (2016). Wide residual networks. arXiv preprint arXiv:1605.07146.

[337] He, K., Zhang, X., Ren, S., & Sun, J. (2016). Deep residual learning for image recognition. In Proceedings of the IEEE conference on computer vision and pattern recognition (pp. 770-778).

[338] Nayak, S. R., Nayak, D. R., Sinha, U., Arora, V., & Pachori, R. B. (2021). Application of deep learning techniques for detection of COVID-19 cases using chest X-ray images: A comprehensive study. Biomedical Signal Processing and Control, 64, 102365.

[339] Bradley, A. P. (1997). The use of the area under the ROC curve in the evaluation of machine learning algorithms. Pattern recognition, 30(7), 1145-1159.

[340] Yaqoob, M. K., Ali, S. F., Bilal, M., Hanif, M. S., & Al-Saggaf, U. M. (2021). ResNet based deep features and random forest classifier for diabetic retinopathy detection. Sensors, 21(11), 3883.

[341] Al, N. M. A. M. M., & Khudeyer, R. S. (2021). ResNet-34/DR: a residual convolutional neural network for the diagnosis of diabetic retinopathy. Informatica, 45(7).

[342] Shanthi, T., & Sabeenian, R. S. (2019). Modified Alexnet architecture for classification of diabetic retinopathy images. Computers & Electrical Engineering, 76, 56-64.

[343] Masood, S., Luthra, T., Sundriyal, H., & Ahmed, M. (2017, May). Identification of diabetic retinopathy in eye images using transfer learning. In 2017 international conference on computing, communication and automation (ICCCA) (pp. 1183-1187). IEEE.

[344] Deshpande, A., & Pardhi, J. (2021). Automated detection of Diabetic Retinopathy using VGG-16 architecture. Irjet, 8(03).

[345] Lam C, Yi D, Guo M, Lindsey T. Automated Detection of Diabetic Retinopathy using Deep Learning. AMIA Jt Summits Transl Sci Proc. 2018 May 18;2017:147-155. PMID: 29888061; PMCID: PMC5961805.

[346] Harry Pratt, Frans Coenen, Deborah M. Broadbent, Simon P. Harding, Yalin Zheng, Convolutional Neural Networks for Diabetic Retinopathy, Procedia Computer Science, Volume 90, 2016, Pages 200-205, SSN 1877-0509, https://doi.org/10.1016/j.procs.2016.07.014.

[347] Math, L., Fatima, R. Adaptive machine learning classification for diabetic retinopathy. Multimed Tools Appl 80, 5173–5186 (2021). https://doi.org/10.1007/s11042-020-09793-7

[348] Yao, L., Zhong, Y., Wu, J., Zhang, G., Chen, L., Guan, P., ... & Liu, L. (2019). Multivariable logistic regression and back propagation artificial neural network to predict diabetic retinopathy. Diabetes, Metabolic Syndrome and Obesity: Targets and Therapy, 1943-1951.

[349] Zaaboub, N., & Douik, A. (2020, September). Early diagnosis of diabetic retinopathy using random forest algorithm. In *2020 5th International Conference on Advanced Technologies for Signal and Image Processing (ATSIP)* (pp. 1-5). IEEE.

[350] Abdelsalam, M. M., & Zahran, M. A. (2021). A novel approach of diabetic retinopathy early detection based on multifractal geometry analysis for OCTA macular images using support vector machine. *IEEE access*, *9*, 22844-22858.

[351] Kaur, J., & Kaur, P. (2023). Automated Computer-Aided Diagnosis of Diabetic Retinopathy Based on Segmentation and Classification using K-nearest neighbor algorithm in retinal images. *The Computer Journal*, *66*(8), 2011-2032.

[352] Ghosh, R., Ghosh, K., & Maitra, S. (2017, February). Automatic detection and classification of diabetic retinopathy stages using CNN. In *2017 4th International Conference on Signal Processing and Integrated Networks (SPIN)* (pp. 550-554). IEEE.

[353] Baba, S.M., Bala, I., Dhiman, G. *et al.* Automated diabetic retinopathy severity grading using novel DR-ResNet + deep learning model. *Multimedia Tools Appl* (2024). https://doi.org/10.1007/s11042-024-18434-2

LIST OF PUBLICATION/S

1. Baba, S. M., Bala, I., Dhiman, G., Sharma, A., & Viriyasitavat, W. (2024). Automated diabetic retinopathy severity grading using novel DR-ResNet+ deep learning model. *Multimedia Tools and Applications*, 1-43.

LIST OF CONFERENCE/S

1. Baba, S. M., & Bala, I. (2022, May). Detection of diabetic retinopathy with retinal images using CNN. In *2022 6th International Conference on Intelligent Computing and Control Systems (ICICCS)* (pp. 1074-1080). IEEE.
2. Baba, S. M., & Bala, I. (2023, June). Severity Grading of Diabetic Retinopathy Using CNN. In *2023 International Conference on Computer, Electronics & Electrical Engineering & their Applications (IC2E3)* (pp. 1-6). IEEE.

LIST OF PATENT/S

S.no	Title	Application Number	Status
1.	Automated Diabetic Retinopathy Severity Grading using Novel DR-ResNet+ Deep Learning Model	202311087882	Patent published